

TECHNISCHE UNIVERSITÄT MÜNCHEN

Lehrstuhl für Technische Chemie II

# **Catalytic Conversion of Methanol to Olefins over HZSM-5 Catalysts**

Xianyong Sun

Vollständiger Abdruck der von der Fakultät für Chemie der Technischen Universität  
München zur Erlangung des akademischen Grades eines

**Doktors der Naturwissenschaften (Dr. rer. nat.)**

genehmigten Dissertation.

Vorsitzender: Univ.-Prof. Dr.-Ing. Kai-Olaf Hinrichsen

Prüfer der Dissertation:

1. Univ.-Prof. Dr. Johannes A. Lercher
2. Univ.-Prof. Dr. Klaus Köhler

Die Dissertation wurde am 05. 11. 2013 bei der Technischen Universität München  
eingereicht und durch die Fakultät für Chemie am 04. 12. 2013 angenommen.

*"The secret to creativity is knowing how to hide your sources."*

Albert Einstein (1879-1955)

## **Acknowledgements**

There is no doubt that I could not have completed this thesis without the tremendous help and supports, technically or spiritually, from everyone involved in this journey.

First of all, I would like to thank Johannes (Prof. Dr. J. A. Lercher) for offering me the valuable opportunity to work and complete my doctoral thesis in his prestigious group. Being involved in a very applied R&D project— that I did not expect actually at the beginning, I managed eventually to present you a piece of scientific work, owing to the trust, freedom and inspirations you've granted to me.

I am extremely grateful to Prof. Dr. Andre C. van Veen, my Ph.D. co-supervisor, who walked me essentially through the whole experimental phase leading to the main scientific findings included in the present thesis work. Dr. Roberta Olindo is gratefully acknowledged for her help and contributions that made me successful in implementing the 10-fold reaction unit during the early phase. I am deeply indebted to Dr. Maricruz Sanchez-Sanchez for the smooth collaborations we have during the final phase, and particularly for correcting my thesis.

The thesis work is completed in the framework of a long-term collaboration between TUM and Clariant produkte GmbH (previous Sud-Chemie AG). I would like to thanks all the project partners from Clariant for the challenges they offered, their trust, encouragement, collaborations, fruitful discussions, and particularly the freedom that they granted to me. In particular, I am very thankful to Prof. Dr. Richard Fischer for his generous supports whenever I needed his hand. Dr. Markus Tonigold is greatly acknowledged for his thoughtful considerations in the MTP project implementation.

I am particularly indebted to my colleague and partner in the lab, Sebastian Mueller, who joined me two years ago. He is always on my side when some challenges come up. And thanks a lot for the comforts you gave to me and the fruitful collaborations.

I am most grateful to my friend and previous lab mate, Hui Shi, for the joy and companion we had during the past years. Thanks a lot for the time and memory. I wish Hui all the best in his life, and hope that our paths will cross again someday in the near future. Thanks a lot for spending time correcting my thesis.

I would like to thank my office mates: Sebastian Foraita, Marco Peroni, Tobias Berto, and Eva Schachtl, Stanislav Kasakov for generating the wonderful atmosphere and funs we have.

I am very grateful to our technical staff in this group for their strong support. I am grateful to all of them: Xaver Hecht for implementing the parallel reactor unit and the commissioning of the Berty reactor. Martin Neukamm for giving suggestions on the handling and disposal of chemicals; Andreas Marx for tackling problems of electronics and computers. Our former and current secretaries, Stefanie Maier, Helen Lemmermöhle, Katharina Thies, Bettina Federmann and Karen Schulz, deserve particular thanks for their help in administrative matters that makes the everyday life easy to go.

Particularly, it has been a great pleasure and unforgettable experience to work with Prof. Mirosław Derewinski in the phosphorous effect, and Prof. Gary L. Haller in the MTP paper corrections during the final stage of my work.

I am very grateful to Prof. Dr. Ing. Kai-Olaf Hinrichsen and Prof. Dr. Klaus Köhler for agreeing on acting as members of the examination committee for my doctoral defense.

Last but not least, I am deeply indebted to my family, relatives and friends from whom I've been receiving endless love and support.

Xianyong Sun  
October, 2013

## Abstract

The reaction patterns of methanol-to-olefins (MTO) conversion over HZSM-5 catalysts have been systematically investigated under industrially relevant conditions. The MTO reaction is of strong autocatalytic nature; olefins and aromatic products act as entrained co-catalysts. While both the aromatics and the olefin based routes are active in methanol conversion, olefin methylation/cracking was identified as the dominant reaction pathway over HZSM-5 zeolite. The aromatics and the olefin based routes produce light ( $C_2$ - $C_4$ ) olefins at distinct selectivities. The aromatics based route produces nearly equal amounts of ethylene and propylene, whereas the olefin-based route is significantly more selective to  $C_{3+}$  olefins than ethylene. Co-feeding of aromatics shifts the product spectrum from predominantly propylene to ethylene and propylene mixtures. It is proposed that a hydrogen transfer pathway involving methanol-derived intermediates exists and proceeds faster than the generally accepted hydrogen transfer between two olefinic species. The catalytic impact of phosphorous anion modifiers on HZSM-5 materials is sensitive to the testing environment and preparation procedures.

Die Reaktionsmuster der Umwandlung von Methanol zu Olefinen (MTO) über HZSM-5-Katalysatoren wurden unter industriell relevanten Bedingungen untersucht. Die MTO-Reaktion ist stark autokatalytisch; olefinische und aromatische Produkte wirken als eingeschlossene Cokatalysatoren. Während sowohl der Aromaten- als auch der Olefin-basierte Reaktionsweg wirken, ist wurde Olefin-Methylierung / Olefincracking als der dominierende Reaktionspfad über HZSM-5 Zeolithe identifiziert. Die Aromaten- und die Olefin-basierten Pfade liefern leichte ( $C_2$ - $C_4$ ) Olefine in bestimmten Selektivitäten. Die Aromaten-basierte Route produziert nahezu gleiche Mengen an Ethylen und Propylen, wohingegen die Olefin-basierte Route deutlich selektiver für  $C_{3+}$  Olefine als Ethylen ist. Das Co-feeding von Aromaten verschiebt das Produktspektrum von vorwiegend Propylen zu Mischungen aus Ethylen und Propylen. Es wird vorgeschlagen, dass ein Wasserstoff-Transfer-Pfad mit aus Methanol gebildeten Zwischenprodukten existiert und schneller als der allgemein akzeptierte Wasserstoff-Transfer zwischen zwei olefinischen Spezies abläuft. Der katalytische Einfluss von anionischen Phosphormodifikatoren auf HZSM-5 Materialien ist empfindlich auf die Testumgebung und die Präparationsmethode.

## Table of contents

<b>Acknowledgements .....</b>	<b>i</b>
<b>Abstract.....</b>	<b>iii</b>
<b>Table of contents.....</b>	<b>iv</b>

### Chapter 1

<b>Introduction.....</b>	<b>1</b>
1.1 General background: market is awaiting more olefins .....	2
1.2 Commercial technologies in methanol conversion .....	4
1.3 Mechanistic aspects in MTO reaction. ....	9
1.3.1. Early proposals of direct C-C coupling.....	10
1.3.2. Autocatalysis .....	11
1.3.3. Hydrocarbon pool mechanism.....	13
1.3.4. Dual cycle concept .....	16
1.4 Phosphorous induced zeolite modificatiaons .....	19
1.5 Scope of the thesis.....	21
1.6 References .....	22

### Chapter 2

#### Impact of Co-feeding Aromatics and Olefins in the Methanol–To-Olefins Conversion over HZSM-5 Catalysts

.....	<b>26</b>
2.1. Introduction .....	27
2.2. Experimental .....	29
2.2.1. Catalyst and reagents .....	29
2.2.2. Catalytic testing .....	30
2.3. Results and Discussion.....	31

2.3.1.	Reaction path of methanol-to-olefins conversion over HZSM-5 catalysts.....	31
2.3.2.	Impact of aromatics co-feeding on the methanol conversion .....	33
2.3.2.1	Impact of co-feeding <i>p</i> - or <i>m</i> -xylene.....	34
2.3.2.2	Impact of toluene and benzene co-feeding on methanol conversion .....	40
2.3.3.	Impact of co-feeding olefins on methanol conversion.....	43
2.3.3.1	Impact of 1-pentene co-feeding on the methanol conversion .....	43
2.3.3.2	Impact of the nature of co-fed olefins on the methanol conversion.....	49
2.4.	Conclusions .....	54
2.5.	Acknowledgements .....	55
2.6.	References .....	55

## Chapter 3

### Insights into Reaction Pathways of Methanol-To-Olefins Conversion over HZSM-5 Zeolite

.....	<b>57</b>	
3.1.	Introduction .....	58
3.2.	Experimental .....	60
	Catalyst and reagents, and Catalytic testing.....	60
3.3.	Results and Discussion.....	62
3.3.1.	Autocatalysis versus hydrocarbon pool proposal.....	62
3.3.2.	Insights from aromatics and olefin co-feeding.....	66
3.3.3.	Comparison with olefin cracking .....	71
3.3.4.	Impact of methanol to co-feed ratio on product distribution.....	78
3.3.5.	Towards elucidating the working mechanism in MTO over HZSM-5.....	82
3.4.	Conclusions .....	85
3.5.	Acknowledgements .....	86
3.6.	References .....	86

**Chapter 4**

**Impact of Reaction Conditions and Catalyst Modifications on the Methanol-To-Olefins Reaction over HZSM-5 catalysts**

.....**89**

4.1. Introduction ..... 90

4.2. Experimental ..... 91

    4.2.1. Sample preparations..... 91

        4.2.1.1 Zeolites..... 91

        4.2.1.2 Phosphorous modifications and steaming ..... 92

    4.2.2. Catalytic testing ..... 93

        4.2.2.1 Activity and reaction pathway evaluations..... 93

        4.2.2.2 Catalytic performance testing..... 94

4.3. Results and Discussion..... 96

    4.3.1. Impact of reaction conditions on MTO reaction..... 96

        4.3.1.1 Effect of reaction temperature..... 96

        4.3.1.2 Impact of reaction temperature on MTO long-term performance..... 101

    4.3.2. Effect of methanol pressure on product selectivity..... 105

    4.3.3. Impact of P doping..... 110

        4.3.3.1 Impact of phosphorous doping of ZSM-5 with various Si/Al ratios .....110

        4.3.3.2 Impact of test conditions and water washing .....116

4.4. Conclusions ..... 123

4.5. Acknowledgements ..... 125

4.6. References ..... 125

**Chapter 5**

**Summary and conclusions.....127**

**Curriculum vitae .....130**

**List of publications to be submitted.....131**

**List of presentations.....132**



# *Chapter 1*

## **Introduction**

## 1.1 General background: market is awaiting more olefins

In organic chemistry, an olefin or alkene is an unsaturated chemical compound containing at least one carbon–carbon double bond [1]. Ethylene represents the simplest mono-olefins with a general formula of  $C_nH_{2n}$ , a family of acyclic hydrocarbons with only one carbon-carbon double bond and no other functional groups. Unlike a carbon-carbon single bond which consists of a single *sigma* bond, a carbon–carbon double bond consists of one *sigma* bond and one *pi* bond [1]. Most reactions of olefins involve the rupture of the reactive *pi* bond and formation of a new single *sigma* bond, which makes olefins suitable for the conversion to a wide variety of products. In particular, the two most important light olefins, ethylene and propylene, are key building blocks for the modern petrochemical industry [2]. The majority of olefins consumption is driven by the production of polymers (i.e. polyethylene and polypropylene) used for plastics, in addition to other important derivatives such as ethylene dichloride, ethylene oxide, propylene oxide, oxo alcohol, polystyrene, acrylic acid and acrylonitrile [2-3].

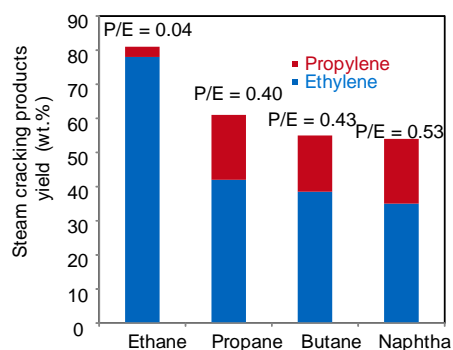


**Figure 1.** Typical propylene/ethylene (P/E) ratios from steam cracking of various feeds including ethane, propane, butane, and naphtha [2,4].

At present, 97% of ethylene is produced from thermal steam cracking [2]. In this process, the hydrocarbon molecules in the feedstock (predominantly naphtha), are broken down at high temperatures in the presence of steam to produce ethylene as the main product and other hydrocarbons. Steam cracking produces propylene as a byproduct with a typical ratio of propylene to ethylene (P/E) of 0.5 (Figure 1), which contributes to 66% of worldwide propylene production. In addition to that, 32% of propylene production is

supplied by fluidized catalytic cracking (FCC) [2]. As FCC units produce primarily gasoline, propylene is again a by-product. The rest 2% of the propylene comes from propane dehydrogenation or metathesis [2].

The global propylene production is currently about half that of ethylene [2,4]. Demand for these light olefins is forecasted to increase over the next decade. The demand by 2015 is projected to grow to 160 million tons for ethylene and 105 million tons for propylene, respectively. However, the demands for ethylene and propylene increase at different rates. The global propylene demand is forecasted to increase by 6 to 8% per year, which exceeds the forecasted growth in global ethylene demand of 4 to 6% per year [2,4]. As the predicted rate in ethylene growth is lower than that in propylene growth, the conventional steam cracking technology itself will not be able to meet the demand for propylene.

With respect to the activities in various regions, the past years has seen new olefin plants mainly in the Middle East and Asia [2,4]. The reason is quite obvious: Asia is one of the fastest growing regions with a very high demand for ethylene and propylene derived consumer products; on the other side, the Middle East acts as an advantageous location for ethylene production as a result of its abundant and cheap feeds (especially ethane) [2]. Although both the Middle East and Asia will gain in ethylene market share, there will still be a gap in propylene supply especially in Asia. The required P/E ratio in Asia is about 0.9 [4]. Compared to the naphtha as the conventional feed for steam crackers which produce ethylene and propylene with a typical P/E ratio of 0.5, ethane cracking does not typically yield an appreciable amount of propylene to meet the demand, as the produced P/E ratio is as low as 0.04 (Figure 1). The increased production of ethylene from ethane and the strong growth of propylene derivatives have driven up the price of propylene compared to ethylene [2,4].

Therefore, this situation results in an increasing gap between propylene demand and production. Not only will the newly implemented ethylene plants be unable to meet the increased propylene demand, the total amount of produced propylene is also less than the market need. It is estimated that 10% of propylene production, equivalent to 10 million

tons, will have to come from other technologies [2]. In this respect, methanol conversion will act as an important alternative for on-purpose propylene production.

## 1.2 Commercial technologies in methanol conversion

Methanol is the simplest alcohol, with a chemical formula of  $\text{CH}_3\text{OH}$ . Methanol can be readily produced by proven technologies from synthesis gas (a mixture of carbon monoxide and hydrogen), which in turn is produced by steam reforming of natural gas or gasification of carbonaceous materials including coal, recycled plastics, municipal wastes, or other organic materials [2]. Although methanol itself is a potential motor fuel or can be blended with gasoline, it would require large investments to overcome the technical problems associated with the direct use [5]. The discovery of methanol-to-hydrocarbons (MTH) reaction was accidental. One group at Mobil was aiming to convert methanol to other oxygen-containing compounds over a ZSM-5 catalyst (Figure 2, left), and they obtained unexpected hydrocarbons. Independently, another Mobil group was trying to alkylate isobutane with methanol over a ZSM-5 catalyst. They observed that isobutane was completely unreactive, and a mixture of paraffins and aromatics in the gasoline boiling range was exclusively formed from methanol [5].

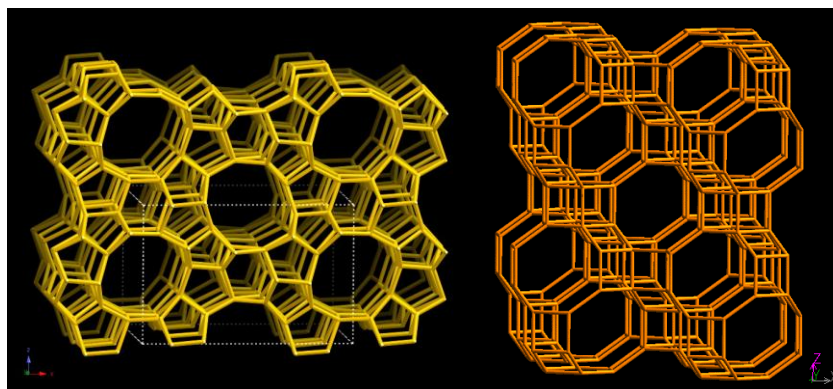


**Figure 2.** Framework topologies of HZSM-5(MFI) of SAPO-34 (CHA) materials. HZSM-5 zeolite is the archetypical catalyst for the Mobil's MTG and MTO, MOGD as well as Lurgi's MTP and Total's OCP processes. SAPO-34 is the key component of the catalysts for UOP/Hydro's MTO and DICI's DMTO processes. The images are from the IZA website.

The oil crisis in 1970s stimulated an intense interest in developing the MTH technology, which was regarded as a vital alternative to the petroleum based route for the production of synthetic fuels and other chemicals [5-7]. In fact, almost anything made out of crude oil can be produced out of coal or natural gas by the MTH technology. At the beginning, the MTH technology was mainly regarded as a vital process to produce high-quality gasoline from natural gas [6]. In 1979 the Mobil's fixed-bed methanol-to-gasoline (MTG) process was first commercialized in New Zealand to produce gasoline from the abundant natural gas resources [6-7]. The New Zealand plant started to come on stream from early 1986 and produce about 600 000 tons gasoline per year, meeting one-third of the local demand for gasoline [6-7]. The gasoline production part of the plant was later shut down, due to the significantly decreased price for gasoline. The methanol production part is still in operation [5-7].

The MTH family has been expanded from the production of specific fuels (MTG) to the production of platform chemicals and especially light olefins (methanol-to-olefins, MTO) [5,7]. As methanol conversion is highly exothermic, the control and dissipation of heat is one of the key issues in the reactor and process design. Conventionally, methanol is partly dehydrated in the first reactor over a slightly acidic catalyst (usually alumina-based) to form an equilibrium mixture of methanol, dimethyl ether and water, prior to being fed into the next reactor [5,7]. In the next reactor, the mixture is converted to either gasoline (MTG) or olefins (MTO), depending on the used catalyst and/or the process operation conditions. The Mobil's fixed-bed MTG reaction operates at temperatures of about 673 K and a methanol partial pressure of several bar, and a ZSM-5 based catalyst is used [6,7]. These reaction conditions favor the hydrogen transfer reactions leading to the formation of paraffins and aromatics from olefins.

Implementation of the MTG process seems to facilitate the development of the MTO process, though independent investigations have been conducted in parallel from the very beginning. The role of light olefins as crucial intermediates in the MTG conversion was recognized very early [8]. It was observed that about 40% carbon –based selectivity to light olefin products was achieved at a certain conversion level in the MTG reaction [5,8]. Intensive efforts were made to develop technologies for selective production of light

olefins from methanol either on the archetypical catalyst, i.e., medium-pore ZSM-5 zeolites, or later on small-pore SAPO-34 zeotype materials (Figure 2, right). On the other hand, the selectivity to light olefins increases remarkably at high temperature (partly thermodynamic effect) and low pressure (kinetic effect) [7]. By a combination of proper choice of catalysts and reaction conditions (for example, a reaction temperature of 773 K), the yield of light olefins can be enhanced significantly. This led to successful development of the fluid-bed MTO process by Mobil [5]. Using a ZSM-5 based catalyst, this process produces propylene and butylene as main products and high-octane gasoline as a byproduct. The Mobil's MTO process has been demonstrated in a plant at Wesseling, Germany [5,7].

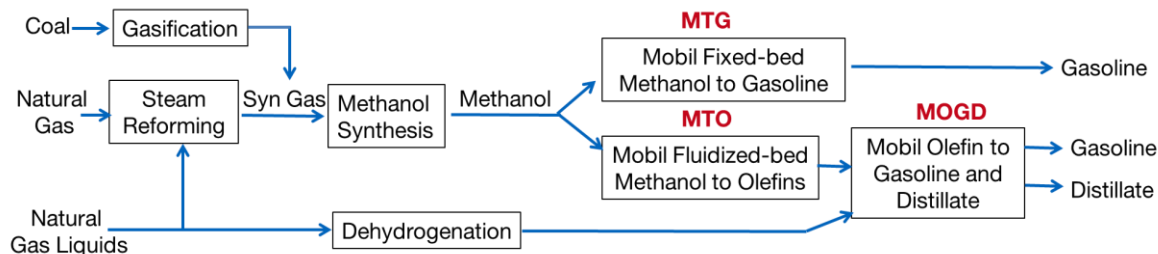


**Figure 3.** Mobil's MTG, MTO, and MOGD processes [5,7].

As depicted in Figure 3, further conversion of the produced light olefins by another ZSM-5 based process results in a full-ranged product spectrum, as light olefins undergo oligomerization reactions, leading to the production of higher olefins which fall in the range of gasoline, or distillate. This is called Mobil's olefin-to-gasoline and distillate process (MOGD), which is well coupled with the MTO process [5,7].

Another MTO process was successfully developed in 1990s by UOP in cooperation with Norsk Hydro (now INEOS) by applying a H-SAPO-34 based catalyst and a low-pressure fluidized-bed reactor design to enable efficient temperature control and continuous regeneration [5,7]. A demonstration unit, with a capacity of 0.5 ton per year, operated by Norsk Hydro verified the olefin yield and catalyst performance [5,7]. SAPO-34 material was invented by researchers at Union carbide (now UOP). It has a unique pore structure (chabazite topology, large cavities connected by 8-rings as the pore openings) [5, 7]. This

favors the production of light olefins, and as high as 80% selectivity to ethylene and propylene can be achieved [5]. However, in stark contrast to H-ZSM-5, coking of H-SAPO-34 is rapid and frequent regenerations are needed. The ratio of propylene/ethylene is around 1.0 and can be altered by adjusting reaction conditions. Further improvement of selectivity to ethylene and propylene was achieved by combining the MTO process with an olefin cracking process (OCP) developed jointly by Total Petrochemicals and UOP (Figure 4) [7]. In 2009 a semi-commercial demonstration unit in Feluy, Belgium, processing up to 10 tonnes per day of methanol feed was brought on-stream. The construction of a 295 kt/y plant in Nanjing, China was announced in 2011 [7].

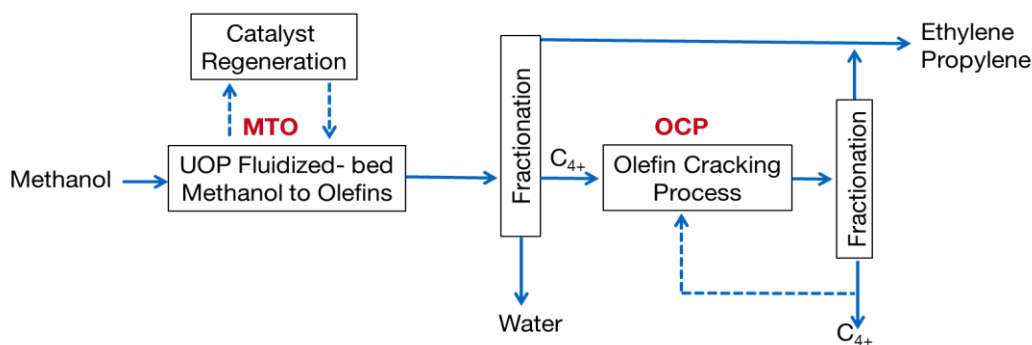


**Figure 4.** UOP's fluidized-bed MTO process combined with UOP/Total OCP olefin cracking process [5,7].

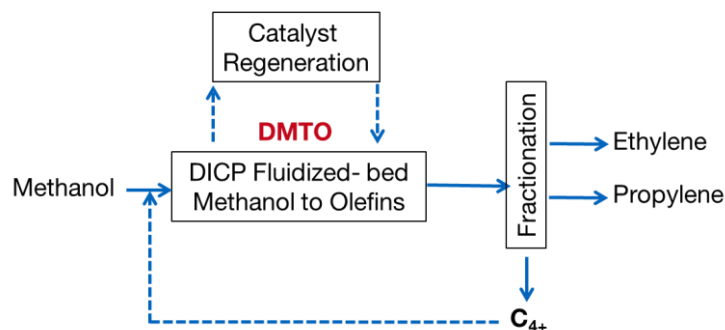


**Figure 5.** DICP's fluidized-bed DMTO process [7].

A similar process, named DMTO, was developed by researchers at Dalian Institute of Chemical Physics (DICP), in which a H-SAPO-34 based catalyst and a fluidized-bed reactor are also applied [7]. Shown in Figure 5, the main difference from the UOP's

MTO process lies in that, instead of applying a separate olefin cracking reactor,  $C_{4+}$  stream is recycled to the MTO reactor for maximizing production of ethylene and propylene. The first commercial MTO plant with a production capacity of 600 000 tons (ethylene + propylene) per year was brought on stream in 2010 [7].

A H-ZSM-5 based fixed-bed Methanol-To-Propylene (MTP) technology was developed by Lurgi with the aim to maximize propylene production, in parallel to the development course of H-SAPO-34 based fluidized-bed MTO technologies for the co-production of ethylene and propylene [8,9]. As depicted in Figure 6, methanol is partly dehydrated in the pre-reactor, and the mixture of methanol and dimethylether is then fed into an adiabatic fixed-bed quench reactor via inter-stage feeding to control the temperature [7-9]. The total pressure is close to atmospheric and the MTP reaction temperatures are about 733-753 K [7]. A highly siliceous H-ZSM-5 based catalyst was used in the process to achieve the high selectivity to propylene [7]. After conversion, the reactor effluent is fractionized, where the undesired products, such as ethylene, butenes and higher aliphatic products, are simply recycled to the methanol conversion reactor for further production of propylene. The process design consists of three parallel fixed-bed reactors, which enable intermittent regeneration [7-9]. Additional recycling of process condensate water acts as a diluting agent and increases the selectivity to olefins. The first MTP plant was brought on stream in China in 2010 with an annual capacity of 500 000 tons of propene per year and 185 000 tons gasoline per year as the main by-product [7].

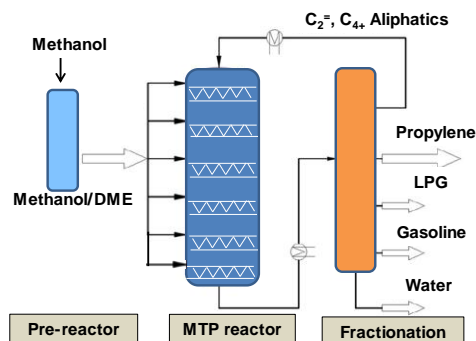


**Figure 6.** A simplified scheme of Lurgi's MTP process. Three parallel adiabatic reactors enable the intermittent regenerations (not depicted). Inter-stage feeding (quench) favors the temperature control, and recycle of process condensate,  $C_2$  and  $C_{4+}$  olefins leads to a higher propylene yield [7].



### 1.3 Mechanistic aspects in MTO reaction

In parallel to the development of the MTO(P) technologies in industry, three decades of intensive experimental and theoretical research efforts have been made in academia to unravel the underlying mechanism, which is believed to benefit the practical development [2,5,7,8]. The extremely complex reaction network makes it a very challenging task to elucidate the MTO mechanistic pathways. Due to the porous nature of the applied zeolite or zeotype materials, particular attention should be paid to desorption and diffusion disguises when deriving mechanistic insights from experimental phenomena, as the secondary reactions often consume the primary products and mask the real pathways [7].

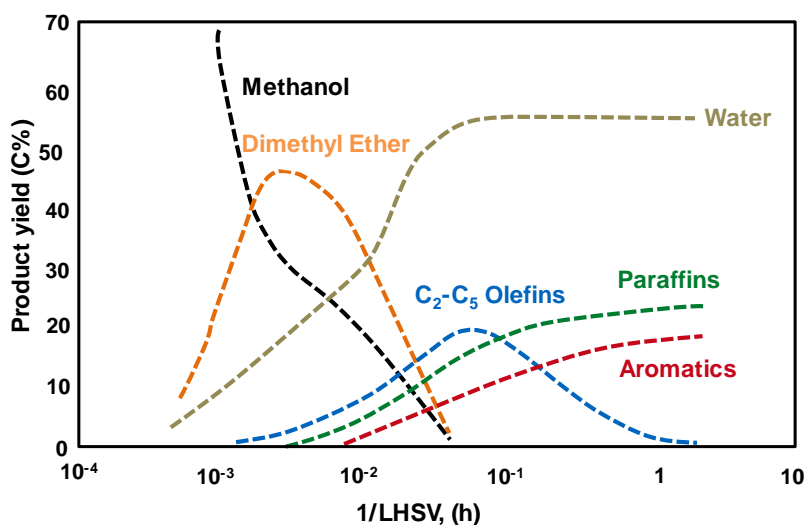
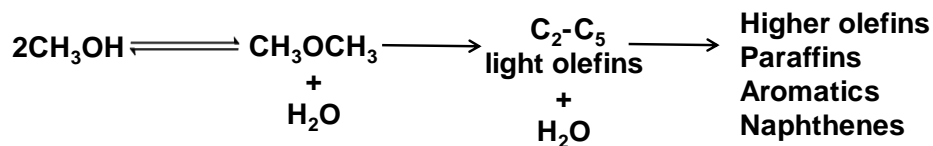


**Figure 7.** Reaction path of the methanol-to-hydrocarbons reaction [5-6].

As the reaction path of the MTH reaction indicates (Figure 7), methanol conversion over acidic HZSM-5 zeolites proceeds via consecutive reaction steps. The main reaction steps can be schemed as follows (Scheme 1):



**Scheme1.** Sequential steps of MTH conversion over ZSM-5 catalysts [5,8].

Methanol is first dehydrated to form an equilibrium mixture of methanol, water and dimethylether. C<sub>2</sub>-C<sub>5</sub> light olefins are produced from this mixture in the subsequent step. In the last step, the light olefins are further transformed to higher olefins, naphthenes, paraffins and aromatics via oligomerization, hydrogen transfer and cyclization reactions. The reaction mechanism of the first step, i.e., DME formation from methanol, is generally accepted as follows: a methanol molecule reacts with a hydroxyl group on the solid acid catalyst to form a surface methoxyl, which then undergoes a nucleophilic attack by another methanol molecule [5]. On the other hand, the third step, i.e., transformation of light olefins to other hydrocarbons, is well known to proceed via the classical carbenium ion mediated chemistry [5]. However, the reaction mechanism in the second step, formation of olefins from C<sub>1</sub> entities, has been the one of the focuses in the heterogeneous catalysis research since the first report by Chang in mid-1970s [2,7,8].

### **1.3.1 Early proposals of direct C-C Coupling**

The initial debate was mainly on how the first C–C bond was formed from methanol/dimethylether or C<sub>1</sub> entities derived from it. Over 20 direct coupling mechanisms were suggested with intermediate species encompassing oxonium ylides, carbenes, carbocations, free radicals or surface bound alkoxy groups (Figure 8), in spite of little direct experimental evidence [5]. Recently, Van Speybroeck et al. conducted an integrated survey via theoretical calculations on the possible direct coupling pathways [11]. It was concluded that direct C–C coupling fails completely due to unstable intermediates and prohibitively high activation barriers [11]. Using highly purified reagents, Song et al. showed that methanol was not reactive without a primordial hydrocarbon species, demonstrating that direct C<sub>1</sub> coupling operated at a rate so low, if any, that it was overwhelmed by trace impurities from methanol feed, carrier gas or catalyst [12]. Given that a kinetic induction period preceding the steady-state hydrocarbon formation is well established on the fresh catalyst, there is a convincing reason to believe that the reaction mechanism prevailing during steady state catalysis is irrelevant to that in the induction period. Furthermore, considering that recycling of hydrocarbons other than the desired products is a frequently adopted operation in realistic

applications for methanol conversion, the direct mechanisms are of little practical significance, though it remains an intriguing question.

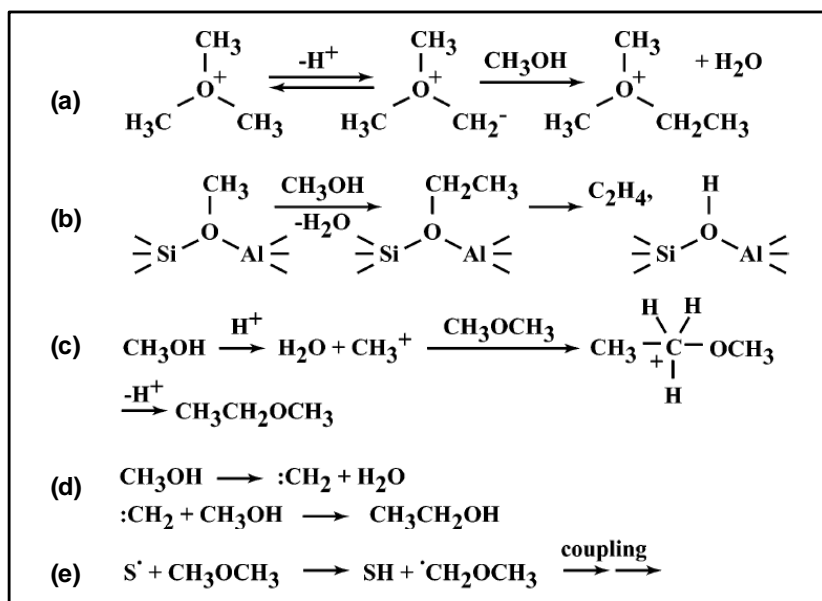
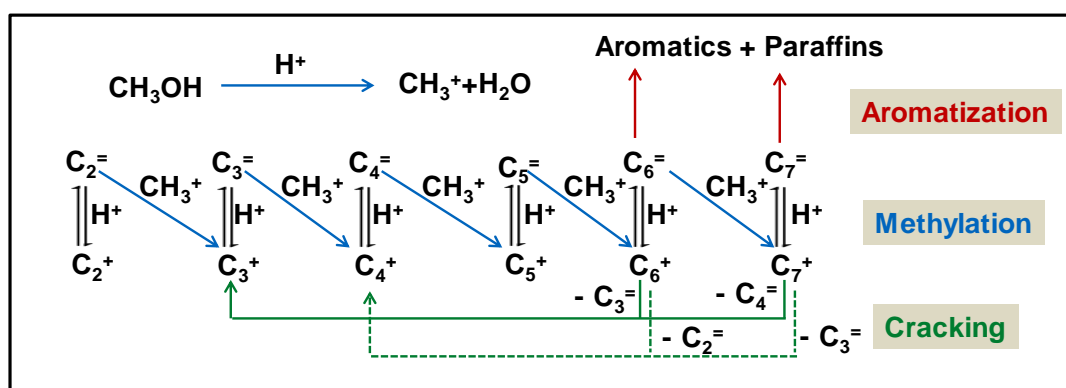


**Figure 8.** Early proposed “direct” mechanisms for the conversion of methanol/dimethyl ether to olefins, sorted by Haw et al. [12]: (a) An abbreviated oxonium-ylide route. (b) An alkoxy chain growth process occurring on a framework site. (c) A pathway showing a carbenium ion alkylating dimethyl ether to form a carbonium ion. (d) One of several proposed carbene pathways. (e) An abbreviation of one of several free radical routes. S\* is an unspecified surface radical species.

### 1.3.2 Autocatalysis

Instead of the direct mechanisms, the indirect mechanisms are generally accepted to explain the light (C<sub>2</sub>–C<sub>4</sub>) olefins formation during steady-state operation. In 1979, Chen and Reagan originally proposed that MTH is an autocatalytic reaction, in the sense that a small amount of initial olefin products, which were believed to be formed with a rather low rate during the induction period, act as co-catalyst leading to the self-accelerated methanol conversion via autocatalytic olefin alkylation [13]. This leads to the increased conversion rate with contact time at the initial stages of the reaction. This is in line with the observation by Langner [14] that the kinetic induction period was significantly shortened by adding very small amount of higher alcohols as olefin precursors. Consistent with the proposal of autocatalytic nature, an olefin homologation/cracking

route was proposed by Dessau and co-workers as the main reaction pathway for the formation of light ( $C_2$ – $C_4$ ) olefins from methanol conversion at the steady-state operation over HZSM-5 catalysts (Scheme 2) [15-16]. After the initial olefins are formed during the induction period, these olefins are consecutively methylated to form higher olefin homologues, which subsequently crack to form lighter olefins such as ethylene and propylene. Hydrogen transfers and cyclization reactions lead to the formation of alkanes and aromatics as end products. Further supports on the olefin-based cycle were obtained from isotopic labeling experiments [17]. In a most recent theoretical study via the ONIOM approach, Lesthaeghe et al. [18] proved the viability of this olefin methylation/cracking cycle for ethylene and propylene formation on HZSM-5, in which the calculated activation barriers for this path were fairly low (60–120  $\text{kJ mol}^{-1}$ ).



**Scheme 2.** An olefin homologation/cracking mechanism proposed by Dessau and co-worker [15,16].

In parallel to the proposal of this olefin based cycle, the important role of aromatics and unsaturated cyclic species in methanol reaction was also reported very early. In as early as 1982, Langner observed that the duration of the induction period decreased by 18-fold when methanol was co-fed with 36 ppm of cyclohexanol over HZSM-5, which indicated the significant role of cyclic unsaturated species in the methanol conversion [14]. Accordingly, Langner proposed the co-catalytic role of methylated cyclic hydrocarbons in producing  $C_3$ – $C_5$  olefins via the paring reaction (Figure 9) [14]. In a parallel study, Mole et al. [19-20] observed an enhanced methanol conversion rate over HZSM-5 when a small amount of toluene or p-xylene was added. This finding led Mole

et al. to propose the aromatics co-catalysis (Figure 9). As methanol reaction produces aromatics, one could also call the aromatics co-catalysis as another autocatalytic effect in addition to the olefin based autocatalysis. These early investigations using ZSM-5 zeolite were very insightful and embodied already the concept of aromatics based cycle. However, these findings remained largely ignored.

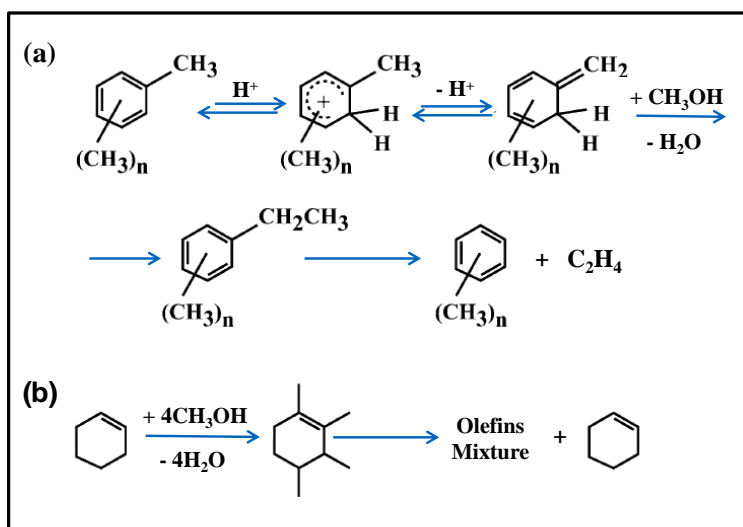
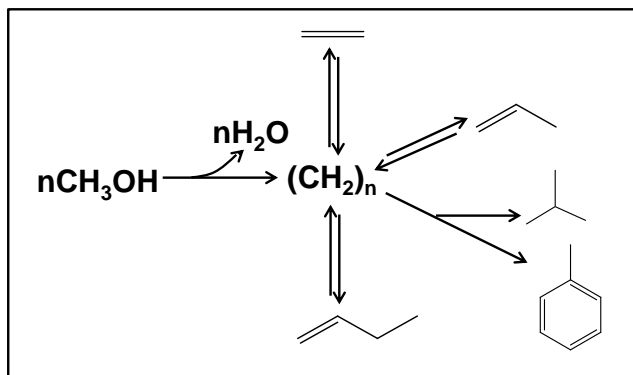


**Figure 9.** Two early proposals that embodied the hydrocarbon pool mechanism in MTO catalysis. (a) mechanism of methylbenzene side-chain alkylation proposed by Mole in 1983 [19-20]. (b) An abbreviated description of the explanation for the dramatic effect of cyclohexanol and other co-feeds of reducing the kinetic induction period by Langner [14].

### 1.3.3 Hydrocarbon pool mechanism

It was the invention of SAPO-34 material in the early 1990s that stimulated again the investigations on role of aromatics in the MTH mechanism. Very interestingly, the investigation by Dahl and Kolboe [21-23] demonstrated that the olefin-based reaction mechanism did not play an important role in the H-SAPO-34 catalyzed methanol conversion under their studied reaction conditions. When co-feeding  $^{13}\text{C}$  labeled methanol with unlabeled ethylene or propylene, these authors observed little carbon scrambling over H-SAPO-34 catalyst; in other words, co-processed ethylene or propylene were basically inactive and most of the products were formed exclusively from methanol. These observations led Kolboe et al. to propose the “hydrocarbon pool”

mechanism (Scheme 3) [21-23]. In the original hydrocarbon pool proposal, the active center is an organic species adsorbed on the surface, located in the pores or cages of a microporous solid. The chemical structure of the pool species was not specified in their first reports.



**Scheme 3.** The originally proposed hydrocarbon pool mechanism by Dahl and Kolboe [21-23].

The unique structure of SAPO-34 material (8-member ring pore opening with super cages) provided the possibility of probing ‘trapped’ carbon intermediate species and thus stimulated intensive investigations in parallel by the research groups of Kolboe, and Haw, independently. They established the role of aromatics, especially methylbenzenes or their protonated counterparts, as the active hydrocarbon pool species in light olefin formation in SAPO-34, H-BEA, and H-MOR catalysts having large pores or cages [23-34]. Accordingly, the active site for MTO was defined as a supramolecular inorganic-organic (zeolite-hydrocarbon species) hybrid, which acts as a scaffold for light olefins formation. In a proposed cycle, methanol successively reacts with the methylbenzenes via methylation, and subsequently the elimination of light olefin products such as ethylene and propene regenerates the initial hydrocarbon pool species, and thus completes the catalytic cycle. In 2000, Mikkelsen et al. [25] observed isotopic scrambling in the olefinic products when co-feeding  $^{12}\text{C}$ -toluene and  $^{13}\text{C}$  methanol over H-ZSM-5, and it was concluded that an arene, or some arene derivative, is involved in forming a substantial part of the propylene. In 2002, Haw et al. showed that polymethylbenzenes fed over H-beta zeolite are active for olefins formation [35].

Bj ørgen et al. investigated also the reactivity of polymethylbenzenes over H-beta zeolite, and the heptamethylbenzenium cation was identified as a key intermediate. [33-34] In 2001, Arstad and Kolboe studied the organic material trapped inside SAPO-34 after switching from a  $^{12}\text{C}$  methanol feed to a  $^{13}\text{C}$  methanol feed [26-27]. They observed isotopic scrambling in all polymethylbenzenes, especially the higher homologues. The analysis of the olefinic products after the  $^{12}\text{C}/^{13}\text{C}$  switch showed that the isotopic distribution of the olefinic products changed only gradually, strongly pointing to polymethylbenzenes acting as the active hydrocarbon pool in the SAPO-34 catalyst. In accord with these findings, Haw and co-workers also identified methylbenzenes as the organic reaction centers for methanol to hydrocarbon catalysis on H-SAPO-34 catalysts [28-32]. Haw and co-workers also investigated the MTH chemistry on an H-ZSM-5 catalyst using solid-state NMR spectroscopy, and it was found that methylated cyclopentenyl cations might also function as reaction centers for alkene formation [12].

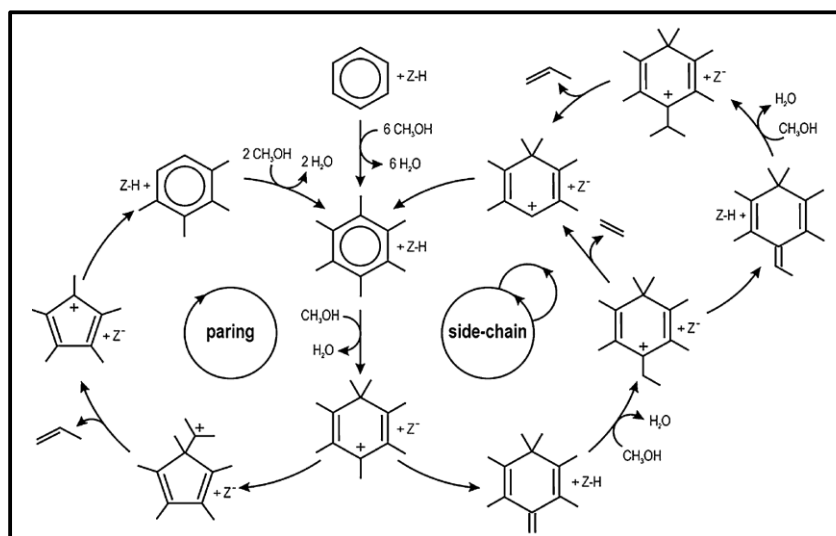


**Figure 10.** Representation of the paring and side-chain reaction concepts in MTH catalysis [7].

In an aromatics-based cycle, light olefins are hypothetically formed via two distinct mechanisms, the paring mechanism and the exocyclic side chain mechanism (Figure 10). Paring mechanism was originally described by Sullivan [36] and it refers to an envisioned process where methyl groups are shaved off from the methylbenzene as light olefins via ring expansion and ring contraction as the key elementary steps. The paring

reaction is known in organic chemistry of alkylated cyclics over superacids. Direct evidence for these paring-type reactions was obtained in investigations of the unimolecular decomposition of protonated methylbenzenes. On the other hand, the side chain methylation Scheme in Figure 10 (right) for propene formation was proposed by Mole and co-workers [19,20] and later refined by Haw and coworkers [12]. Key elementary steps in this mechanism include the formation of exocyclic double bond and a subsequent methylation reaction as well as protonation/deprotonation steps. Employing *in-situ* NMR techniques, Hunger et al. [37-39] obtained spectroscopic evidence supportive of side-chain methylation on H-ZSM-5 catalysts. Although hexamethylbenzene and heptamethylbenzenium are shown as the active intermediates in the scheme, it should also be noted that a lower homologue, the gemdimethyl isomer of the pentamethylbenzenium ion, has been reported to be present in H-ZSM-5 zeolite.

#### 1.3.4 Dual cycle concept

Recent experimental and theoretical work suggested that focusing on aromatics as the sole active species would cause a biased understanding of the hydrocarbon pool mechanism, and that catalyst topology dictates to a large extent the identity of active hydrocarbon pool species. While aromatic intermediates seem to be kinetically relevant for catalysts with large pores or voids like SAPO-34 and beta zeolite, olefins may act as another kind of active hydrocarbon pool species in medium-pore zeolites, such as the ZSM-5 zeolite with 3-D 10-ring channels, where the internal spaces are too small to activate the bulkiest polymethylbenzenes. Davis et al. observed in an early study that the isotopic distribution pattern of ethylene was different from other olefins when co-feeding unlabeled higher alcohols with  $^{14}\text{C}$  labeled methanol over a H-ZSM-5 catalyst, indicating that the mechanism of ethylene formation is distinct from the mechanism of higher olefins formation under the reported reaction conditions [40]. In line with this finding, a renewed study on ZSM-5 [41-42] demonstrated very recently by means of a transient  $^{12}\text{C}/^{13}\text{C}$  isotope-switching experiment zeolite that under their studied reaction conditions, ethylene and lower methylbenzenes (xylenes and trimethylbenzenes) showed comparable  $^{13}\text{C}$  incorporation rates, and  $\text{C}_{3+}$  showed the distinct isotopic incorporation rates from those of ethylene and aromatics. Accordingly, a dual-cycle mechanism was



proposed (Figure 11) [41-42]: two catalytic cycles operate simultaneously over HZSM-5 zeolite under the studied reaction conditions, an aromatics-based cycle which involves ethylene and methylbenzenes, and the olefin-based methylation/cracking cycle which produces  $C_{3+}$  olefins.

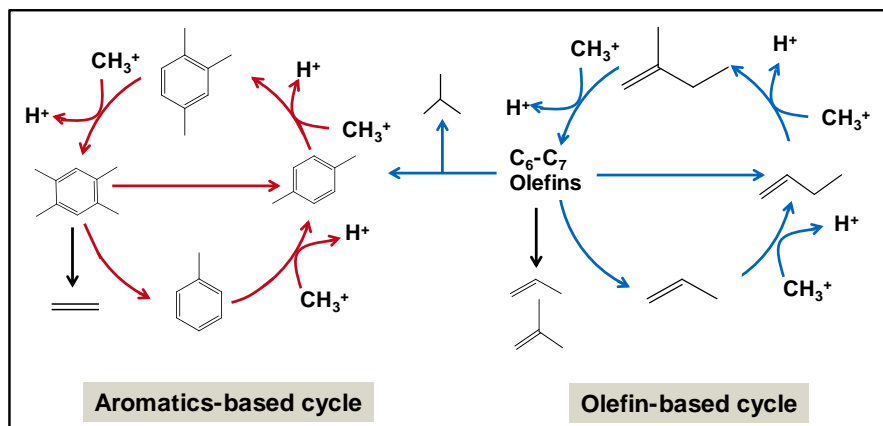


**Figure 11.** The suggested dual-cycle concept for the conversion of methanol over H-ZSM-5 [42].

The emergence of the dual cycle concept, which includes reaction steps of olefin methylation and cracking, aromatics methylation and cracking, and hydrogen transfer as a bridge step, was a seminal contribution in the context of rationalizing the zeolite-specific product distribution through understanding the kinetic consequences of the zeolite topology and the identity of the active hydrocarbon species. The investigation of MTH reaction on ZSM-22 zeolite discovered an extreme case [43]. The unidimensional 10-MR zeolite topology of ZSM-22 (Figure 12, left) determines the olefin based cycle as the prevalent reaction mechanism, and very low selectivity to ethylene and aromatics was observed. However, ZSM-22 appears to be inactive for the olefin cracking step, leading to a product spectrum rich in  $C_{5+}$  branched olefins rather than the more desired propylene [43]. For the other often studied zeolites, such as H-BEA, SAPO-34 or H-ZSM-5, where probably both catalytic cycles work, the relationship has not been fully established yet. For instance, although several reports have shown that aromatics, especially higher polymethylbenzenes, are active hydrocarbon pool species in H-BEA zeolite (Figure 12, right) working at a reaction temperature around 623 K, recent

investigations by Iglesia et al. [44,45] demonstrated that, over H-BEA, the olefin based cycle can be selectively favored over the aromatics based cycle, and the carbenium-ion chemistry dictates the formation of a product pool rich in highly branched C<sub>4</sub> and C<sub>7</sub> aliphatics by using low temperatures (473 K) and moderate DME partial pressures (>50 kPa). Therefore, the reaction conditions, in addition to zeolite topology, play a remarkable role in dictating the reaction pathways and finally the product distribution.

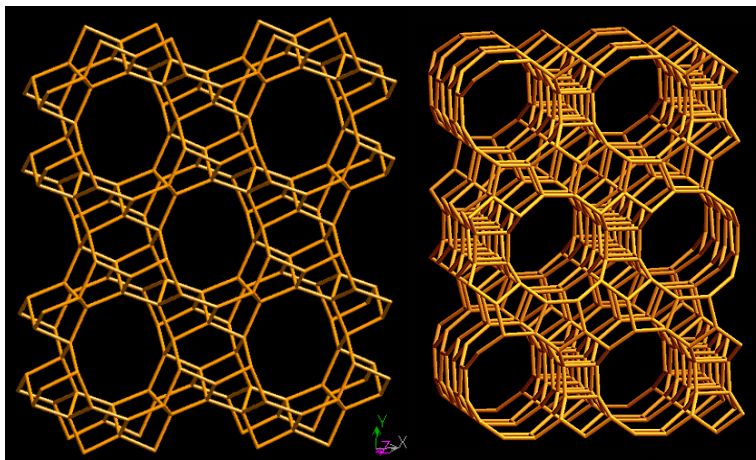


**Figure 12.** Framework topologies of ZSM-22 (TON, left) and beta (BEA, right) zeolites. The images are from the IZA website.

To summarize, the understanding of the MTH mechanism has advanced significantly in recent years. Instead of direct C-C coupling, it is now generally accepted that the conversion of MTH proceeds via indirect reaction pathways, in which aromatics and olefins act as co-catalysts undergoing repeated methylation and cracking reactions [46]. These insights are at best schemed by the current dual-cycle concept. Under this concept, a general rationale on the zeolite-specified product distribution can be established. However, for zeolites where both aromatics and olefin based cycles operates, such as ZSM-5, controversial observations exist. The reason is that, in addition to the zeolite topology, reaction conditions play an important role in dictating the reaction mechanism. As shown in this section, under the conditions employed by Mobil's MTG (the reaction temperature 673 K and methanol partial pressure is several bars), gasoline-range paraffins and aromatics are produced. On the other hand, under

reaction conditions employed by Lurgi's MTP process, light olefins, especially propylene, are the dominant products.

While it is well known that reaction conditions shall play an important role in dictating the actual working reaction mechanism, all the reported MTO mechanistic understandings have been achieved under rather narrow range of reaction conditions, most of which are irrelevant to the practical operations. Therefore, for a specific zeolite, such as the HZSM-5 catalyst which is of particular interest to the industry, spaces and challenges still exist on the elucidation of how reaction conditions influence the nature of active hydrocarbon species in realistic process operations, the kinetic behaviors of these species and the interactions between the aromatic- and olefin- based cycles, which dictate the final product distribution.

## 1.4 Phosphorous induced zeolite modifications

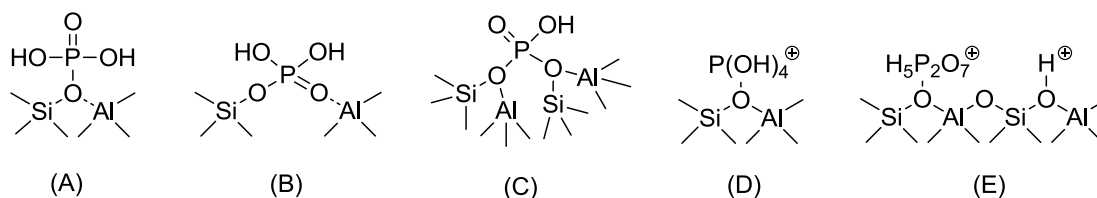
Compared to the MTO process in which fluidized-bed reactors and the zeotype silicoaluminophosphate SAPO-34 catalyst are employed as the key components, Lurgi's MTP processes utilize adiabatic fixed-bed reactors and HZSM-5-based catalysts as the key features [7]. Accordingly, a strong resistance to deactivation for the employed catalyst is needed in the ZSM-5 based processes, to reduce the operation cost in intermittent catalyst regenerations via carbon burn-off by diluted air. On the other side, compared to the reported selectivity to light olefins demonstrated in the MTO technologies, the selectivity to the targeted product, i.e., propylene, needs to be further improved in the current MTP technology [47-53]. Optimization of both the inorganic catalyst and the organic feed compositions will contribute remarkably to meeting these specific demands.

ZSM-5 catalyst, of the MFI topology, is a zeolite, which represents a family of microporous, crystalline, acidic aluminosilicates. In addition to methanol conversion, HZSM-5 is extensively applied as catalysts in a wide variety of other industrial processes. Their catalytic performance relies, to a large extent, on their acidity. In addition to various hydrothermal synthesis strategies, several post-synthetic modification approaches

have been invented as well, among which steam treatment and phosphorous doping are two frequently adopted methods to tune the acidity and consequently their catalytic properties in terms of activity, selectivity and stability [5].

Steam treatment of ZSM-5 zeolite at moderate temperatures is able to induce partial dealumination and healing of the defects in zeolite. The effect of mild steaming on the properties of a high Si/Al MFI zeolite was examined in detail by this group recently [54]. On the other hand, zeolite modification by phosphorous anions doping is also a frequently reported approach [55-72]. Various inorganic and organic phosphorous precursors (trimethylphosphite, orthophosphoric acid, trimethylphosphine, and so forth) were reported to have been successfully used [55-72]. After wet impregnation and subsequent calcination in air at elevated temperatures, the modified zeolites usually showed improved catalytic performance for reactions including toluene alkylation, fluid catalytic cracking, and C<sub>4</sub> olefin cracking in addition to the MTO reaction [55-72]. However, its application to the ZSM-5 zeolites of high Si/Al ratios, which are usually regarded as a key requirement for maximizing the selectivities to olefins and especially propylene, has not been fully discussed.

Since the first report by Butter and Kaeding, intense efforts have been made to understand the interaction of the MFI zeolite framework with the phosphorous species, and the species generated by the modification [55-72]. Several models were proposed, as shown in Scheme 4.



**Scheme 4.** Proposed models on the interaction of phosphorus with the zeolite framework of ZSM-5 prepared by impregnation with orthophosphoric acid and calcination, as proposed by (A) V édrine et al. [59], Kaeding et al. [55,56], (B) Lercher et al. [57,58,60], (C) Xue et al.[66], (D) Corma et al. [67].

Three intriguing impacts of phosphorous introduction were demonstrated, but controversy exists regarding the structure and the attribution. Phosphorous-containing

zeolites show enhanced hydrothermal stability against dealumination under steaming conditions [55-62]. Several authors attributed this effect to the interaction between phosphorus and the zeolite framework, which stabilized the tetrahedrally coordinated framework aluminum [55-60]. Introduction of phosphorous species significantly reduced the Brønsted acidity. Whereas most of the proposed models suggested the through-bonding interaction of phosphorous with bridging hydroxyl groups (Scheme 4), there was a lack of definitive experimental evidence, e.g., Si-O-P bond formation, for such direct interactions. On the other hand, several authors attributed the acidity decrease exclusively to the phosphorous-induced dealumination of tetrahedrally coordinated aluminum in the zeolite lattice with simultaneous formation of amorphous extra-framework aluminum phosphates [60-72], which are basically insoluble in water. Elution of phosphorous by washing impregnated ZSM-5 samples with water prior to calcination, however, could lead to complete restoration of Brønsted acidity as well as its textual properties [64]. The reversibility of dealumination apparently contradicts explanations invoking the formation of insoluble extra-framework aluminum phosphates from dealumination. The underlying mechanism for this reversibility was hardly discussed. In spite of intensive investigations [55-72], fundamental questions concerning the chemical nature of the species formed during various treatments of P-modified ZSM-5 zeolites, as well as the mechanism of their formation, are at best hypothesized without being unequivocally established.

On the one hand, although there are several reports on the impact of phosphorous doping on ZSM-5 catalyst of low Si/Al ratios applied to MTO reaction, the impact of P doping on the high Si/Al ZSM-5 zeolites was scarcely reported. On the other hand, impact of the test conditions on the catalytic performance has drawn little attention so far.

## 1.5 Scope of the thesis

A fundamental understanding of the working MTO mechanism is essential for optimizing the practical process operations. It is now generally accepted that the conversion of MTH proceeds via indirect reaction pathways, in which both aromatics- and olefins-based cycles operate in producing light olefins from methanol. A general rationale on the correlations of zeolite topology and active catalytic cycles and product distribution can be

established for a few particular types of zeolite, such as ZSM-22. However, for some zeolites, such as the archetypical MTO catalyst ZSM-5, where both aromatics and olefin based cycles operates, the relationships are less clearly elucidated. The reason is that, in addition to the zeolite topology, reaction conditions play an important role in dictating the working mechanism.

In this context, we made efforts on the detailed elucidation of the MTO reaction pathways over HZSM-5 zeolites under reaction conditions closely relevant to practical MTO(P) operations. In particular, we investigated how the nature of active hydrocarbon species is affected by process conditions, how kinetic behaviors of these species evolve, and how the interplay between the aromatic- and olefin- based cycles dictates the final product distribution.

In *Chapter 2*, we investigated the impact of co-feeding aromatics and olefins on the MTO reaction over a HZSM-5 catalyst with a Si/Al ratio of 90. Considering that both aromatics and olefins exist in the zeolite pores, the corresponding olefins- and methylbenzenes-mediated routes operate on a competing basis. Taking advantage of the different activities and selectivities of olefin- and aromatics- populated cycles towards ethylene and propylene formation, one could envision the optimization the product distribution through selectively propagating or suppressing one of the two (aromatics- and olefin-based) catalytic cycles. Therefore, we explored the possibility of tuning the MTO product distribution over the HZSM-5 catalyst (Si/Al = 90) by co-feeding various aromatics including benzene, toluene and xylenes, or olefins including ethylene, propylene, 1-butene, 1-pentene, and 1-hexene.

In *Chapter 3*, we discussed the MTO reaction pathways under the studied reaction conditions that are closely relevant to practical MTO(P) operations. Efforts were made on the elucidation of kinetic aspects of the actual working mechanism, i.e., the intrinsic selectivities towards ethylene and propylene formation of the aromatics- or olefins- based cycle, respectively; how the dominant reaction pathway is influenced by feed composition; how it changes during the reaction course, and subsequently the contribution of each cycle on the methanol conversion which finally influences the specific product distribution.

In *Chapter 4*, we investigated and tried to understand the effects of process conditions, especially reaction temperature and methanol partial pressure, on the MTO(P) process over HZSM-5 catalysts. On the other hand, we performed an extensive investigation into the catalytic consequences of the steam treatment and phosphorous modifications in the MTP reaction. Several zeolites with varying Si/Al ratios were employed in the study of phosphorous modification, in which the phosphorous loadings and modification procedures were also varied.

The final chapter concludes the whole body of research and generalizes some insights into the mechanistic aspects in the MTO (P) reaction over HZSM-5 catalysts under reaction conditions close to practical MTO(P) operations.

## 1.6 References

- [1] Wade, L.G. (Sixth Ed., 2006). *Organic Chemistry*. Pearson Prentice Hall. p. 279. ISBN 1-4058-5345-X.
- [2] T. Mokrani, M. Scurrrell, *Catal. Rev. Sci. Eng.* 51 (2009) 1.
- [3] G.A. Olah, *Angew. Chem. Int. Ed.* 44 (2005) 2636.
- [4] Data from the [www.kbr.com](http://www.kbr.com)
- [5] M. Stöcker, *Micropor. Mesopor. Mater.* 29 (1999) 3.
- [6] C. D. Chang, *Catal. Today* 13 (1992) 103.
- [7] U. Olsbye, S. Svelle, M. Bjorgen, P. Beato, T.V.W. Janssens, F. Joensen, S Bordiga, K.P. Lillerud, *Angew. Chem. Int. Ed.* 51 (2012) 5810.
- [8] C. D. Chang, *Catal. Rev. Sci. Eng.* 25 (1983) 1.
- [9] G. Birke, H. Koempel, W. Liebner, H. Bach, 2006, EP2006048184.
- [10] M. Rothaemel, U. Finck, T. Renner, 2006. EP 2006/136433 A1.
- [11] D. Lesthaeghe, V. Van Speybroeck, G. B. Marin, M. Waroquier, *Ind. Eng. Chem. Res.* 46 (2007) 8832.
- [12] J. F. Haw, W. Song, D.M. Marcus, J.B. Nicholas, *Acc. Chem. Res.* 36 (2003) 317.
- [13] N.Y. Chen, W.J. Reagan, *J. Catal.* 59 (1979) 123.
- [14] B.E. Langner, *Appl. Catal.* 2 (1982) 289.
- [15] R.M. Dessau, *J. Catal.* 99 (1986) 111.
- [16] R.M. Dessau, R.B. LaPierre, *J. Catal.* 78 (1982) 136.
- [17] S. Kolboe, I. M. Dahl, *Stud. Surf. Sci. Catal.* 94 (1995) 427.
- [18] D. Lesthaeghe, J. Van der Mynsbrugge, M. Vandichel, M. Waroquier, V. Van Speybroeck, *ChemCatChem* 3 (2011) 208.
- [19] T. Mole, J. Whiteside, D. Seddon, *J. Catal.* 82 (1983) 261.
- [20] T. Mole, G. Bett, D, Seddon, *J. Catal.* 84 (1983) 435.

- [21] I.M. Dahl, S. Kolboe, *Catal. Lett.* 20 (1993) 329.
- [22] I.M. Dahl, S. Kolboe, *J. Catal.* 149 (1994) 458.
- [23] I.M. Dahl, S. Kolboe, *J. Catal.* 161 (1996) 304.
- [24] J.F. Haw, W. Song, D.M. Marcus, J.B. Nicholas, *Acc. Chem. Res.* 36 (2003) 317.
- [25] Ø. Mikkelsen, P. O. Rønning, S. Kolboe, *Microporous Mesoporous Mater.* 40 (2000) 95.
- [26] B. Arstad, S. Kolboe, *Catal. Lett.* 71 (2001) 209.
- [27] B. Arstad, S. Kolboe, *J. Am. Chem. Soc.* 123 (2001) 8137.
- [28] W. Song, J. F. Haw, J. B. Nicholas, C. S. Henghan, *J. Am. Chem. Soc.* 122 (2000) 10726.
- [29] W. Song, H. Fu, J. F. Haw, *J. Am. Chem. Soc.* 123 (2001) 4749.
- [30] W. Song, H. Fu, J. F. Haw, *J. Phys. Chem. B* 105 (2001) 12839.
- [31] H. Fu, W. Song, J. F. Haw, *Catal. Lett.* 76 (2001) 89.
- [32] J. F. Haw, D. M. Marcus, *Catal. Lett.* 34 (2005) 41.
- [33] M. Bjørgen, U. Olsbye, S. Kolboe, *J. Catal.* 215 (2003) 30.
- [34] M. Bjørgen, U. Olsbye, D. Petersen, S. Kolboe, *J. Catal.* 221 (2004) 1.
- [35] A. Sassi, M. A. Wildman, J. F. Haw, *J. Phys. Chem. B* 2002, 106 (2002) 8768.
- [36] R. F. Sullivan, C. J. Egan, G. E. Langlois, R. P. Sieg, *J. Am. Chem. Soc.* 83 (1961) 1156.
- [37] M. Hunger, T. Horvath, *J. Am. Chem. Soc.* 118 (1996) 12302.
- [38] M. Seiler, U. Schenk, M. Hunger, *Catal. Lett.* 60 (1999) 139.
- [39] M. Seiler, W. Wang, M. Hunger, *J. Phys. Chem. B* 105 (2001) 8143.
- [40] L. M. Tau, B. H. Davis, *Energy & Fuels* 7 (1993) 249
- [41] S. Svelle, F. Joensen, J. Nerlov, U. Olsbye, K. P. Lillerud, S. Kolboe, M. Bjørgen, *J. Am. Chem. Soc.* 128 (2006) 14770.
- [42] M. Bjørgen, S. Svelle, F. Joensen, J. Nerlov, S. Kolboe, F. Bonino, L. Palumbo, S. Bordiga, U. Olsbye, *J. Catal.* 248 (2007) 195.
- [43] S. Teketel, S. Svelle, K. P. Lillerud, U. Olsbye, *ChemCatChem* 1 (2009) 78.
- [44] J.H. Ahn, B. Temel, E. Iglesia, *Angew. Chem.* 121 (2009) 3872.
- [45] D.A. Simonetti, J.H. Ahn, E. Iglesia, *J. Catal.* 277 (2011) 173.
- [46] I. M. Hill, Y. S. Ng, A. Bhan, *ACS Catal.* 2 (2012) 1742.
- [47] H. Koempel, W. Liebner, *Stud. Surf. Sci. Catal.* 167 (2007) 261.
- [48] H. Bach, L. Brehm, S. Jensen, 2004, EP 2004/018089 A1.
- [49] G. Birke, H. Koempel, W. Liebner, H. Bach, 2006, EP2006048184.
- [50] M. Rothaemel, U. Finck, T. Renner, 2006. EP 2006/136433 A1.
- [51] B. V. Vora, T. L. Marker, P. T. Barger, H. R. Nielsen, S. Kvisle, T. Fuglerud, *Stud. Surf. Sci. Catal.* 107 (1997) 87.
- [52] *Chem. Eng. News* 2005, 83 (50) 18.
- [53] J. Liang, H. Li, S. Zhao, W. Guo, R. Wang, M. Ying, *Appl. Catal.* 64 (1990) 31.



- [54] L. H. Ong, M. Domok, R. Olindo, A. C. van Veen, J. A. Lercher, *Micropor. Mesopor. Mater.* 164 (2012) 9.
- [55] W. W. Kaeding, C. Chu, L. B. Young, B. Weinstein, S. A. Butter, *J. Catal.* 67 (1981) 159.
- [56] W. W. Kaeding, C. Chu, L. B. Young, S. A. Butter, *J. Catal.* 69 (1981) 392.
- [57] J. A. Lercher, G. Rumpfmayr, *Appl. Catal.* 25 (1986) 215.
- [58] J. A. Lercher, G. Rumpfmayr, H. Noller, *Acta Phys. Chem.* 31 (1985) 71.
- [59] J. C. Vedrine, A. Auroux, P. Dejaifve, V. Ducarme, H. Hoser, S. Zhou, *J. Catal.* 73 (1982) 147.
- [60] H. Vinek, G. Rumpfmayr, J.A. Lercher, *J. Catal.* 115 (1989) 291.
- [61] J. Caro, M. Bülöw, M. Derewinski, J. Haber, M. Hunger, J. Kärger, H. Pfeifer, W. Storek, B. Zibrowius, *J. Catal.* 124 (1990) 367.
- [62] G. Seo, R. Ryoo, *J. Catal.* 124 (1990) 224.
- [63] G. Oehlmann, H.G. Jerschke, G. Lischke, R. Eckelt, B. Parltitz, E. Schreier, B. Zibrowius, E. Loeffler, *Stud. Surf. Sci. Catal.* 65 (1991) 1.
- [64] G. Lischke, R. Eckelt, H.G. Jerschke, B. Parltitz, E. Schreier, W. Storek, B. Zibrowius, G. Oehlmann, *J. Catal.* 132 (1991) 229.
- [65] D. Liu et al. *Catalysis Today* 164 (2011) 154.
- [66] N. Xue, X. Chen, L. Nie, X. Guo, W. Ding, Y. Chen, M. Gu, Z. Xie, *J. Catal.* 248 (2007) 20.
- [67] T. Blasco, A. Corma, J. Martinez-Triguero, *J. Catal.* 237 (2006) 267.
- [68] D. Van VU, Y. Hirota, N. Nishiyama, Y. Egashira, K. Ueyama, *J. Japan Petroleum Inst.* 53 (2010) 232.
- [69] W. Dehertog, G. Froment, *Appl. Catal.*, 71 (1991) 153.
- [70] S. Abubakar, D. Marcus; J. Lee; et al. *Langmuir* 22 (2006) 4846.
- [71] J. Liu, C. Zhang, Z. Shen, M. Hua, Y. Tang, W. Shen, Y. Yue, H. Xu, *Catal. Comm.* 10 (2009) 1506.
- [72] J. Nunan, H. Cronin, J. Cunningham, *J. Catal.* 87 (1984) 77.

# Chapter 2

## Impact of co-feeding aromatics and olefins in the methanol-to-olefins conversion over HZSM-5 catalysts

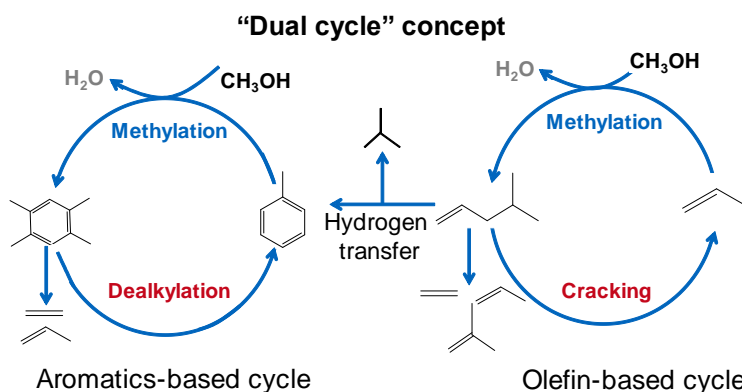
*The impact of co-feeding various aromatics including benzene, toluene and xylenes, or olefins including ethylene, propylene, 1-butene, 1-pentene, and 1-hexene on the conversion of methanol (10 kPa) to olefins was systematically studied over a HZSM-5 catalyst under industrially relevant reaction conditions (723 K). Co-feeding low concentrations of aromatic molecules (16~32 C%), which are free of diffusion constraints, significantly propagates the aromatics based catalytic cycle and greatly suppresses the olefin based cycle, leading to enhanced methane, ethylene formation and aromatics methylation at the expense of propylene and C<sub>4+</sub> higher olefins. The ratio of propylene to ethylene could be adjusted by the concentration of the aromatics co-feeds. Co-feeding the same molar concentration of benzene and toluene influences the methanol conversion in a similar way to that of p-xylene, as they all experience no transport limitation and the lower aromatics get methylated to form the same active carbon species as in the case of p-xylene. In stark contrast, co-feeding small amount (10~40 C%) of C<sub>3-6</sub> olefins with 100 C% methanol does NOT selectively suppress the aromatics based cycle, resulting in unchanged selectivities to ethylene and higher olefins (C<sub>3+</sub>). Within the C<sub>3+</sub> fraction, propylene selectivity decreases and the selectivity to butenes is enhanced with increasing concentration of the co-fed olefin. Due to the relatively high rates in methylation and cracking of C<sub>3-6</sub> olefins in the olefin-based cycle, the same product distributions at high methanol conversion were observed when co-feeding C<sub>3-6</sub> olefins with the same carbon concentrations. This work provides further insights into the two distinct catalytic cycles operating for the methanol conversion HZSM-5 catalysts.*

## 2.1. Introduction

Methanol-to-hydrocarbons processes using microporous zeolites or zeo-type catalysts are regarded as a vital family of conversion technologies to bypass petroleum-based routes for the production of specific fuels and platform petrochemicals [1-3]. Methanol can be readily produced by proven technologies from synthesis gas, which in turn is generated by reforming any gasifiable carbon resource including coal, natural gas, and biomass. On the other hand, special significance of the methanol chemistry originates from its versatility of enabling selective transformations towards various products by proper choice of catalysts and reaction conditions [1-3]. Successfully implemented processes include Methanol-To-Gasoline [4-5], Methanol-To-Propylene (both based on archetypical HZSM-5 catalysts) [6-9], and Methanol-To-Olefins (based on SAPO-34 catalysts, producing both ethylene and propylene) [10-12]. However, the typical single-pass selectivity for any of the processes has remained limited and recycling is necessary. Fundamental insights into the reaction mechanism play a vital role in achieving selectivity control. Ever since the first report by Chang [13], three decades of considerable experimental and computational research efforts have been dedicated to unraveling the complex reaction mechanism. Instead of the direct mechanisms which involve the initial C-C bond formation directly from  $C_1$  entities, the indirect “hydrocarbon pool” mechanism [14-16] is generally accepted for explaining the formation of light ( $C_2$ – $C_4$ ) olefins from methanol during steady-state operation. In the original “hydrocarbon pool” concept, the active center is proposed to be located in the pores or cages of a microporous solid, comprised of an hydrocarbon species (organic part) and a Brønsted acid site (inorganic part) in proximity [14-16]. It is described to act as a virtual scaffold for the assembly of light olefins and avoids unstable and high-energy intermediate species required for the direct C–C coupling mechanisms [14-20]. In a proposed cycle, methanol successively reacts with the hydrocarbon species via methylation, and subsequently elimination of light olefin products such as ethylene and propene regenerates the initial hydrocarbon species, and thus completes the catalytic

cycle [14-20].

Recent experimental and theoretical work demonstrated, that focusing on polymethylbenzenes as the solely active species would cause a biased understanding on the MTO mechanism, and olefins may act as another kind of active “hydrocarbon pool” species in zeolites such as the medium-pore ZSM-5 zeolite with 3-D 10-ring channels, while aromatic intermediates seem to be kinetically relevant for catalysts with large pores or voids [21-22]. This leads to the proposal and establishment of the “dual-cycle” mechanism [21-22], as shown in Scheme 1. Thus, considering that both aromatics and olefins exist in the zeolite pores, the corresponding olefins- and methylbenzenes-mediated routes operate on a competing basis. Taking advantage of the different activities and selectivities of olefin- and aromatics- populated cycles towards ethylene and propylene formation, one could optimize the product distribution through selectively propagating or suppressing one of the two (aromatics- and olefin- based) catalytic cycles.



Scheme 1. Proposed “dual-cycle” mechanism in methanol-to-olefins conversion over HZSM-5 [21-22].

Accordingly, three potential strategies can be conceived for achieving selectivity control. Given that turnover of the aromatics-based cycle demands generally a larger space than the olefin-based cycle does, one approach is to adjust the hosting space by varying zeolite topologies [23-24]. Indeed, very recent experiments on methanol conversion over the one-dimensional 10-MR H-ZSM-22 zeolite without intersections

showed that the sterically restricted topology suppressed selectively the reactions via the aromatics-based cycle and secondary aromatization via hydrogen transfer which would require larger transition states and reaction intermediates [25-28]. Thus, methanol conversion at 673 K proceeded exclusively via the olefin-based cycle, leading to a product mixture rich in C<sub>3+</sub> branched alkenes and very low in ethylene and almost negligible in aromatics [25-28]. The second conceived strategy is to tune the inorganic part, i.e., the Brønsted acidity, through zeolite synthesis or post-synthetic anion or cation modifications, which have been documented in a large body of literature [2]. Another conceived approach for selective propagation of a catalytic cycle is to tune the organic part, the olefin or aromatic species, by enhancing the local competition through co-processing methanol with some specific hydrocarbons.

We intended to explore the latter approach, i.e., varying the nature and concentration of the co-processed hydrocarbons, to adjust the product selectivity under industrially relevant reaction conditions. We note that there have been several reports on co-reacting hydrocarbons with methanol including various olefins and aromatics, but their main intentions were to elucidate the mechanistic considerations via isotopic labeling under conditions irrelevant to industrial MTO(P) operations, and the impacts of co-feeding on product distribution have not been demonstrated in detail [29-38]. Most recently, Ilias and Bhan reported the impact on product distributions by co-processing low concentrations of toluene and/or propylene with dimethylether, but the experiments were mainly performed at a reaction temperature as low as 548 K and a dimethylther pressure of 70 kPa [37]. In the present work, to simulate industrial process conditions, experiments were performed with methanol pressure fixed at 10 kPa over a high siliceous HZSM5 catalyst at 723 K. Low ratios of co-feeds to methanol, relevant to industrial on-site MTP operations, were adopted. Various aromatic co-feeds including benzene, toluene and xylenes, and olefins including ethylene, propylene, 1-butene, 1-pentene, and 1-hexene were evaluated.

## **2.2. Experimental**

### **2.2.1 Catalyst and reagents**

The synthesis method of the HZSM-5 catalyst (Si/Al=90) was reported in the publication by Ong et al. [39]. The as-synthesized material has a crystal size of 500 nm. The zeolite powder was pressed into a wafer, crushed, and sieved to a fraction of particle size in the range of 200–280  $\mu\text{m}$ . Methanol (99.93%), 1-hexene, 1-heptene, benzene, toluene, *para*- and *meta*-xylenes (99.0%) were supplied by Sigma-Aldrich. Gases of C<sub>2-5</sub> olefins (5 or 10% in volume diluted in N<sub>2</sub>) were supplied by Westfalen GmbH.

### 2.2.2 Catalytic testing

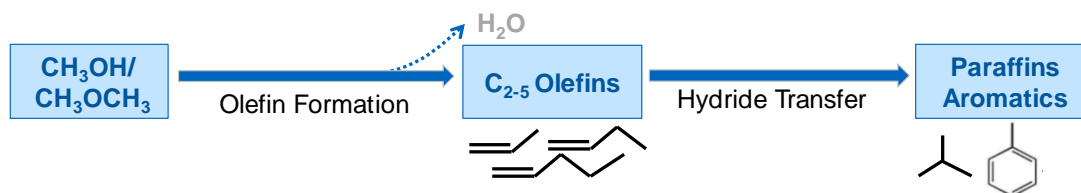
All catalytic tests were performed on a bench-scale plug flow reaction unit. The catalyst pellets were homogeneously diluted with silicon carbide (ESK-SIC, 1:15 wt:wt) with a comparable particle size to ensure temperature uniformity. Catalysts were placed in a quartz tube (26 cm in length, 6.0 mm i.d.) and supported between two quartz wool plugs. The samples were activated at 753 K with the temperature control at the external surface of the quartz tube with 50 ml min<sup>-1</sup> N<sub>2</sub> for 2 h prior to switching to feed. The reaction temperature was held at 723 K, and the total pressure was 108 kPa. The methanol partial pressure was maintained at 10 kPa. The total flow rate was held at 55 ml min<sup>-1</sup>. Methanol vapor was fed by passing dry N<sub>2</sub> flow (29 ml min<sup>-1</sup>) through a methanol-containing saturator which was thermo-stated at 298 K. Flow rates of gaseous olefin co-feeds (C<sub>2-5</sub>) were controlled by mass flow controllers (Bronkhorst). For aromatics, 1-hexene or 1-heptene, the co-fed vapor was introduced by passing dry N<sub>2</sub> flow through a saturator containing the liquid reactant. Catalyst loading (2 to 100 mg) and reactant flow velocity were varied to achieve a wide range of contact time and methanol conversion. Here the contact time is defined as the ratio of catalyst mass to the molar flow rate of methanol. The reactor effluent was kept at 393 K and transferred via a heated line into a gas chromatograph (HP 5890) equipped with a HP PLOT-Q column (30 m  $\times$  0.32 mm  $\times$  0.5  $\mu\text{m}$ ) connected to a flame ionization detector for on-line analysis. Product analysis was performed at steady-state conversions.

Both methanol and dimethylether were treated as reactants. The concentration of a co-feed is given as a molar ratio of its partial pressure to methanol partial pressure (10 kPa).

The product distributions (concentration and yield) were given on a carbon basis, and the carbon in the methanol feed with a partial pressure of 10 kPa was defined as 100%. For instance, a feed of 0.4 kPa toluene and 10 kPa methanol is depicted as co-feeding 4 mol.% toluene. As one toluene molecule has seven carbon atoms, 28% toluene with 100% methanol in carbon, the feed was referred to as containing a total carbon concentration of 128% (28 C% from toluene with 100 C% from methanol) in the feed. In the experiments of methanol conversion with aromatic co-feeds, the final aromatics increment after reaction is defined as the aromatics concentration (in C%) from which the initial concentration of the aromatics co-feed (in C%) is subtracted.

## 2.3. Results and Discussion

### 2.3.1 Reaction path of methanol-to-olefins conversion over HZSM-5 catalysts



**Scheme 2.** A simplified reaction path of methanol conversion over HZSM-5 catalysts.

At 723 K and methanol pressure of 10 kPa, a detailed view on MTO conversion and product yields as a function of contact time over HZSM-5 is depicted in Figure 1(a). Methanol conversion leads to a wide span of products including methane, ethylene, propylene, butenes, C<sub>5</sub> hydrocarbons, C<sub>6+</sub> aliphatics, other light paraffins (C<sub>2-4</sub>), and aromatics. Hereby, the C<sub>5</sub> fraction designates all hydrocarbons with five carbon atoms, and the C<sub>6+</sub> aliphatics encompass other heavier hydrocarbons other than aromatics. Light paraffins include methane, ethane, propane, n-butane and isobutane, while aromatics include benzene, toluene, xylenes, trimethylbenzenes, and tetramethylbenzenes. Hydrogen transfer (HT) products include aromatics and C<sub>2-4</sub> light paraffins. In the absence of any co-feed, the effect of contact time on methanol conversion is characterized by an induction period preceding the on-set of methanol conversion.

During the induction period, methanol is dehydrated to dimethyl ether (DME) till a thermodynamic equilibrium is established. After a certain amount of hydrocarbon species was built up, the methanol conversion started up at a critical contact time ( $0.03 \text{ min mg}_{\text{cat}} \text{ mol}_{\text{MeOH}}^{-1}$ ). The methanol conversion showed a self-acceleration and was complete within a narrow range of contact times. The typical S-shaped curve, characteristic of an autocatalytic phenomenon, indicates that some of the products act as co-catalysts for methanol conversion [46].

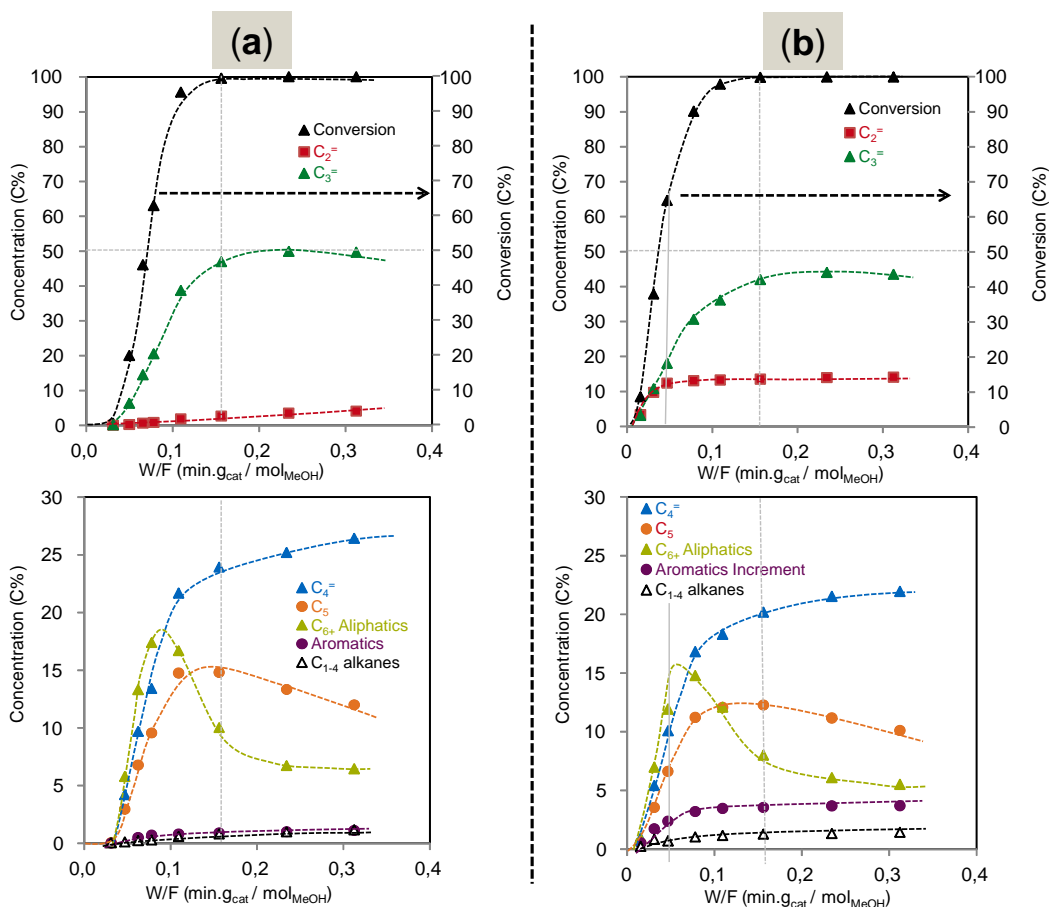


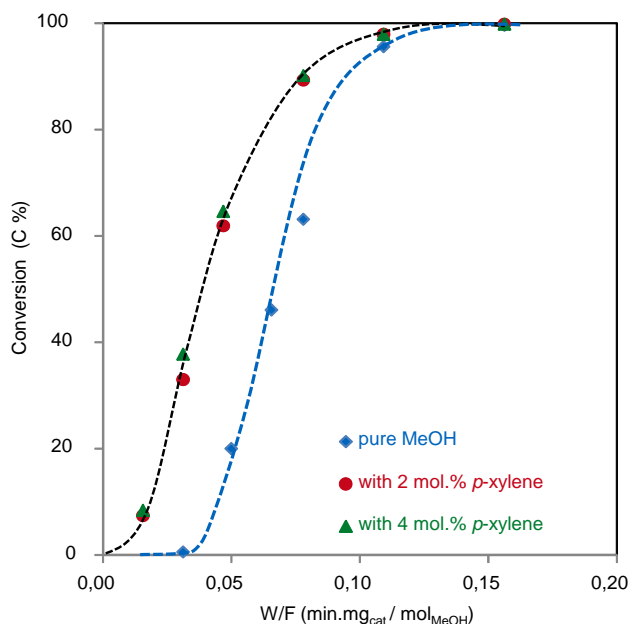
**Figure 1.** Conversion/concentration profiles as a function of contact time for feeds of pure methanol (a) and methanol with 4 mol.% *p*-xylene (b) over HZSM-5 catalyst at 723 K. Product concentrations were calculated on the carbon-number basis through defining the carbon concentration in methanol as 100 C%. Hereby the aromatics increment was calculated by subtracting the product concentration (in C%) by 32 C% (the initial carbon in 4 mol.% *p*-xylene which contained eight carbon atoms).



The concentrations of propylene and C<sub>5</sub> hydrocarbons reached a maximum more or less at the contact time when methanol conversion just attained 100%, followed by declining trends at increased contact times (Figure 1a). Ethylene, light paraffins (C<sub>1-4</sub>) and aromatics were formed with low concentrations (ca. 8 C% in total), which all increased with increased contact time. This is generally in line with the simplified pathway shown on Scheme 2. However, there are two product groups, C<sub>6+</sub> aliphatics and ethylene, which deserve further attention. The concentrations of C<sub>6+</sub> aliphatics peaked when methanol conversion was ca. 80%, then decreased with further increases in methanol conversion and finally leveled off at even longer contact times (Figure 1a). Considering that methanol inhibits olefin adsorption, even in low concentrations (e.g., until only 20% remaining) [38], we attribute the formation of C<sub>6+</sub>, particularly at lower contact times, mainly to the methylation of C<sub>3-5</sub> olefins, instead of their oligomerization. Further conversion of these higher olefins leads to the formation of C<sub>3-5</sub> light olefins instead of aromatics. Thus, this behavior indicates that olefin methylation to higher olefins (mainly C<sub>6</sub><sup>-</sup> and C<sub>7</sub><sup>-</sup>) and cracking of these higher olefins are two critically important steps in the reaction network, and C<sub>6+</sub> olefins act as reaction intermediates [41-42]. Very different from C<sub>3+</sub> olefins, ethylene formation followed a similar trend to that of aromatics with increasing contact time (Figure 1a), suggesting that ethylene formation has a mechanistic relationship with the formation of aromatic molecules [22].

### 2.3.2 Impact of aromatics co-feeding on the methanol conversion

To investigate the influence of specific aromatic co-feeds on the methanol conversion, experiments were performed with various aromatics at 723 K and methanol partial pressure of 10 kPa. The aim was to study whether co-feeding a low concentration of aromatics could selectively propagate the aromatics based cycle and if so, to study the effect of co-feeding aromatics on modulating the product distribution. First, the impact of co-feeding different concentrations (molar ratios of aromatics to methanol being 2 or 4 to 100% methanol) of *p*-xylene was shown, followed by comparison with that of co-feeding *m*-xylene. Then the effect of co-feeding lower (and cheaper) aromatics, toluene and benzene, was examined.

2.3.2.1 Impact of co-feeding *p*- or *m*-xylene

**Figure 2.** Impact of *p*-xylene co-feeding on methanol conversion as a function of contact time. Methanol pressure was 10 kPa and reaction temperature was 723 K. The partial pressure of *p*-xylene was 0, 0.2, 0.4 kPa, leading to a ratio of *p*-xylene to methanol being 0, 2 or 4 to 100 (0, 2 or 4%).

Co-processing of methanol with xylenes was carried out at reaction conditions similar to the experiments in the absence of co-feed. The feed was composed of methanol and *p*-xylene in a molar ratio of 100 to 2 or 100 to 4 (2 or 4 mol.% of *p*-xylene). In contrast to most previous reports [38,43-44], low molar ratios of co-feeds to methanol was used in this study according to multiple considerations: 1) to mimic the realistic on-site conditions of a MTP operation; 2) to avoid methylation of aromatics rather than methanol conversion as the main catalytic reaction; 3) to keep the initial catalyst surface covered mainly by methanol or its derived species instead of the intensive competitive adsorption by the co-fed aromatics. The induction period for methanol conversion was greatly shortened when *p*-xylene (2 mol.%) was co-fed. However, the S-shaped curve still remained. Further increase in *p*-xylene concentration from 2 to 4 mol.% led to insignificant and finite enhancement in the methanol conversion at any contact time (Figure 2). According to autocatalysis kinetics, increased concentrations of co-catalytic

product species would result in progressively higher conversion rates; therefore, *p*-xylene cannot be the main product responsible for autocatalysis under conditions of these experiments.

The effect of contact time on product concentrations, with a mixed feed of methanol and *p*-xylene in a molar ratio of 100 to 4, was shown in Figure 1(b). At methanol conversion of 8.4%, the main products were ethylene and propylene, the selectivity being 39% and 36%, respectively, and the other products were mainly butene isomers (10%) and C<sub>5-7</sub> olefins (4 and 6% each). At higher methanol conversions, propylene concentration greatly increased and surpassed that of ethylene by a factor of ca. 3 at the longest studied contact time. As shown in Figure 1b, while ethylene concentration nearly leveled off at methanol conversion of 70%, propylene concentration continued to increase. Concurrently, butenes and C<sub>5-7</sub> olefins evolved in a manner similar as that observed with pure methanol feed. During the increase of methanol conversion from 70 to 100%, 30% carbon in methanol, together with 10% carbon in C<sub>6-7</sub> aliphatics, was converted to C<sub>3-5</sub> olefins (Figure 1b). This indicates that, under reaction conditions studied, although the aromatics based cycle contributes significantly to methanol conversion and ethylene formation, the olefin based cycle which contributes to the formation of propylene and higher olefins is not completely suppressed by co-feeding *p*-xylene.

The yields of ethylene, aromatics and methane increased, while those of propylene and higher olefins decreased, with increasing concentration of *p*-xylene in the feed (Figure 3). In particular, the yields of ethylene and aromatics increased by ca. 4 times, from 3.5 to 14 C% and from 0.8 to 3.6 C%, respectively, when the feed changed from pure methanol to 4 mol.% *p*-xylene-containing methanol. These observations, along with the high fractions of trimethylbenzenes and tetramethylbenzenes in aromatics (Figure S2), demonstrated that co-feeding *p*-xylene propagates the aromatics based cycle via aromatics methylation and split-off of methane and light olefins (predominantly ethylene and propylene). On the other hand, the olefins based cycle was suppressed when *p*-xylene was co-fed, as shown by the lower yields of propylene and C<sub>4-7</sub> olefins.

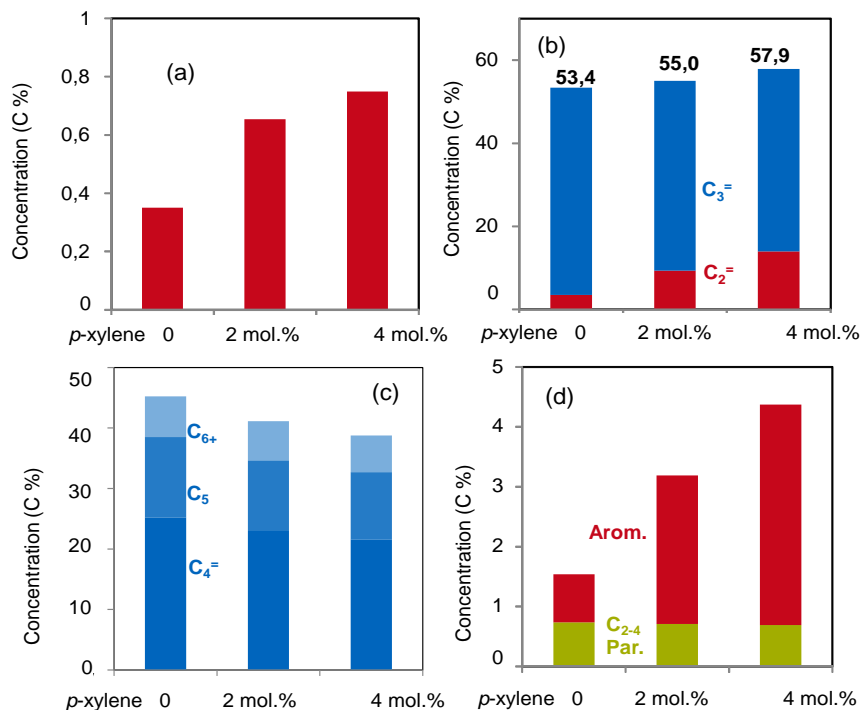


**Figure 3.** Influence of the *p*-xylene addition on the product distribution in terms of methane (a), ethylene and propylene (b), C<sub>4</sub>=, C<sub>5</sub>, and C<sub>6+</sub> aliphatics (c), C<sub>2-4</sub> paraffins and aromatics increment (d) at a contact time of 0.23 min mg<sub>cat</sub> mol<sub>MeOH</sub><sup>-1</sup>. Reaction temperature was 723 K, methanol partial pressure 10 kPa and partial pressures for *p*-xylenes 0, 0.2 or 0.4 kPa.

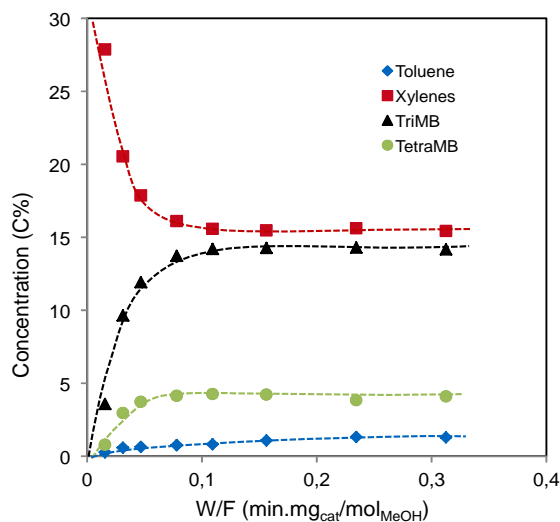


**Figure S2.** Concentrations of various aromatics as a function of contact time. Reaction temperature was 723 K, methanol partial pressure 10 kPa, *p*-xylene partial pressure 0.4 kPa. Concentrations were shown on the carbon basis.

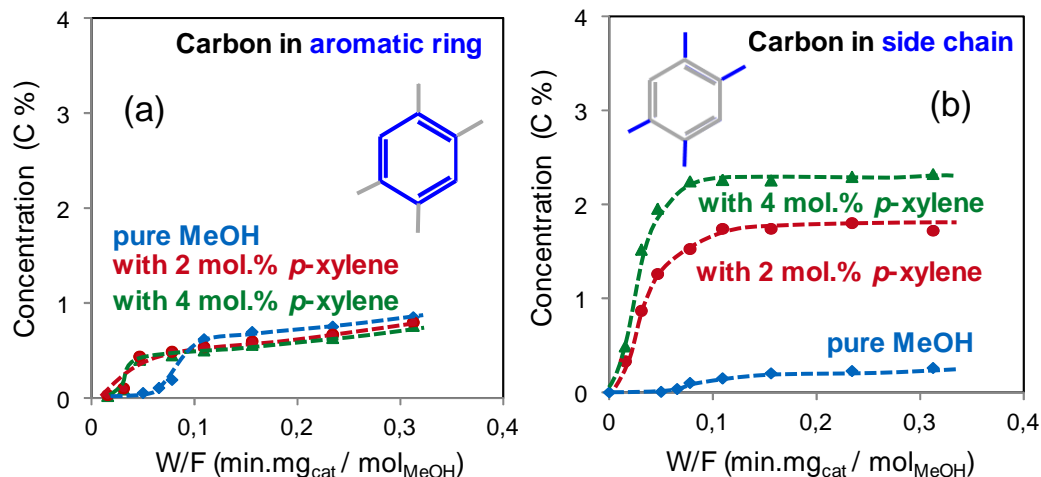
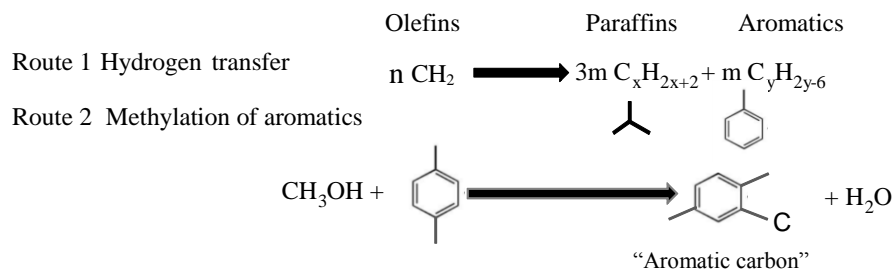


**Figure S3.** Carbon concentrations of aromatics (increments) as a function of contact time, in terms of carbon concentration in the aromatic rings (a) and in the alkyl chains (b) for the feeds of pure methanol or methanol with 2 or 4 mol.% *p*-xylene. Methanol partial pressure was 10 kPa. *p*-xylene partial pressure was 0.4 kPa. Reaction temperature was 723 K.

The total yield of ethylene and propylene slightly increased with increasing *p*-xylene concentration in the feed (Figure 3b). Therefore, by varying the concentration of co-fed *p*-xylene, the ratio of propylene to ethylene can be tuned without loss of selectivity to total light olefins, and both propylene-targeted and light-olefins-targeted production can be realized without changing the reaction temperature and methanol pressure. As depicted in Figure 4a, the yields of C<sub>2-4</sub> paraffins, formed via hydrogen transfer reactions of olefins, were comparable between pure methanol and feeds containing *p*-xylene. In a typical hydrogen transfer reaction, the paraffin and aromatics molecules are produced with a stoichiometric ratio of three to one during hydrogen transfer between olefins (Scheme 3, route 1). As a result, aromatics produced from such routes should have been observed with at most one third of the yield of C<sub>2-4</sub> paraffins. As the actual aromatics increment was significantly higher than C<sub>2-4</sub> paraffin yield when co-feeding *p*-xylene (Figure 4b), the aromatics surplus must come from the incorporation of carbon in methylating C<sub>1</sub> species derived from methanol (Scheme 3, route 2). This interpretation is further supported by the detailed analysis on the carbon distribution in aromatics increment, shown in Figure S3. While the fraction of carbon in the aromatic ring (Figure

S3a) is comparable for the feeds with *p*-xylene co-feeding or of pure methanol, co-feeding *p*-xylene enhances the aromatics methylation, leading to the significantly increased carbon concentration in the side chains.



**Scheme 3.** Two representative routes for aromatics increment

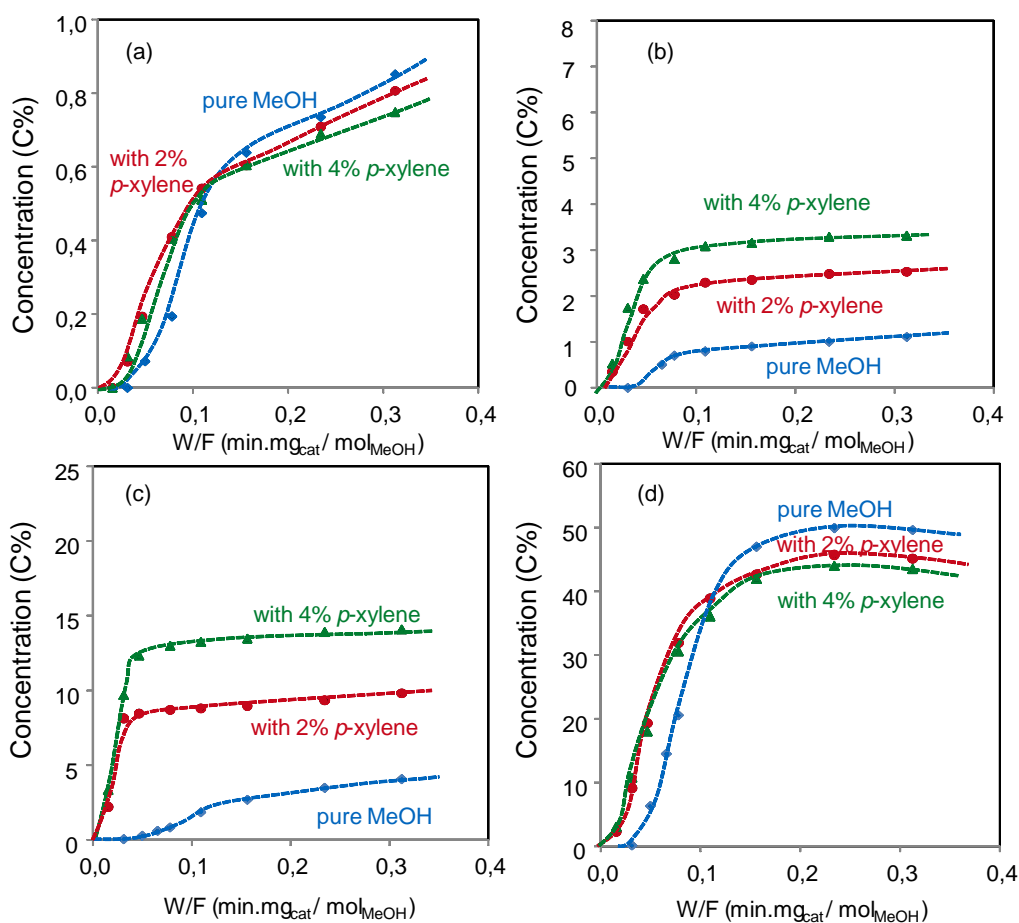


**Figure 4.** Impact of co-feeding different concentrations (2 or 4 mol.%) of *p*-xylene on the yield of C<sub>2.4</sub>

paraffins (a), aromatics increment (b), ethylene (c) and propylene (d). Reaction temperature was 723 K, methanol partial pressure 10 kPa and partial pressures for xylenes 0, 0.2 or 0.4 kPa.

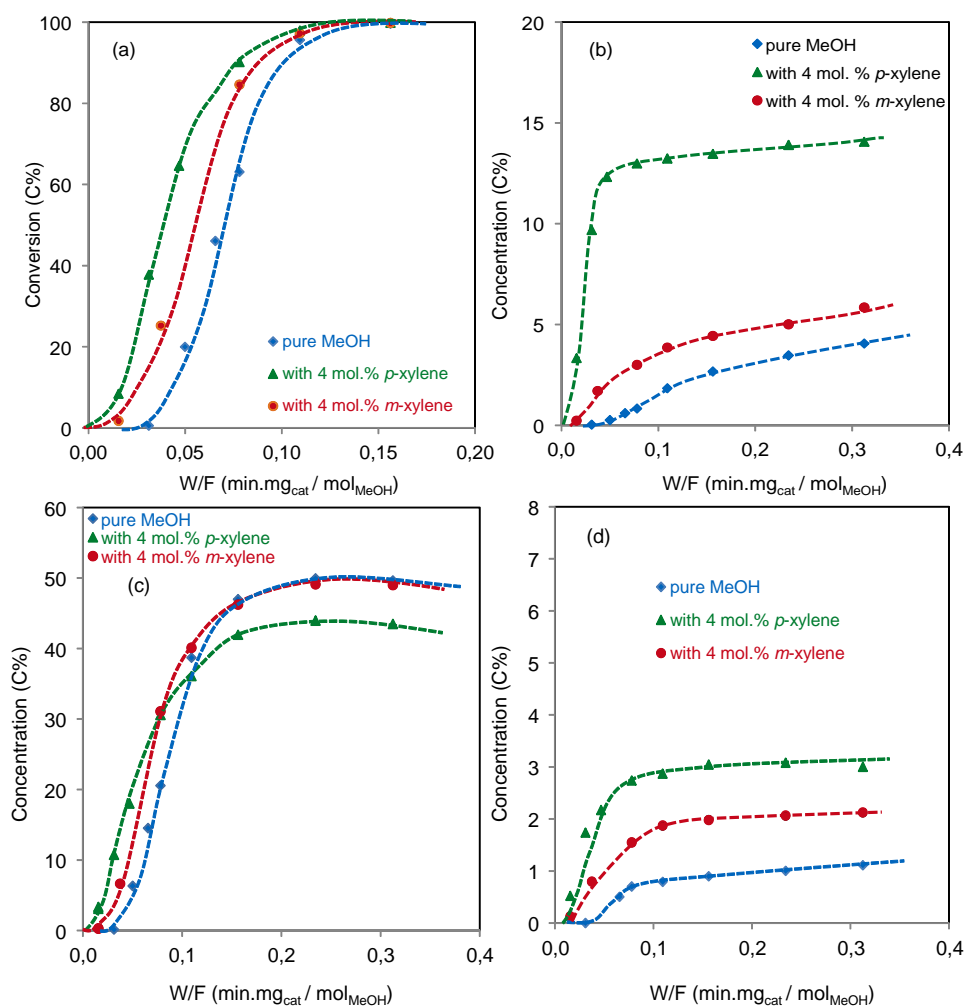


**Figure 5.** Impact of *m*-xylene co-feeding on methanol conversion (a), the yield of ethylene (b), propylene yield (c) and aromatics increment (d). Pure methanol feed and *p*-xylene co-feeding were included as references. Reaction temperature was 723 K, methanol partial pressure 10 kPa and partial pressures for xylenes 0.4 kPa.

When *m*-xylene was used as the co-feed with a xylene-to-methanol molar ratio of 4 to 100, the initiation phase, i.e., the critical contact time after which methanol conversion become detectable, was shortened by about 50% (Figure 5a). Compared to the values observed for pure methanol feed, ethylene yield was promoted from 3.5 to 5.1 C%,

while the propylene yield decreases slightly from 49.9 to 49.0 C% when 4 mol.% *m*-xylene was co-fed (Figure 5c). These effects were much less significant compared to those imposed by co-feeding of *p*-xylene.

The main reason resides in steric constraints. The dimension of the pore size of MFI zeolite is about 0.6 nm, while the molecular size for *p*- and *m*-xylene is 0.58 and 0.68 nm, respectively. The diffusion rate for *m*-xylene to access the Brønsted acid sites which are located in the zeolite channels is lower than that of *p*-xylene. Therefore, the propagating effect of *m*-xylene on the aromatics based cycle is less prominent than that of *p*-xylene. This is also in line with the increment of aromatics concentration (Figure 5d). The aromatics increment (2 C%) in the feed containing *m*-xylene was significantly lower than the increase (3.1 C%) with the feed containing *p*-xylene, indicating that *m*-xylene has difficulty in diffusing into the channel where the Brønsted acid sites are located and being methylated, a pre-requisite for the aromatics based cycle to initiate and turnover.

#### 2.3.2.2 Impact of toluene and benzene co-feeding on methanol conversion

We have demonstrated that the aromatics based cycle operates over HZSM-5 and can be selectively propagated through co-feeding low concentrations of xylenes. Correspondingly, the olefin based cycle can be suppressed. The next question is whether co-feeding aromatics other than xylenes, such as toluene and benzene, could serve the same purpose of tuning product selectivities.

At a molar aromatics-to-methanol ratio of 4 to 100, methanol conversion changed with increasing contact time in a manner independent of the nature of co-fed aromatics, be it toluene, benzene or *p*-xylene (Figure 6). After full methanol conversion was reached, ethylene and propylene yields from a toluene-containing feed were slightly lower than those from a feed containing *p*-xylene. Co-feeding with benzene led to even lower yields to ethylene and propylene, 12.8% and 40.4%, respectively. Compared to the feed containing *p*-xylene, the toluene-containing feed gave rise to significantly larger aromatics increment (6.0% vs. 3.1%), while yielding a comparable amount of C<sub>2-4</sub> light paraffins. Apparently, this resulted from more methylation of toluene than *p*-xylene. In



turn, the aromatics increment when co-feeding benzene was ca. 4% higher than that from toluene, indicating that all the co-fed 4% benzene got methylated. As more methanol was consumed by aromatics methylation on benzene and toluene than *p*-xylene, it accounts for the slightly lower formation of ethylene and propylene than those with *p*-xylene co-feeding. A similar trend was also observed from comparison of the impact of co-feeding 2 mol.% benzene, toluene, and *p*-xylene, as shown in Figure S4. Given that toluene has the same kinetic diameter as *p*-xylene (0.58 nm), it could easily access the acid sites inside the pores and get methylated. For the feeds with toluene or *p*-xylene addition, the essential working aromatics species for the hydrocarbon pool are the same.

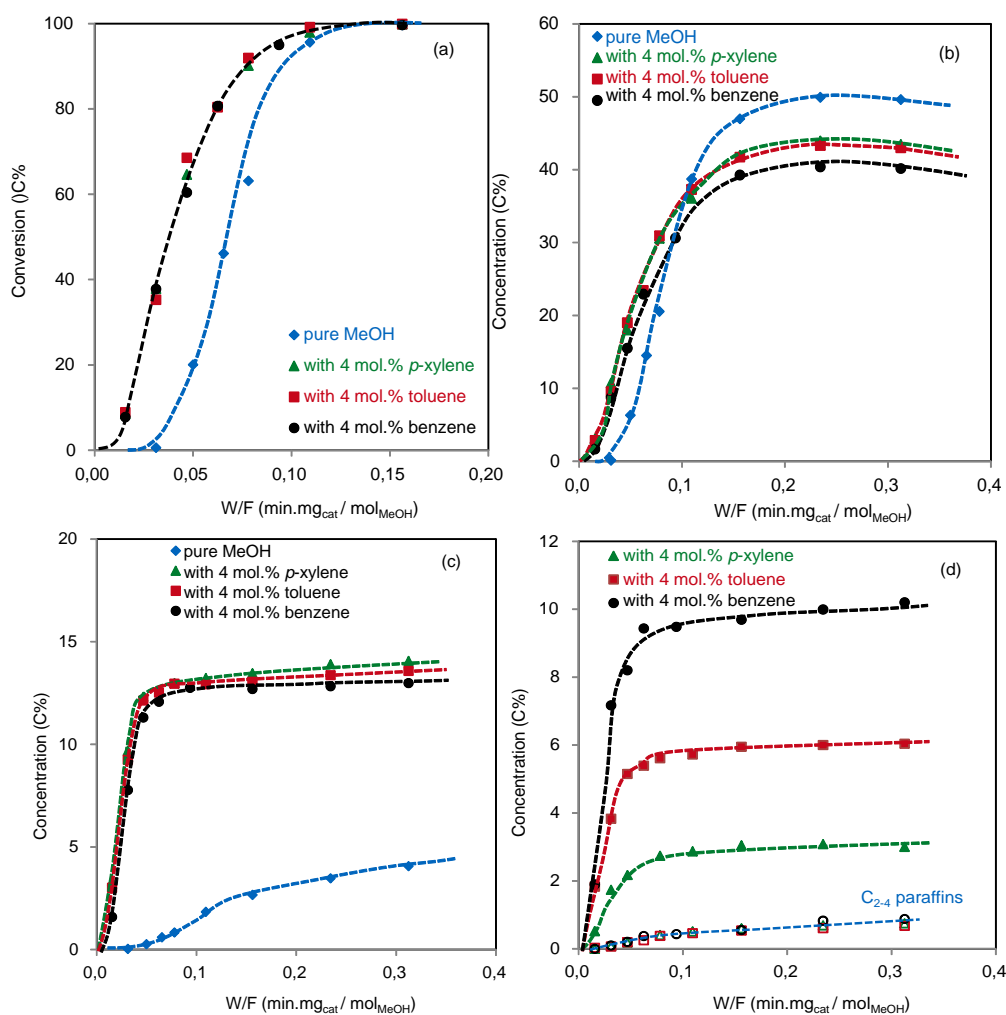


**Figure 6.** Impact of co-feeding 4 mol.% toluene or benzene on methanol conversion (a), propylene yield (b), ethylene yield (c), the yield of C<sub>2-4</sub> paraffins (d, open symbols), and concentration increment of aromatics (d, closed symbols). Pure methanol and 4% *p*-xylene were shown as references.

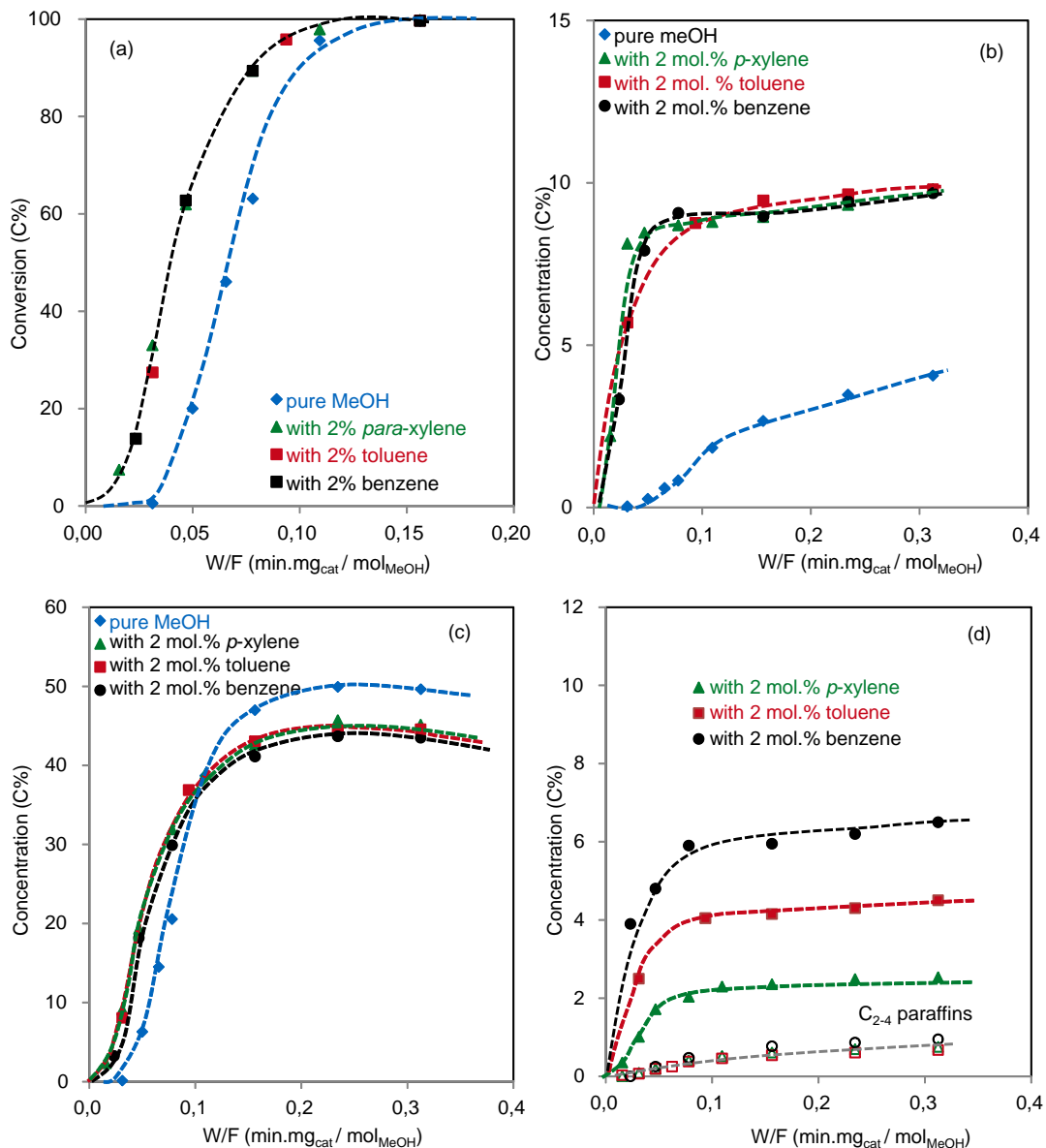


**Figure S4.** Comparison on the impact of co-feeding 2 mol.% *para*-xylene, toluene or benzene on the methanol conversion (a), ethylene (b) and propylene (c) yield, the yield of C<sub>2-4</sub> paraffins (d, open symbols) and concentration increment of aromatics (d, closed symbols). Pure methanol conversion was shown as a reference in (a-c). Reaction temperature was 723 K, methanol partial pressure was 10 kPa, and partial pressures for *p*-xylene, toluene or benzene were 0.2 kPa.

Therefore, considering that the lower methylbenzenes (mainly toluene, xylenes and trimethylbenzenes) are the prevalent aromatics that are on-site produced and available in the MTP process, the selectivity to ethylene and propylene can be modulated by recycling a suitable fraction of aromatics products. As co-feeding of benzene, toluene and xylenes essentially influences the methanol conversion in a unified way, the extent to which the aromatics based cycle is selectively propagated and, consequently, the ethylene yield can be controlled by the molar ratio of aromatics co-feeds to methanol.

### **2.3.3 Impact of co-feeding olefins on methanol conversion**

Analogous to the experiments carried out with various aromatics, the impact of co-feeding a specific olefin on methanol conversion is investigated in this section. Experiments were performed with various olefins at 723 K and methanol partial pressure of 10 kPa. The aim was to study whether co-feeding a certain concentration of olefins could selectively propagate the olefin based cycle and the impact on the product distribution. First, the impact of co-feeding different concentrations of 1-pentene (molar ratios of olefin to methanol being 2, 4, or 8 mol.% to 100%) was shown, followed by comparison with that of co-feeding various olefins including ethylene, propylene, 1-butene, 1-hexene.

#### *2.3.3.1 Impact of 1-pentene co-feeding on the methanol conversion*

Co-feeding olefins is another conceived potential strategy for tuning product selectivities. To mimic the practical operation, 1-pentene was co-fed with methanol in a molar 1-pentene-to-methanol ratio of 2, 4 or 8 to 100 (a C-based ratio of 10, 20 or 40 to 100). Analogous to the case of co-feeding aromatics, co-feeding 1-pentene led to the bypassing of the induction period (Figure 7). In stark contrast to the case of aromatics co-feeding, however, further increase in 1-pentene concentration from 10 to 40 C% in the feed resulted in higher methanol conversions at a certain contact time before 100% methanol conversion. Therefore, it is the olefins, rather than aromatics, that act as the crucial species responsible for the autocatalytic behavior. The S-shaped curve

characteristic of autocatalysis persisted even with 8% co-fed 1-pentene, a different finding from the report by Wu et al. [38]. These authors found that with 1-pentene co-feeding the methanol conversion followed a pseudo first-order kinetics instead of a Sigmoid curve [38]. It is believed that the main difference lies in the different concentrations of pentene co-feed. In Xiao's report [38], a molar ratio of pentene to methanol of 100:100 was adopted, which was significantly higher than the highest ratio employed in this study (molar 1-pentene/methanol ratio of 8:100). Methanol tends to convert via methylation with the pentene co-feed when the molar concentration of olefin is comparable to, or even higher than, the methanol concentration. In this case, a first-order conversion kinetics for methanol was observed, as methylation of 1-pentene holds a higher rate constant than the methylation of any other lower olefins. When only a low concentration of pentene was co-fed with methanol, as in this study, most methanol molecules would undergo autocatalytic MTO reaction, rather than methylation.

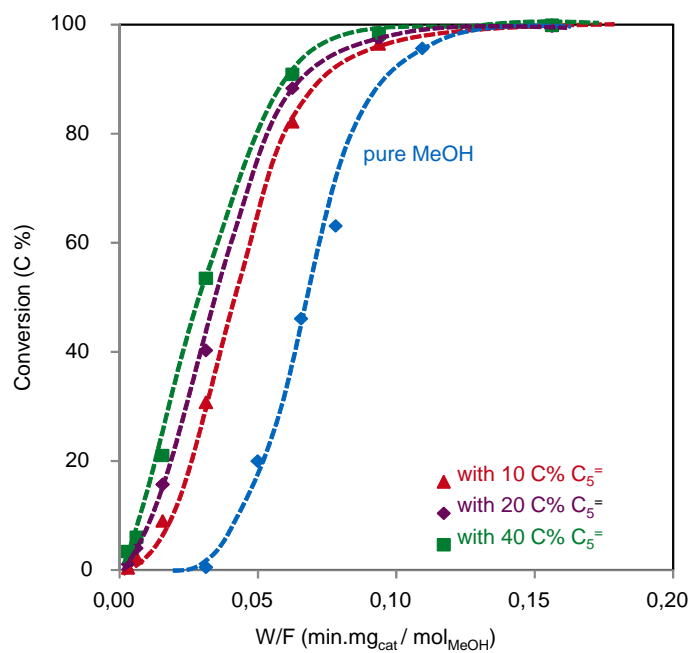


**Figure 7.** Impact of the concentration of co-fed 1-pentene on the methanol conversion. Reaction temperature was 723 K, methanol partial pressure 10 kPa, 1-pentene partial pressure 0.2, 0.4, 0.8 kPa, respectively.

Figure 8 depicts the evolution of product concentrations with increasing contact time for

the feed containing 1-pentene (20 C%). At the shortest contact time, 1-pentene (and likely its isomers) underwent a rapid methylation, evidenced by the rapid increase in the concentration of  $C_{6+}$ . The product distribution at the shortest contact time studied is listed in Table 1. According to these selectivity values at differential conditions, the conversion rate of methanol is estimated to be 2.1 times the rate of pentene disappearance. This might suggest in part that pentenes are not methylated by methanol in a 1:1 ratio, and that multiple methylation events of pentenes to heptenes likely occur. Alternatively, this can be ascribed to the fact that a part of the methanol is not consumed in methylating pentenes; this fraction converts to olefins, as evidenced by the formation of  $C_{2-4}$  olefins at such a short contact time (Table 1).

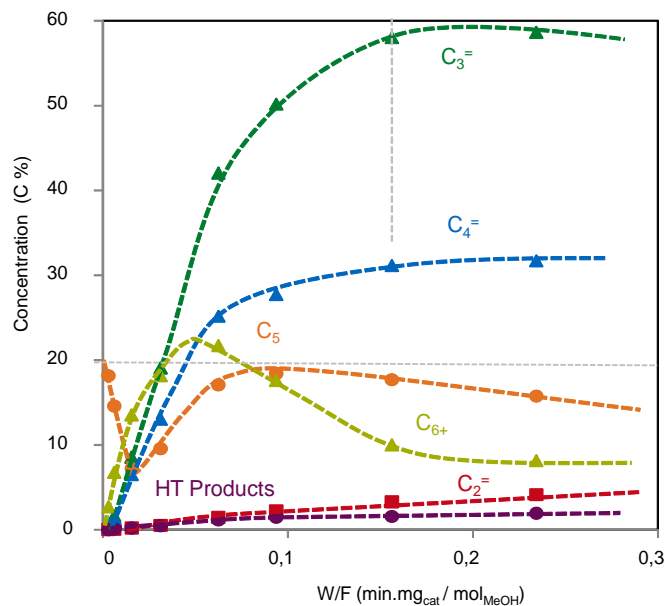


**Figure 8.** Concentration of various hydrocarbons as a function of contact time for the feed of methanol with 20 C% from 1-pentene. Reaction temperature was 723 K, methanol partial pressure 10 kPa, 1-pentene co-feed partial pressure 0.4 kPa. The horizontal dashed line indicated the concentration of initial 20 C% from 1-pentene. The vertical dashed line indicated the contact time at which the 100% conversion of methanol was reached.

After a certain contact time, the pentene concentration started to increase, and the following trend for each group was similar to that observed for conversion of methanol alone (Figure 1a), indicating that co-feeding 1-pentene does not alter the dominant

reaction pathway. At a certain contact time, the yield of a specific product or group, e.g., propylene, from methanol with co-fed pentene was higher than that from pure methanol (Figure 8 compared with Figure 1a). This is because that 1-pentene co-feed is fully converted. In addition to the carbon from converted methanol, all these carbons are distributed and incorporated into each product.

**Table 1.** Conversions and product distributions at low contact times, i.e.,  $<0.01$  ( $\text{min mg}_{\text{cat}} \text{mol}_{\text{MeOH}}^{-1}$ ). Reaction temperature was 723 K, methanol partial pressure 10 kPa, co-feeding 20 C% from propylene, 1-butene, 1-pentene or 1-hexene. The flow rate was kept identical at  $55 \text{ ml min}^{-1}$

Co-feed (20 C%)	Catalyst amount (mg)	Methanol conversion*	Hydrocarbons (C%)							HT products
			C <sub>1</sub>	C <sub>2</sub> <sup>=</sup>	C <sub>3</sub> <sup>=</sup>	C <sub>4</sub> <sup>=</sup>	C <sub>5</sub>	C <sub>6</sub>	C <sub>7+</sub>	
C <sub>3</sub> <sup>=</sup>	2.5	1.9	0.04	0.01	17.4	2.52	0.82	0.63	0.45	
1-C <sub>4</sub> <sup>=</sup>	2.5	4.1	0.06	0.04	1.38	14.4	4.16	2.89	1.09	0.05
1-C <sub>5</sub> <sup>=</sup>	1	1.5	0.04	0.02	0.37	0.32	17.8	2.22	0.43	
1-C <sub>6</sub> <sup>=</sup>	5	13.9	0.09	0.21	8.80	6.69	4.56	8.29	0.93	0.17

\* The lowest conversion for each co-feeding experiment.

Figure 9 shows the comparison of the product distribution for the feeds without or with various amounts of 1-pentene co-feed at the same contact time of  $0.23 \text{ min mg}_{\text{cat}} \text{mol}_{\text{MeOH}}^{-1}$ .

In stark contrast to that observed when co-feeding aromatics, co-feeding 10 to 40 C% 1-pentene significantly reduced the formation of the undesired methane, which was mainly formed via demethylation of polymethylaromatics. In the cases of pure methanol conversion or co-feeding aromatics, the initial phase for the methanol reaction is dominated by the aromatics based cycle which inevitably promotes methane formation. When the methanol is co-fed with pentene, the olefin based cycle dominates the conversion pathway, in which  $\beta$ -scission would necessarily lead to insignificant formation of methane. On the other hand, co-feeding 1-pentene showed little impact on the selectivities to ethylene and C<sub>2-4</sub> paraffins resulting from hydrogen transfer. In marked contrast to the case of co-feeding aromatics, addition of low concentrations of 1-pentene neither suppressed the aromatics based cycle nor promoted significantly the olefin based cycle. The main consequence of co-feeding 1-pentene was altering the

selectivities from propylene to butenes (Figure 9).

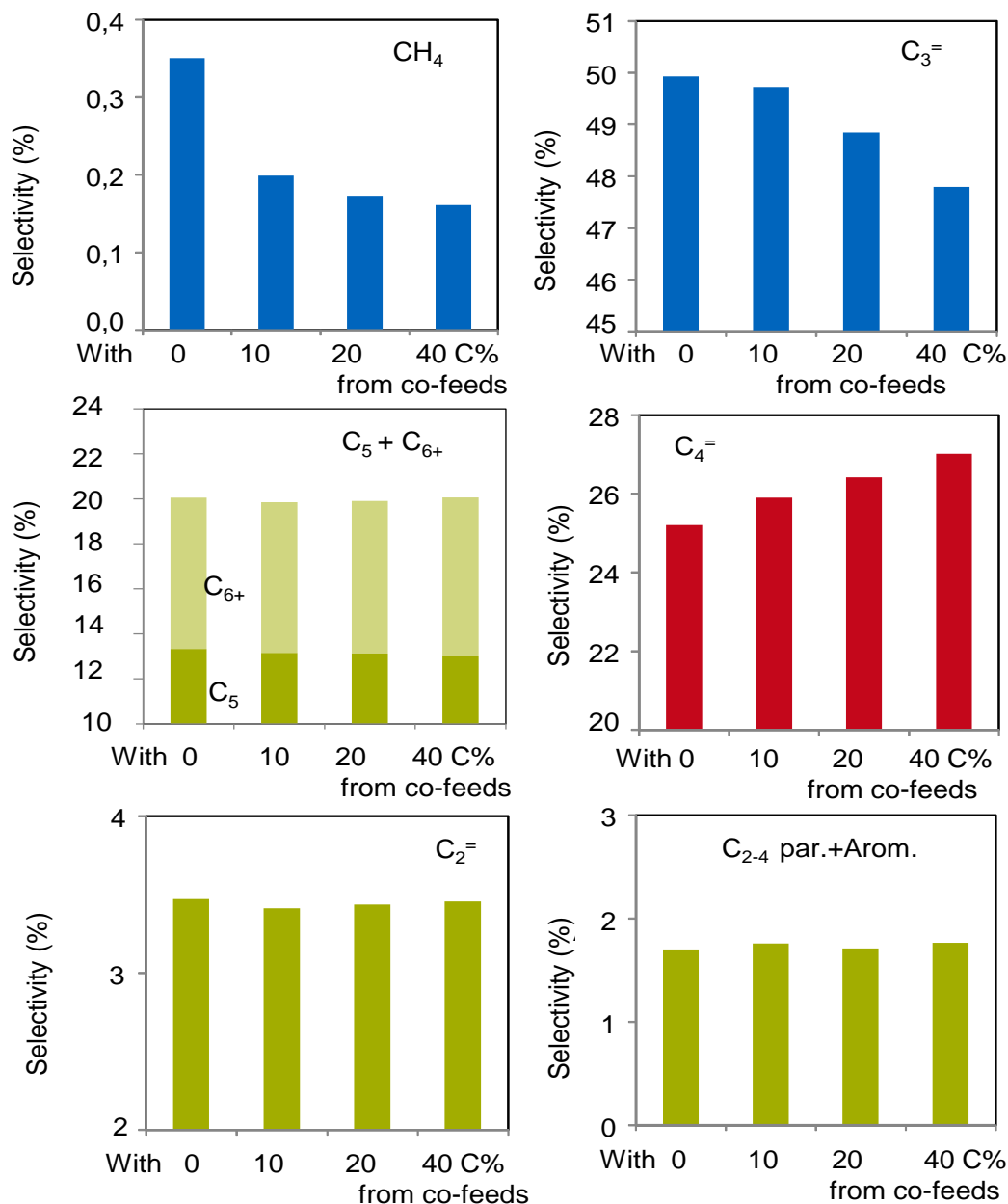


**Figure 9.** Influence of the concentration of co-fed 1-pentene on the total product distribution. Reaction temperature was 723 K, methanol partial pressure 10 kPa, 1-pentene co-feed partial pressure 0.2, 0.4, 0.8 kPa, respectively, contact time  $0.23 \text{ min mg}_{\text{cat}} \text{ mol}_{\text{MeOH}}^{-1}$ .

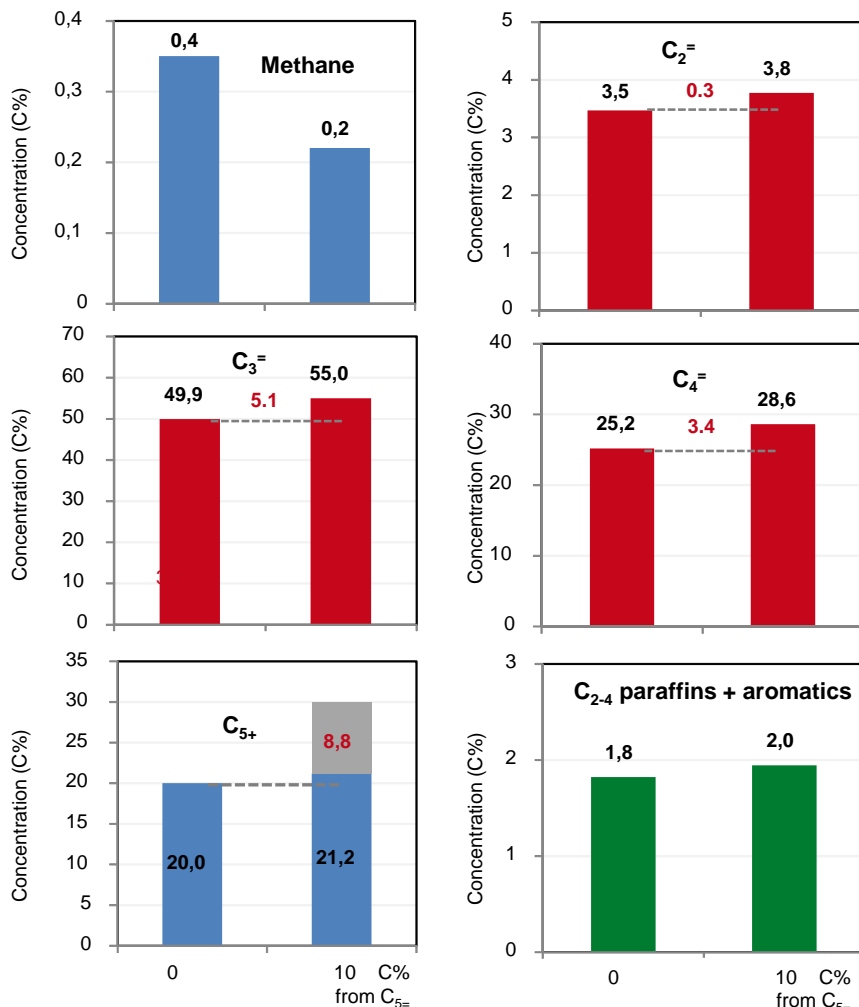


**Figure S5.** Effect of co-feeding 10 C% 1-pentene on product concentration. Reaction temperature was 723 K, methanol partial pressure 10 kPa, 1-pentene co-feed partial pressure 0 or 0.2 kPa, and the contact time  $0.23 \text{ min mg}_{\text{cat}} \text{ mol}_{\text{MeOH}}^{-1}$ .

This impact can also be demonstrated with Figure S5. A direct comparison was performed on production concentrations at a contact time of  $0.23 \text{ min mg}_{\text{cat}} \text{ mol}_{\text{MeOH}}^{-1}$ . Compared to the pure methanol feed, the feed with 10 C% from 1-pentene produced 0.3 C% more ethylene, 5.1 C% propylene and 3.4 C% more butenes (in total 8.8 C% to C<sub>2</sub>-C<sub>4</sub> olefins). On the other hand, the yield of C<sub>5</sub> fraction was 1.2 C% higher for the feed with 1-pentene. Considering that 10 C% was co-fed, the net impact is that 8.8% of the co-fed C<sub>5</sub> was transformed into C<sub>2-4</sub> olefins, while the selectivities to other products from methanol conversion remained almost unchanged.



## 2.3.3.2 Impact of the nature of co-fed olefins on the methanol conversion

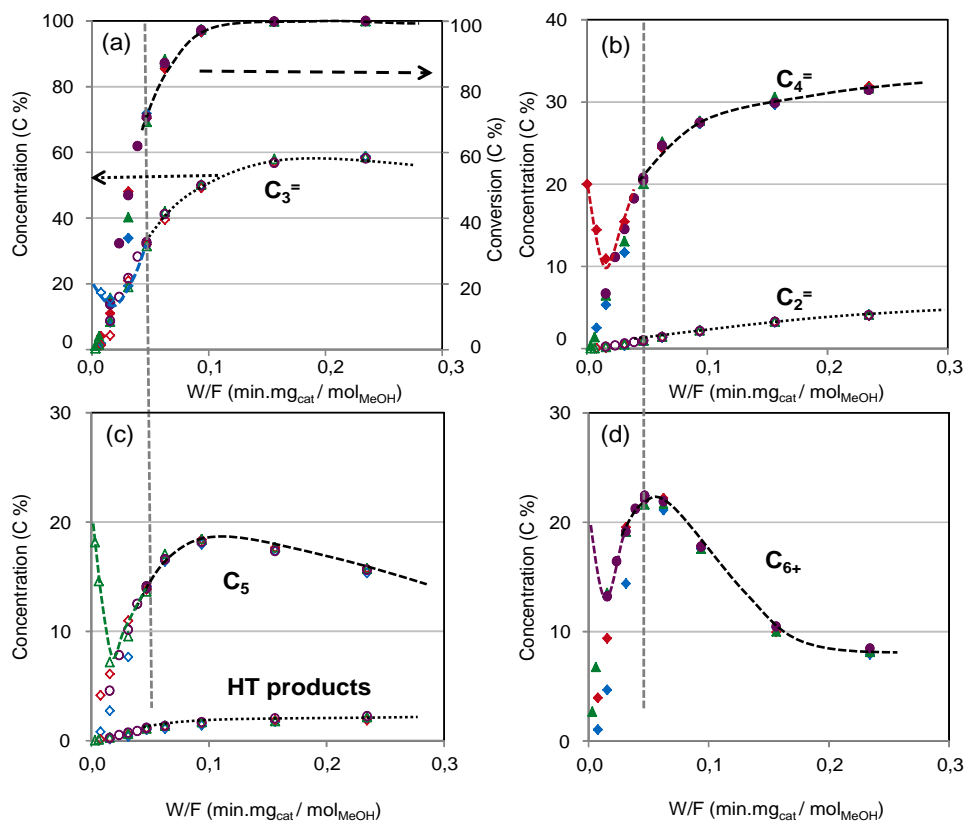


**Figure 10.** Reaction path for the conversion of 100% methanol with 20% carbon from propylene (blue), 1-butene (red), 1-pentene (green), 1-hexene (purple), in terms of conversion and propylene (a), butenes and ethylene (b),  $C_5$  and HT products (c), and  $C_{6+}$  (d). Reaction temperature was 723 K, methanol partial pressure 10 kPa. Partial pressures for propylene, 1-butene, 1-pentene or 1-hexene were 0.67, 0.5, 0.4, 0.33 kPa, respectively, leading to an equivalent 20% co-fed carbon in each feed mixture.

Figure 10 shows the methanol conversion and product yields as a function of contact time for a methanol-olefin mixture, which contained 100% C from methanol and an equal amount of 20% C from one of the  $C_{3-6}$  1-olefins, i.e., propylene, 1-butene, 1-pentene, or 1-hexene. At methanol conversions below 50%, the nature of co-fed olefin showed an impact on methanol conversion and product distribution. As methylation of the co-fed  $C_n$  olefins was the main reaction (Table 1), the  $C_{n+1}$  olefins were the main product except for the case of 1-hexene.

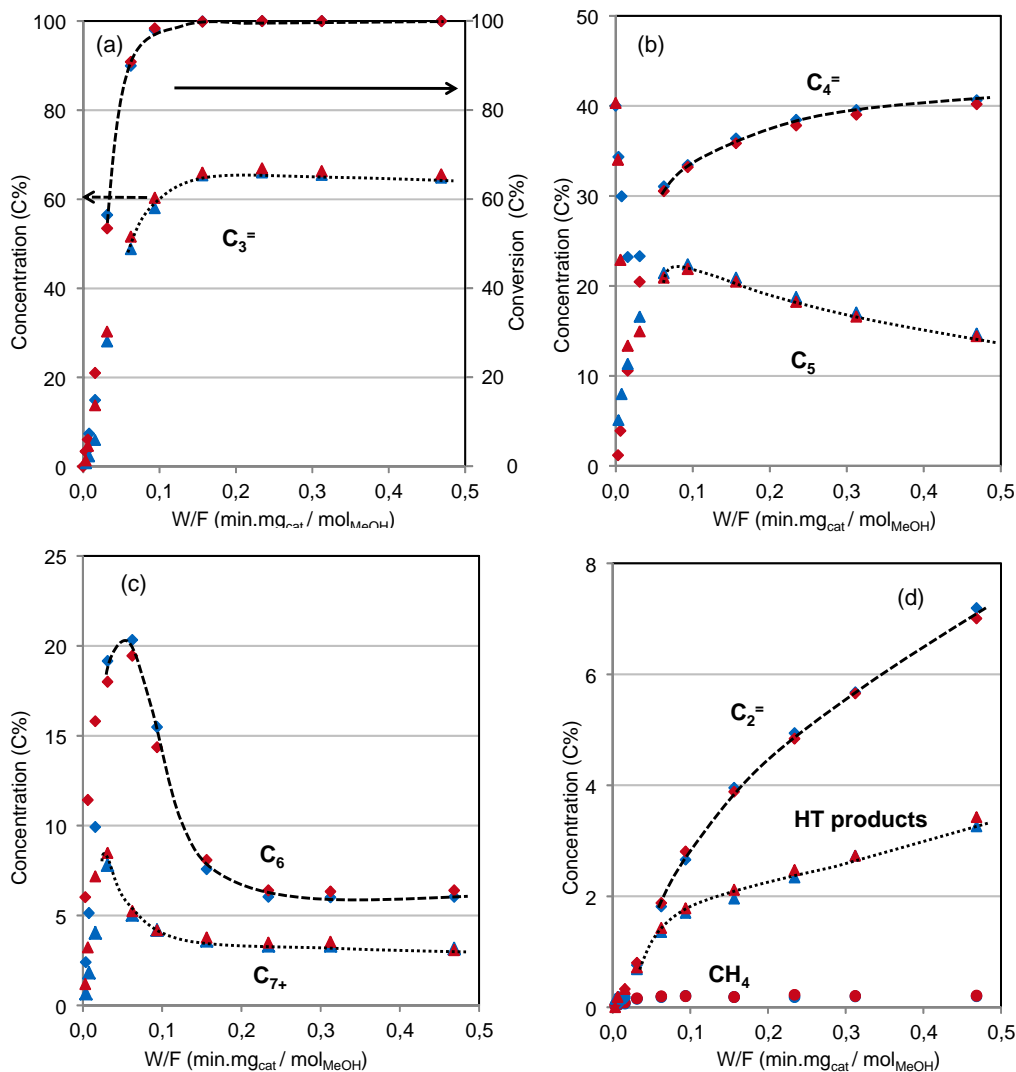


**Figure S6.** Reaction paths for the conversion of 100% methanol with 40% carbon from 1-butene (in blue) or 1-pentene (in red), in terms of methanol conversion and propylene (a), butenes and C<sub>5</sub> (b), C<sub>6</sub> and C<sub>7+</sub> (c), and ethylene and HT products (d). Reaction temperature was 723 K. Methanol partial pressure was 10 kPa, and partial pressures for 1-butene and 1-pentene were 1 and 0.8 kPa, respectively, leading to the equivalent 40 C% in each feed mixture.

At methanol conversion higher than 70%, the product distribution became no longer dependent on the nature of the olefin co-feeds (Figure 10). The methylation rate coefficients for C<sub>3+</sub> olefins increase in order of carbon chain length [45]. Taking the propylene co-feeding as an example, the propylene molecules are methylated to form

butenes, which have higher methylation reactivities than propylene. This results in further methylation of butenes to pentenes, which are in turn more active than butenes and propylene in methylation and thus have a high tendency to be methylated further to hexenes. At the prevalent reaction conditions, hexenes are much more reactive than butenes and pentenes in cracking, so some hexene is desorbed as product, some cracked to propylene, and some further methylated to heptene which either desorbs (minor) as product or undergoes cracking (major) to form propylene and butenes. Cracking of hexenes and heptenes is relatively fast. Therefore, the carbon chain growth terminates at the heptenes. The fast methylation and cracking of  $C_{3+}$  higher olefins results in the fast scrambling of the co-fed carbon, and thus the final product distribution is dictated by the amount of the added carbon, irrespective of the nature of the co-fed olefin. When  $C_{3+}$  olefins were co-fed with 40 C% concentration with respect to methanol (100 C%), which is close to the recycle limit in practical operations, product distribution also remained unchanged at methanol conversions  $> 60\%$  for any  $C_{3-6}$  olefin fraction (Figure S6). Accordingly, there is practically no need to co-feed a specific olefin fraction, except for ethylene (vide infra). As shown in Figures 8, S5 and 10, the yield of propylene could be improved, e.g., from 50 to 60%, by co-feeding  $C_{3-6}$  olefin with methanol, but the total C-based selectivity to propylene was either indifferent or slightly lower by olefin co-feeding (Figure 9).

Compared to the co-feeding of  $C_{3-6}$  olefins, co-feeding ethylene led to a different curve of methanol conversion with increasing contact time (Figure 11). The reactivity of ethylene in methylation is reported to be at least one order of magnitude lower than the  $C_{3+}$  olefins. The low activity of ethylene would lead to a slower conversion of methanol compared to the addition of other higher olefins. It also indicates a slow incorporation and scrambling of the carbon of ethylene into the other higher products.

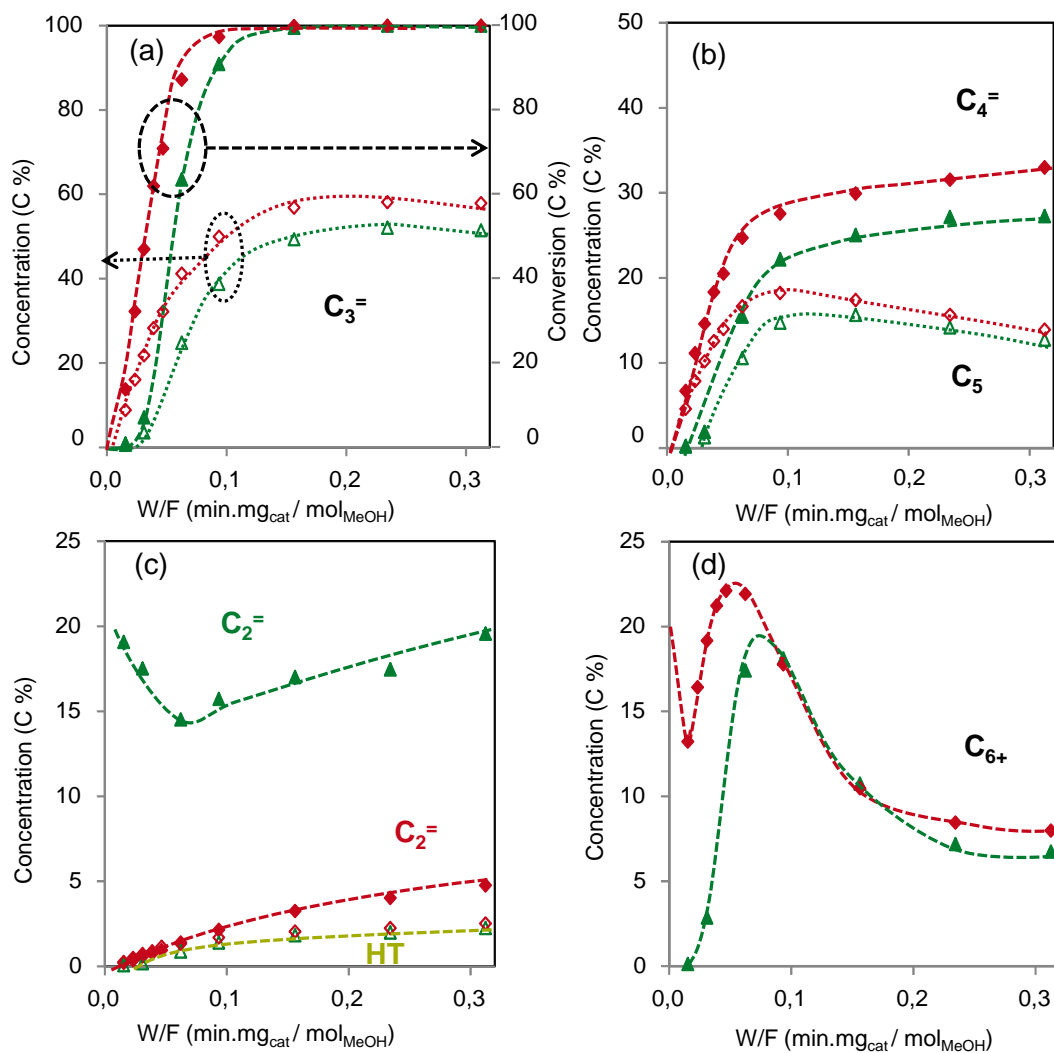


**Figure 11.** Comparison of reaction path for 100% methanol with 20% carbon from ethylene (green) and 1-hexene (red), in terms of methanol conversion and propylene (a), butenes and C<sub>5</sub> (b), ethylene and HT products (c), and C<sub>6+</sub> (d). Reaction temperature was 723 K. Methanol partial pressure was 10 kPa, and partial pressures for ethylene and 1-hexene were 1 and 0.33 kPa, respectively, leading to the equivalent 20 C% in each feed mixture.

That the product distribution independent from the nature of olefin co-feeds is further evidence for the olefin based cycle to be the dominant reaction pathway over HZSM-5 under the studied reaction conditions (at higher conversion of methanol). However, in the meantime, addition of olefins in the feed favors the hydrogen transfer and the formation of aromatics. In turn, the aromatics based route remains active, as shown by

the methanol conversion rates in Section 3.3.1. The overall consequence is, therefore, that co-feeding olefins does not selectively propagate the olefin-based cycle. In other words, the ratio of activities of aromatics and olefins based cycles is not significantly changed by co-feeding small amount of olefins compared to that in the case of a pure methanol feed.

We note, however, that the results of impact of co-feeding olefins demonstrated in Figure 9 is in marked contrast with the recent work by Bhan et al. [37], who claimed that co-processing propylene significantly propagates the olefin-based cycle. In Bhan's case, results were reported at a reaction temperature of as low as 548K and the comparison was made at a DME conversion of around 20% [37]. These conditions are highly different from the realistic industrial MTO(P) operations (reaction temperature higher than 723K and methanol/DME conversion nearly 100%) and the reaction conditions adopted in the present work. Under such lower reaction temperature and low methanol/DME conversion, methylation was much more favored than cracking. This led these authors to observe a remarkable increase in the selectivity of C<sub>4</sub>-C<sub>7</sub> aliphatics when co-processing propylene [37]. However, as showed in the present work, in a complete reaction pathway, these methylated higher olefins would undergo rapid cracking at higher methanol conversion facilitated by the high reaction temperature. This essentially leads to the scrambling and re-distribution of the co-fed carbon, instead of selectively promoting the olefin-based cycle, as shown in Figures 9 and S5. This is further evidence for the olefin based cycle to be the dominant reaction pathway over HZSM-5 under the studied reaction conditions (at higher conversion of methanol).

The present work provides insights into the practical MTO(P) applications, such as Lurgi's MTP process[6-9,38]. In this process, Methanol/DME is introduced to the HZSM-5 catalyst bed loaded in an adiabatic fix-bed reactor [6-9]. After fractionalization of the reactor effluent, the alkene products other propylene, such as C<sub>2</sub><sup>=</sup> and C<sub>4</sub>-C<sub>6</sub> aliphatics, are recycled to the reactor for further conversion to maximize propylene production [6-9,38]. Globally, this process converts about 65% carbon to propylene, balanced by LNG and gasoline (mainly aromatics).

- 1) Utilizing the results derived from the present work, the MTP process operation

has a great potential to be tuned from maximum propylene production into producing both ethylene and propylene to meet the fluctuated market demand. Conceptually this could be achieved through recycling on-site produced aromatic by-product without any change on the reactor configuration and the employed catalyst. Furthermore, the ratio of propylene to ethylene could be adjusted by altering the concentration of recycled aromatic fraction.

- 2) On the other hand, the presented work demonstrated that co-feeding a certain amount of C<sub>4</sub>-C<sub>6</sub> olefins leads to the product distribution independent of the nature of olefinic co-feeds. This indicates that practically there is no need to consider a more fractionalized separation or recycle some specific olefinic fraction. Co-processing the higher olefinic fraction with methanol yield more propylene than the mere methanol conversion, because part of the carbon in co-feeds was scrambled and re-distributed into the propylene fraction through fast olefin methylation and cracking.

## 2.4. Conclusions

Under reaction conditions close to those of the industrial MTP process operation, co-feeding a small concentration of aromatic molecules (16~32 C%), which are free of diffusion constraints, significantly propagates the aromatics based catalytic cycle and greatly suppresses the olefin based cycle, leading to enhanced methane, ethylene formation and aromatics methylation at the expense of propylene and C<sub>4+</sub> higher olefins. The ratio of propylene to ethylene could be easily controlled by modulating the concentration of the aromatics co-feeds. Co-feeding the same molar concentration of benzene and toluene influences the methanol conversion in a similar way to that of *p*-xylene, as they all experience no transport hindrance and these lower aromatics get methylated to form the same active carbon species as in the case of *p*-xylene. In stark contrast, co-feeding small amount (10~40 C%) of C<sub>3-6</sub> olefins with 100 C% methanol does not selectively suppress the aromatics based cycle, resulting in unchanged selectivities to ethylene and higher olefins (C<sub>3+</sub>). Within the C<sub>3+</sub> fraction, propylene

selectivity decreases and the selectivity to butenes is enhanced with increasing concentration of the co-fed olefin. Due to the relatively fast methylation rate of C<sub>3-6</sub> olefins, the same product distribution at 100% methanol conversion and identical impact were observed when co-feeding C<sub>3-6</sub> olefins. This work provides further insights into the two distinct catalytic cycles operating for the methanol conversion to produce ethylene and propylene over HZSM-5 catalysts.

## 2.5 Acknowledgements

The financial support from Clariant Produkte (Deutschland) GmbH and fruitful discussion within the framework of MuniCat is gratefully acknowledged.

## 2.6 References

- [1] C. D. Chang, Catal. Rev. Sci. Eng. 25 (1983) 1.
- [2] M. Stöcker, Micropor. Mesopor. Mater. 29 (1999) 3.
- [3] T. Mokrani, M. Scurrell, Catal. Rev. Sci. Eng. 51 (2009) 1.
- [4] S. Yurchak, Stud. Surf. Sci. Catal. 36 (1988) 251.
- [5] C. D. Chang, Catal. Today 13 (1992) 103.
- [6] H. Koempel, W. Liebner, Stud. Surf. Sci. Catal. 167 (2007) 261.
- [7] H. Bach, L. Brehm, S. Jensen, 2004, EP 2004/018089 A1.
- [8] G. Birke, H. Koempel, W. Liebner, H. Bach, 2006, EP2006048184.
- [9] M. Rothaemel, U. Finck, T. Renner, 2006. EP 2006/136433 A1.
- [10] B. V. Vora, T. L. Marker, P. T. Barger, H. R. Nielsen, S. Kvisle, T. Fuglerud, Stud. Surf. Sci. Catal. 107 (1997) 87.
- [11] Chem. Eng. News 2005, 83 (50) 18.
- [12] J. Liang, H. Li, S. Zhao, W. Guo, R. Wang, M. Ying, Appl. Catal. 64 (1990) 31.
- [13] C. D. Chang, A. J. Silvestri, J. Catal. 47 (1977) 249.
- [14] I. M. Dahl, S. Kolboe, Catal. Lett. 20 (1993) 329.
- [15] I. M. Dahl, S. Kolboe, J. Catal. 149 (1994) 458.
- [16] I. M. Dahl, S. Kolboe, J. Catal. 161 (1996) 304.
- [17] J. F. Haw, W. Song, D. M. Marcus, J. B. Nicholas, Acc. Chem. Res. 36 (2003) 317.
- [18] U. Olsbye, M. Bjørgen, S. Svelle, K. P. Lillerud, S. Kolboe, Catal. Today 106 (2005) 108.
- [19] W. Song, D. M. Marcus, H. Fu, J. O. Ehresmann, J. F. Haw, J. Am. Chem. Soc. 124 (2002) 3844.

- [20] J. F. Haw, J. B. Nicholas, W. Song, F. Deng, Z. Wang, T. Xu, C. S. Heneghan, *J. Am. Chem. Soc.* 122 (2000) 4763.
- [21] S. Svelle, F. Joensen, J. Nerlov, U. Olsbye, K. P. Lillerud, S. Kolboe, M. Bjørgen, *J. Am. Chem. Soc.* 128 (2006) 14770.
- [22] M. Bjørgen, S. Svelle, F. Joensen, J. Nerlov, S. Kolboe, F. Bonino, L. Palumbo, S. Bordiga, U. Olsbye, *J. Catal.* 248 (2007) 195.
- [23] Z.-M. Cui, Q. Liu, S.-W. Bain, Z. Ma, W.-G. Song, *J. Phys. Chem. C* 112 (2008) 2685.
- [24] Z.-M. Cui, Q. Liu, Z. Ma, S.-W. Bain, W.-G. Song, *J. Catal.* 258 (2008) 83.
- [25] S. Teketel, S. Svelle, K. P. Lillerud, U. Olsbye, *ChemCatChem* 1 (2009) 78.
- [26] S. Teketel, U. Olsbye, K. P. Lillerud, P. Beato, S. Svelle, *Microporous Mesoporous Mater.* 136 (2010) 33.
- [27] J. Li, Y. Wei, Y. Qi, P. Tian, B. Li, Y. He, F. Chang, X. Sun, Z. Liu, *Catal. Today* 164 (2011) 288.
- [28] J. Li, Y. Wei, G. Liu, Y. Qi, P. Tian, B. Li, Y. He, Z. Liu, *Catal. Today* 171 (2011) 221.
- [29] T. Mole, G. Bett, D. Seddon, *J. Catal.* 84 (1983) 435.
- [30] B. E. Langner, *Appl. Catal.* 2 (1982) 289.
- [31] M. M. Wu, W. W. Kaeding *J. Catal.* 88 (1984) 478.
- [32] L. M. Tau, A. W. Fort, S. Bao, B. H. Davis, *Fuel Process. Technol.* 26 (1990) 209.
- [33] S. Svelle, P. O. Rønning, S. Kolboe, *J. Catal.* 224 (2004) 115.
- [34] L.-M. Tau, B. H. Davis, *Energy Fuels*, 7 (1993) 249.
- [35] S. Svelle, P.O. Rønning, U. Olsbye, S. Kolboe, *J. Catal.* 234 (2005) 385.
- [36] T. Behrsing, T. Mole, P. Smart, R.J. Western, *J. Catal.* 102 (1986) 151.
- [37] S. Ilias, A. Bhan, *J. Catal.* 290 (2012) 186.
- [38] W. Wu, W. Guo, W. Xiao, M. Luo, *Chem. Eng. Sci.* 66 (2011) 4722.
- [39] L. H. Ong, M. Domok, R. Olindo, A. C. van Veen, J. A. Lercher, *Micropor. Mesopor. Mater.* 164 (2012) 9.
- [40] N. Y. Chen, W.J. Reagan, *J. Catal.* 59 (1979) 123.
- [41] R. M. Dessau, *J. Catal.* 99 (1986) 111.
- [42] R. M. Dessau, R. B. LaPierre, *J. Catal.* 78 (1982) 136.
- [43] S. Svelle, P. O. Rønning, U. Olsbye, S. Kolboe, *J. Catal.* 234 (2005) 385.
- [44] O. Mikkelsen, P. O. Ronning, S. Kolboe, *Micropor. Mesopor. Mater.* 40 (2000) 95.
- [45] S. Ilias, A. Bhan, *ACS Catal.* 3 (2013) 18.



# Chapter 3

## Insights into reaction pathways of methanol-to-olefins conversion over HZSM-5 zeolite

*It was concluded that two distinct catalytic cycles operate for methanol conversion to produce ethylene and propylene over HZSM-5 catalysts under industrially relevant conditions. However, their essential contributions to the final product distribution depend on both their activities and intrinsic selectivity. The aromatics based cycle produces ethylene and propylene with an almost equal carbon based selectivity, while the olefin based methylation/cracking cycle favor  $C_{3+}$  olefins over ethylene. The co-existence of olefins and aromatics species in the zeolite pores leads to the competition between the two cycles. Therefore, their activities depend on the local concentrations of specific carbon species and methanol conversion. Due to the faster autocatalytic feature of the olefin based cycle, olefin homologation/cracking are more active than the aromatics based route and responsible for most of methanol conversion, contributing to  $C_{3+}$  higher olefins formation irrespective of the nature of co-feeds, aromatics or olefins. On the other hand, ethylene comes from both the aromatics based route (intrinsic selectivity contributes) and the olefin based cycle (overall activities contribute). Their contribution depends to a large extent on the reaction conditions. With an aromatics-enriched feed or at a low reaction temperature, the aromatics based cycle contributes more, while the olefin based cycle contributes significantly at a high reaction temperature (such as in the MTO process). In addition to the classical hydride transfer between light olefins, a distinct and kinetically faster hydrogen transfer pathway involving methanol-derived intermediates, other than classic hydride transfer, was proposed.*

### 3.1. Introduction

The catalytic conversion of methanol to olefins (MTO) has been getting particular attention from both industrial and academic sides in recent years, as this process is believed to alleviate the dependence on crude oil for the production of some platform petrochemicals, i.e., ethylene and propylene [1-4]. The control of product selectivity, as one of the key issues in MTO, necessitates an in-depth fundamental understanding on the reaction mechanism. The extremely complex reaction network in the MTO conversion, however, makes it a very challenging task [5-7]. The initial debate was mainly on how the first C–C bond was formed from methanol/dimethylether or C<sub>1</sub> entities derived from it. Over 20 direct coupling mechanisms were suggested in spite of little experimental evidence [2,8-9]. Recent experimental and theoretical investigations concluded that direct C–C coupling fails completely due to unstable intermediates and prohibitively high activation barriers [8-10]. Instead of the direct mechanisms, the indirect mechanisms are getting more acceptances to account for the steady-state formation of light (C<sub>2</sub>–C<sub>4</sub>) olefins.

In 1979, Chen and Reagan originally proposed that MTH is an autocatalytic reaction [11]. Consistent with this proposal, an olefin homologation/cracking route was proposed by Dessau and co-workers as the main reaction pathway at steady-state operation over HZSM-5 catalysts [12-13]. After the initial olefins are formed during the induction period, these olefins are consecutively methylated to form higher olefin homologues, which subsequently crack into lighter olefins such as ethylene and propylene. Hydrogen transfers and cyclization reactions lead to the formation of alkanes and aromatics as end products. In parallel to the proposal of this olefin based cycle, the important role of aromatics and unsaturated cyclic species in methanol reaction was also reported from early on. In 1982, Langner reported that co-feeding 36 ppm of cyclohexanol significantly reduced the duration of the induction period [14]. In a parallel study, experiments of co-feeding toluene or *p*-xylene with methanol led Mole et al. to observe a co-catalytic effect of methylbenzenes on methanol conversion [15-16]. As the conversion of methanol produces aromatics, one could also call the aromatics co-catalysis as another autocatalytic effect in addition to the olefin based autocatalysis. These early investigations were very insightful and embodied already the concept of aromatics based cycle. However, these findings remained largely ignored.

It was the invention of SAPO-34 material in the early 1990s that stimulated again the investigations of the role of aromatics in the MTH reaction and subsequently the proposal of the “hydrocarbon pool” concept by Kolboe et al. [17-19]. In the original proposal, the active center was a “coke-like” organic species adsorbed on the surface [17-19]. The active site for MTO was later defined as a supramolecular inorganic-organic (zeolite-hydrocarbon species) hybrid, which acts as a scaffold for light olefins formation [20-21]. The unique structure of SAPO-34 material provided the possibility of trapping carbon intermediate species and thus stimulated intensive investigations in parallel by groups of Kolboe and Haw, respectively, which established the role of aromatics, especially polymethylbenzenes or their protonated counterparts, as the active hydrocarbon pool species in SAPO-34, H-BEA, and H-MOR catalysts having large pores or cages [20-31]. Recent experimental and theoretical works proposed that olefins may act as another kind of active hydrocarbon pool species, particularly in medium-pore zeolites, such as the ZSM-22 zeolite with 1-D 10-ring channels, in which the internal spaces are too small to activate the bulkiest polymethylbenzenes [32-35].

In retrospect, MTO history clearly demonstrated that the actual course of the mechanistic understanding develops like a spiral cycle, and the key mechanistic aspects that are generally accepted today were reported already in some very early literature [5]. Both the olefin-based cycle and the aromatic-based route are well accepted by researchers favoring either the early “autocatalysis” proposal or the later “hydrocarbon pool” concept [5-6]. However, further insights into the dynamic course of the interactions of zeolite (acid sites), hydrocarbon species, and methanol are yet to be developed, which we try to address in the present work.

Although a general rationale has been achieved on the zeolite-specific product distribution through understanding the kinetic consequences of the zeolite topology and the identity of the active hydrocarbon species, for some often studied materials, such as H-BEA, SAPO-34 or HZSM-5, where probably both catalytic cycles work, the relationship has not been fully established yet [5-6]. For instance, although several reports have shown that aromatics, especially higher polymethylbenzenes, are active hydrocarbon pool species in H-BEA zeolite working at 623 K [30-31], recent investigations by Iglesia et al. [36-37] demonstrated that, over H-BEA, the olefin based cycle can be selectively favored over the aromatics based cycle, and the carbenium-ion chemistry dictates the formation of a product pool rich in

highly branched C<sub>4</sub> and C<sub>7</sub> aliphatics by using low temperatures (473 K) and moderate DME partial pressures (>50 kPa). Therefore, the reaction conditions, in addition to zeolite topology, play a remarkable role in dictating the active hydrocarbon species, and by doing so, tuning the product selectivity.

The same situation applies to HZSM-5 zeolite, the archetypical catalyst for methanol conversion to gasoline—and in recent years light olefins, especially propylene which is of the most interest, has attracted tremendous efforts to elucidate the working mechanism [1-2,5-6]. A renewed study recently led Olsbye et al. to propose a dual-cycle mechanism on HZSM-5: An aromatics-based cycle involved ethylene and methylbenzenes, and the olefin-based methylation/cracking cycle produces C<sub>3+</sub> olefins [38-39]. This is a seminal contribution to the interpretation of HZSM-5 specified product distributions. However, compared to the typically chosen temperatures ( $\leq 623$  K) for these mechanistic studies, significantly higher reaction temperatures ( $\geq 723$  K) are used in the case of HZSM-5 facilitated industrial processes, such as the Lurgi's MTP process, and a recycling operation of the aliphatic products other than propylene is incorporated [40-43]. As a result, the working mechanism entails a detailed study under realistic reaction conditions and specific operation modes.

This constitutes the other aspect to be addressed in the present work. Efforts were made on the elucidation of kinetic aspects of the actual working mechanism under reaction conditions closely relevant to the practical MTO(P) operations, i.e., the intrinsic selectivities towards ethylene and propylene formation of the aromatics- or olefins- based cycle, how the dominant reaction pathway is influenced by feed composition, how it changes during the reaction course, and subsequently the contribution of each cycle on the methanol conversion which finally influences the specific product distribution.

## **3.2. Experimental**

### **Catalyst, reagents, and catalytic testing**

The employed catalyst and other reagents are the same as the materials used in the previous report [44]. The catalytic tests were performed on either a bench-scale plug flow

reaction unit (with nitrogen dilution) or a home-made 10-fold parallel testing unit (with water dilution). The zeolite catalyst is diluted, placed and processed with the identical procedures as in the previous work.

- 1) In the experiment of MTO reaction cycles, a fixed catalyst amount of 20 mg was charged and placed into the reactor. The methanol partial pressure in the flow is kept at 10 kPa by maintaining the temperature of methanol saturator at 299 K. The total flow rate was systematically changed to achieve different space velocities. After the reaction temperature was stabilized under 50 ml/min nitrogen flow at 723 K for 1h, the ball valve is switched, and nitrogen flow passes through the methanol saturator to carry methanol with a partial pressure of 10 kPa. After reaction for 5 minutes, the GC was started to measure the conversion, and subsequently the ball valve for the feed control was switched to the pure nitrogen flow mode and nitrogen flow rate was set to the demanded value. When the GC was standing by, the ball valve was switched to carry methanol again, and GC was started again after 5min methanol introduction, identical to the previous procedures.
- 2) The experiments for the aromatics co-feeding were performed in line with the previous tests. Methanol partial pressure was 10 kPa, and *para*-xylene partial pressure was 0.2 kPa, diluted by nitrogen. The total flow rate was maintained, while the catalyst charge was changed to reach different levels of conversions.
- 3) In the experiments for conversion of pure olefins (120 C%), i.e., 1-pentene, 1-hexene or 1-heptene, experiments were performed under reaction conditions as close as possible to those applied in the MTO reaction of a feed containing 10 kPa methanol (100 C%) and 0.4 kPa 1-pentene (20 C%). 10 kPa water vapor was introduced with the olefin, to mimic the water concentration formed during the MTO reaction (i.e., the outlet partial pressure of water at 100% conversion of 10 kPa methanol). Identical to the experiments of toluene co-feeding, the total flow rate was unchanged, while the catalyst weight was systematically changed to reach different levels of conversions.
- 4) In the experiment of the impact of carbon ratio of methanol to co-feed (butene or pentene), experiments were performed on the home-made 10-fold parallel

reaction unit at 748 K with water dilution. 2-butanol or 2-pentanol was used as co-feed, as they were under fast and complete dehydration on acidic zeolite to butenes and pentenes, respectively. Defining the carbon based concentration in a mixture of methanol and water (weight ratio 1:2) as 100%, different compositions of the same carbon based concentration were used: a) 100 C% from methanol, methanol partial pressure 0.22 kPa, b) 83.3 C% from methanol with 16.7 C% from co-feed (2-butanol or 2-pentanol), c) 62.5 C% from methanol with 37.5 C% from co-feed (2-butanol or 2-pentanol), d) 37.5 C% from methanol with 62.5 C% from co-feed 2-butanol. Essentially these systems with alcohol co-feeds contained identical carbon concentrations.

### 3.3. Results and discussions

#### 3.3.1 Autocatalysis versus hydrocarbon pool proposal

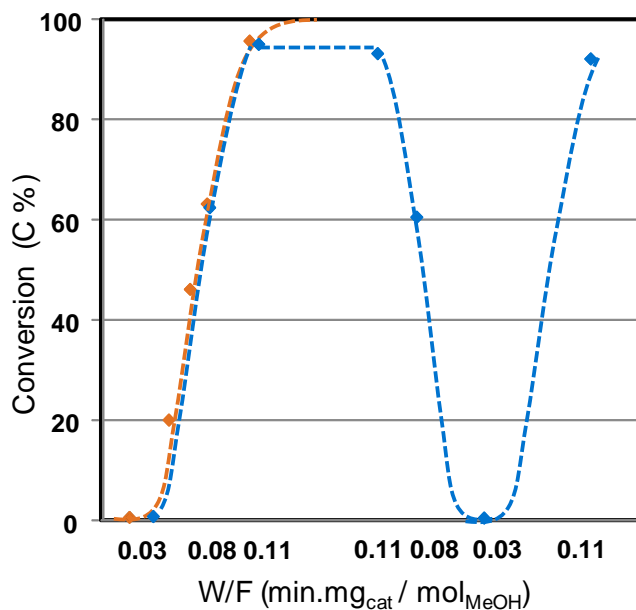
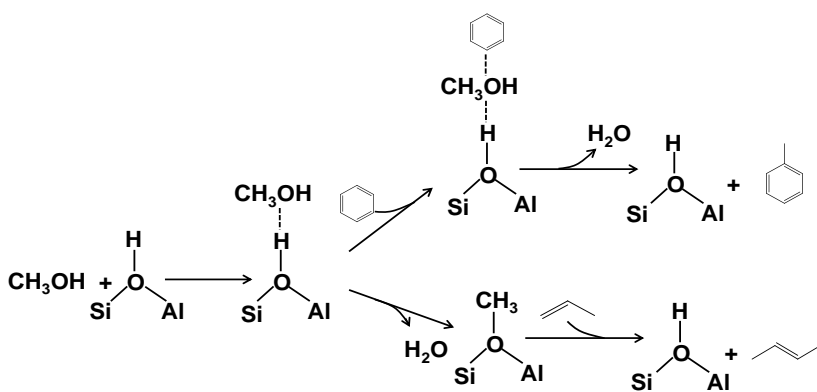


**Figure 1.** Methanol conversion in repeated cycles by varying the flow rates at 723 K and methanol partial pressure of 10 kPa. The orange trace represents methanol conversion as a function of contact time (W/F), in which the methanol conversion at each space velocity was measured with a fresh catalyst loading while the flow rate was kept constant. The blue trace represents the reversible cycle of methanol conversion with a fixed catalyst charge and varied flow rates.

Figure 1 depicts the effect of repeated switches of methanol contact time on the catalytic performance of a fixed catalyst loading. When a methanol conversion of 93% was reached at a contact time of  $0.11 \text{ min mg}_{\text{cat}} \text{ mol}_{\text{MeOH}}^{-1}$ , a subsequent increase of flow rate led to a decrease of contact time to  $0.03 \text{ min mg}_{\text{cat}} \text{ mol}_{\text{MeOH}}^{-1}$ , and the methanol conversion dropped to nearly zero. A further decrease of flow rate brought the contact time back to  $0.11 \text{ min mg}_{\text{cat}} \text{ mol}_{\text{MeOH}}^{-1}$  and restored the methanol conversion to 93%. These repeated switches of flow rate led to the fully reversible conversion cycles as shown in blue (Figure 1) in accordance with the results of the Olsbye et al. [5]. In addition, the results obtained with a fixed catalyst charge and varied flow rates overlapped with those obtained with a fixed flow rate and fresh catalyst of varied amounts.



**Scheme 1.** The generally accepted mechanisms for methylation of olefins or aromatics, in which a gas-phase olefin or aromatic molecule attacks a pre-adsorbed methanol or its derived species.

This complete reversibility is apparently against our understanding on the strictest description of a hydrocarbon pool. According to this concept [17-19], it was believed that a surface carbon pool, which was supposed to be formed on the zeolite surface and act as active centers when a high methanol conversion was reached, should have a longer residence time than the formed products [53]. If this was the case, the following switch of contact time from  $0.08$  to  $0.03 \text{ min mg}_{\text{cat}} \text{ mol}_{\text{MeOH}}^{-1}$  would have generated an appreciable methanol conversion higher than the conversion obtained in the first experiment with a contact time of  $0.03 \text{ min mg}_{\text{cat}} \text{ mol}_{\text{MeOH}}^{-1}$ . However, this is obviously against the

observations here, where the conversion was nearly zero and the activity of a “pre-activated” catalyst was identical to that with a fresh catalyst (Figure 1). The fully reversible conversion cycles may indicate that the carbon species are unstable, decomposing rapidly when the flow rate is increased, and being formed rapidly after switching back to a lower flow rate or a higher bed residence time.

An indirect catalytic MTO cycle starts with consecutive steps of methylation, the kinetics of which has been well reported [45-51]. The well-accepted mechanism for methylation is the Eley-Rideal mechanism, as depicted in Scheme 1, where a gas-phase hydrocarbon molecule (either olefin or aromatics) interacts with a pre-adsorbed methanol or a surface methoxide, and a methylated hydrocarbon is formed and desorbed as gas-phase product [6]. The formed higher hydrocarbon molecules undergo further interaction with another pre-adsorbed methanol or its derivative to undergo further methylation until the higher homologue is formed and ready for cracking on the acid site. The reaction rate of methylation is reported to have a zero order and first order dependence on the partial pressures of methanol and hydrocarbons (olefin or aromatics), respectively [45-51]. This is in line with the general description for the rate of an autocatalytic reaction where the methanol conversion follows a characteristic S-shape as a function of contact time, as shown in

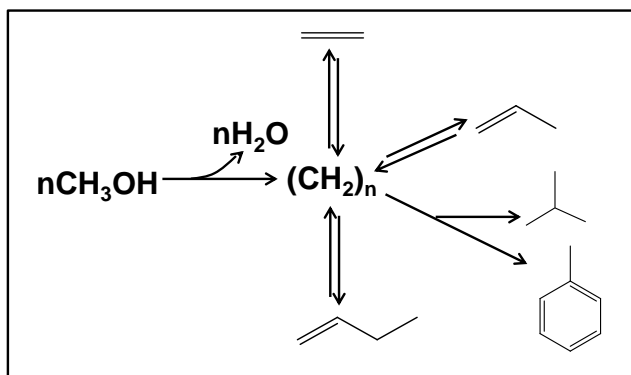
$$r = -k[M]^x[P]^y \quad (1)$$

where the [M] and [P] represent the concentrations of methanol and hydrocarbon products, respectively. Although the calculated reaction orders with respect to methanol deviate from zero and they are usually slightly below one at practical MTO reaction temperatures [54], it is well accepted that methanol adsorbs on the active sites of zeolite more strongly than the light hydrocarbons. Therefore, the MTO mechanism can be envisioned as an analogue of the methylation mechanism depicted in Scheme 1: the zeolite surface is predominantly covered by methanol, and the hydrocarbon species exist in the zeolite pores with a significantly weaker interaction with zeolite than methanol. The Brønsted acid sites activate methanol molecules and are responsible for the final step of cracking of the highest hydrocarbon intermediates, acting as one type of catalytic center. On the other hand, the entrained lower hydrocarbons accommodate the “activated” CH<sub>2</sub>



entities, and the further cracking of the highest homologues produces the light olefins as products. The original lower hydrocarbon is regenerated in the meantime. In this way, the lower hydrocarbon, which is the starting point of a catalytic cycle, could be defined as the other type of catalytic center or co-catalyst.

Therefore, the dynamic course of the interactions of zeolite (acid sites), hydrocarbon species, and methanol, demonstrated by the results obtained in the repeated cycles (Figure 1), are better described by the autocatalysis mechanism as described above, than by the original hydrocarbon pool proposal as shown in Scheme 2. Although both autocatalysis and hydrocarbon pool proposals recognize the critical roles of acid site and lower hydrocarbons (olefins or aromatics), the main distinction lies in the roles that the acid site and the hydrocarbons play. In autocatalysis, the acid site is covered dominantly by methanol and attacked by gas-phase hydrocarbon; while in the strictest understanding of a hydrocarbon pool concept, the acid site adsorbs certain hydrocarbon species, constituting the reaction centers and then a surface pool of “-CH<sub>2</sub>” is formed via contributions by methanol, which split off gas phase light olefins as products.



**Scheme 2.** The originally proposed hydrocarbon pool mechanism by Dahl and Kolboe [17-19].

Based on the above analysis of the description of the interactions between zeolite, hydrocarbons and methanol, we are now in a position to unify the autocatalysis and the hydrocarbon pool concepts. A generalized hydrocarbon pool mechanism should define the entrained hydrocarbons in the zeolite pores, other than the surface carbon species, as the working hydrocarbon pool species. Following this definition, when the generalized

hydrocarbon pool species are free of diffusion constraints, such as in the case of HZSM-5 zeolite, they act also as entrained co-catalysts in the autocatalysis concept. Thus, a generalized hydrocarbon pool mechanism is essentially in full accordance with the autocatalysis concept.

### 3.3.2 Insights from aromatics and olefin co-feeding

Based on the analysis in the previous section of working MTO mechanism over HZSM-5 zeolite, methanol conversion proceeds via consecutive methylation reactions, in which the hydrocarbon species interact with the pre-adsorbed methanol. Therefore, competitive methylation of entrained aromatics and olefins in the zeolite pores will influence the locally prevalent hydrocarbon pool species which finally propagate each cycle. In turn, their gas phase concentrations play a remarkable role. Along with this understanding, a series of experiments with co-feeding various benzenes and olefins were performed, as demonstrated in the previous report [44]. Derived from these experiments, further insights into the MTO reaction pathways are discussed in this section.

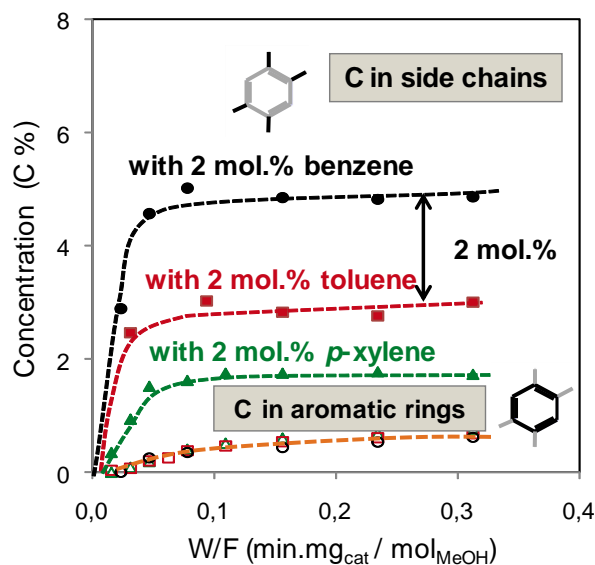


**Figure 2.** The carbon distribution in the aromatics increment by co-feeding benzene, toluene, *para*-xylene, in terms of carbon in the aromatic ring and carbon in the side chain. Methanol partial pressure was 10 kPa, aromatic co-feed partial pressure 0.2 kPa, reaction temperature 723 K.

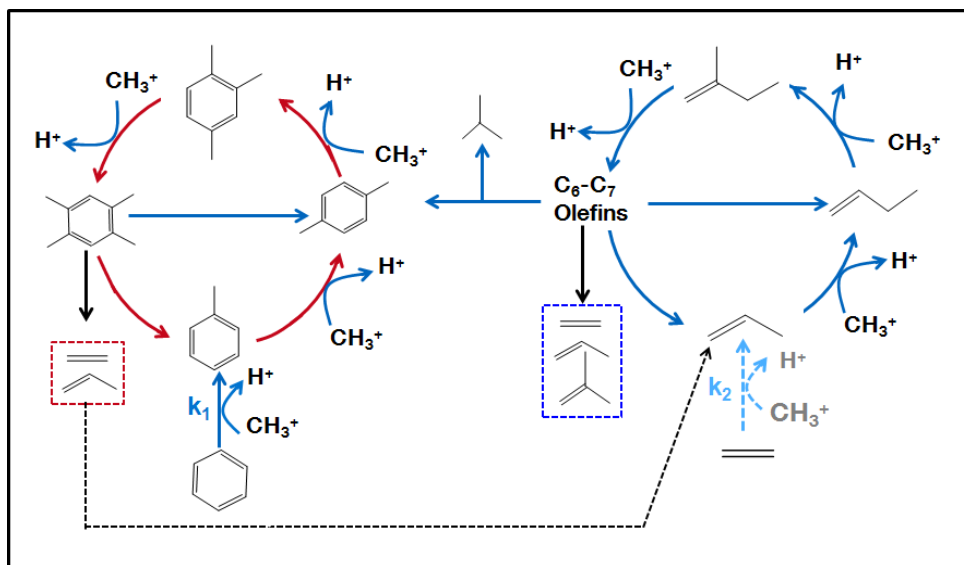


**Figure 3.** A modified dual-cycle mechanism in operation during methanol-to-hydrocarbons catalysis over HZSM-5 under industrially relevant MTO conditions.

An increase in the abundance of aromatics in the feed leads to the selective propagation of the aromatics based cycle, especially at low methanol conversions. Therefore, compared to the conversion of the feed of pure methanol, propagation of the aromatics based cycle shifts the product distribution towards ethylene and methylated aromatics. As *meta*-xylene has a larger kinetic diameter than the HZSM-5 zeolite pore, it can not effectively diffuse into the channel to propagate the aromatics based cycle, which led to the significantly less impact than the co-feeding of *para*-xylene.

Further insights into the aromatics based cycle can be deduced from the experiments by co-feeding of toluene and benzene. As shown in the previous work [44], co-feeding toluene of the same molar concentration as that of *para*-xylene leads to an identical impact on propagation of the aromatics based route. In other words, as shown in Figure 3, the toluene and *para*-xylene are both involved in one cycle as active intermediates and they play an identical role. This is due to the comparable diffusion coefficients and methylation rates for toluene as for *para*-xylene. On the other hand, co-feeding benzene also leads to an identical degree of propagation of the aromatics based cycle, but it results in stoichiometrically more methylation of aromatics than that of toluene. As shown in

Figure 2, co-feeding 2 mol.% benzene led to 2 % more side chain methylation than the case of toluene co-feeding.. This suggests that benzene is outside the aromatics based cycle; however the comparable rate co-efficient for benzene methylation makes it fast transformed to toluene which is actively involved in the cycle, as shown in Figure 3.

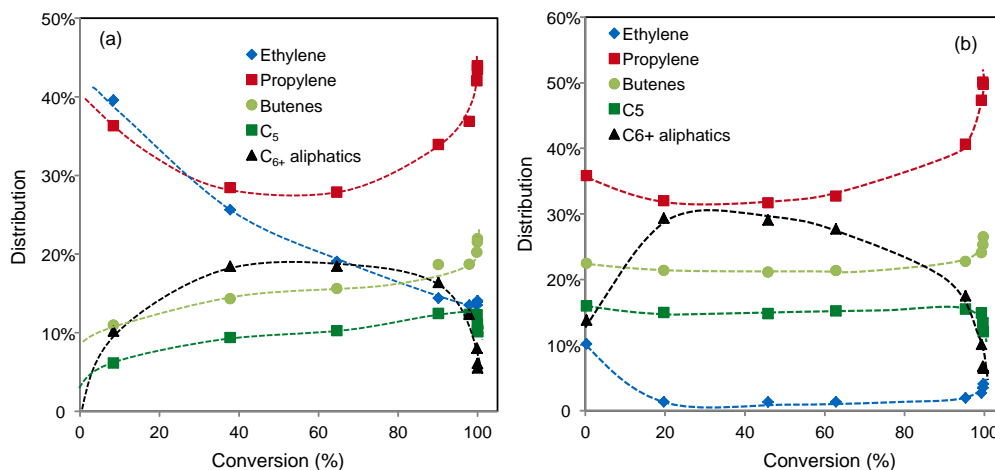


**Figure 4.** Carbon-based C<sub>2+</sub> aliphatic product distributions as a function of methanol/dimethylether conversion. Reaction temperature was 723K, methanol partial pressure 10 kPa, *para*-xylene co-feed partial pressure (a) 0.4 or (b) 0 kPa.

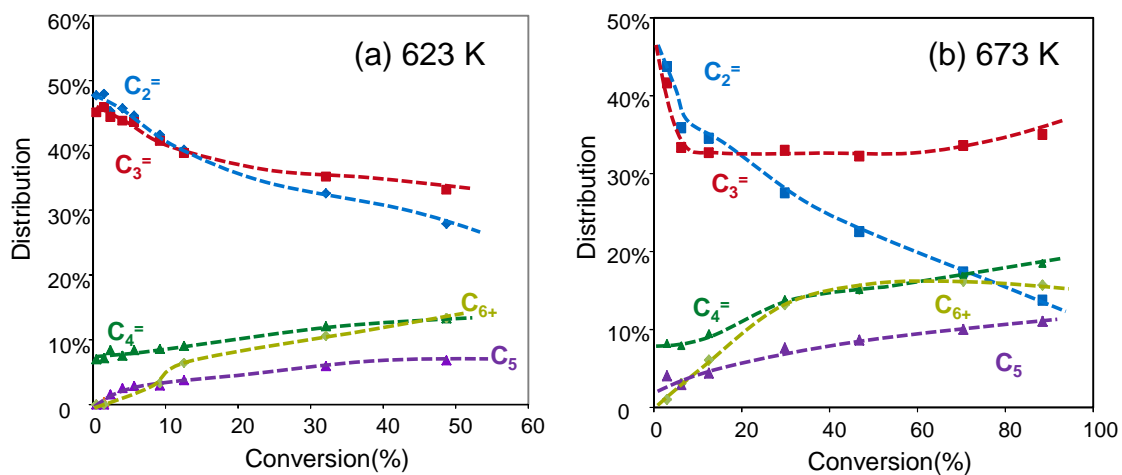


**Figure 5.** Aliphatic products distributions versus of methanol conversion with a feed of mixed methanol and toluene at reaction temperatures of 623 (a) and 673 K (b). Methanol partial pressure was 10 kPa, *p*-xylene co-feed partial pressure 0.4 kPa.

Figure 4 (a) depicts the carbon-based product selectivities as a function of methanol/dimethylether conversion for a feed of methanol and 4 mol.% *para*-xylene. At the lowest methanol conversion in this study, a carbon-based ethylene selectivity of 39% and a propylene selectivity of 36% were observed. Considering that ethylene is very unreactive in further secondary reactions such as methylation or dimerization, and a small portion of propylene is possibly methylated to higher olefins even at this low conversion, it is concluded that the aromatics based cycle, which has proven to be responsible for a dominant fraction of methanol conversion at low conversions, produces simultaneously ethylene and propylene with almost equal carbon-based selectivities. This is further supported by the aromatics co-feeding experiments at relatively lower reaction temperatures. Figure 5 (a) and (b) depict the aliphatic products distribution as a function of methanol conversion at reaction temperature of 623 and 673 K, respectively, for a feed containing 2 mol.% *para*-xylene. It is clearly demonstrated that the extrapolated carbon based selectivities to ethylene and propylene are nearly equal at zero methanol conversion. This observation is in line with those by Bjørgen et al. in which a HZSM-5 zeolite (Si/Al = 45) and a reaction temperature of 623 K were adopted [52]. Therefore, it is proposed that the aromatics based cycle produces ethylene and propylene with equal carbon-based selectivities over HZSM-5 zeolites independent of MTH reaction temperatures.

In the aromatics-cofeeding experiments, although the olefin based cycle plays a minor role at low methanol conversions as a result of the low concentration of olefins, the significance of the olefin based cycle increases with increasing methanol conversion. The reason is that the aromatics based cycle produces ethylene and propylene in equal amounts; despite that ethylene has a low reactivity, the produced propylene is able to compete with aromatics and propagate the olefin based cycle at higher concentrations, resulting in the formation of most of the C<sub>3+</sub> in the final product pool, shown schematically in Figure 3. For instance, in the test with a feed containing 4 mol.% *p*-xylene in which the aromatics based cycle is largely propagated, a maximum of 13 C% ethylene is formed at nearly 100% methanol conversion [44, Figure 1(b)]. If we make the extreme assumption that all the ethylene was formed from the aromatics-based cycle, having established that the aromatics based cycle produces ethylene and propylene with

equal carbon based rates, 13% methanol is then supposed to be converted concurrently to propylene via the aromatics based route. Thus, less than 30% methanol is believed to be converted via the aromatics based cycle, and the remaining 70% methanol is thus converted via the olefin methylation/cracking route. Therefore, although the aromatics based route dominates the initial conversions with a feed abundant in aromatics, the olefin based cycle is dominant during the overall conversion. This is more evident for the conversion of methanol in the absence of any co-feed. At very low conversion (below 0.1%), the ratio of carbon based selectivity of ethylene to propylene is close to 50 to 50 [52]. Therefore, the methanol conversion is proposed to be initiated by the aromatics based cycle. However, formed olefins will rapidly compete with the initial aromatic hydrocarbon pool species. The olefin based cycle starts to dominate the methanol conversion, as shown in Figure 4 (b).

Inspired by the analyses that co-feeding the same concentration of benzene, toluene, *para*-xylene leads to the identical impact on the aliphatic product distribution, we designed similar experiments on the olefins based cycle by co-feeding various C<sub>2</sub>-C<sub>6</sub> olefins of the same carbon-based concentration. Indeed, very similar to the situation in the aromatics based cycle, it was demonstrated that co-feeding a low concentration of olefins (up to 40 C% in this study) leads to the product distribution independent of the identity of the co-fed C<sub>3+</sub> olefins at higher conversions [44]. As shown schematically in Figure 2, similar to the roles that toluene and xylene play in the aromatics based cycle, C<sub>3</sub>-C<sub>6</sub> olefins take part in the olefin methylation/cracking cycle as active intermediates via rapid scrambling and incorporation of co-fed olefins by methylation and cracking with comparable rate constants. Ethylene co-feeding is the only exception. As ethylene is reported to have an activity in methylation at least one magnitude lower than the C<sub>3+</sub> higher olefins, it can not be effectively involved in the olefin methylation/cracking, mostly staying unreacted, as shown schematically in Figure 3.

The observation, that the final product distribution is independent of the nature of the co-fed olefins, is further evidence for the olefin based cycle as the dominant reaction pathway over HZSM-5 under the studied reaction conditions (at higher conversions of methanol). On the other hand, addition of olefins in the feed favors hydrogen transfer and aromatization. Even though the aromatics concentration is low compared to the olefins,

aromatics have a relatively lower diffusion rate than the olefins. Therefore these aromatics tend to stay in pores and compete with olefins. In turn, the aromatics based hydrocarbon pool route remains active. The overall consequence is, therefore, that co-feeding olefins does not selectively propagate the olefin-based cycle. In other words, the ratio of activities of aromatics and olefins based cycles does not significantly change compared to that in the case of a pure methanol feed.

### 3.3.3 Comparison with olefin cracking

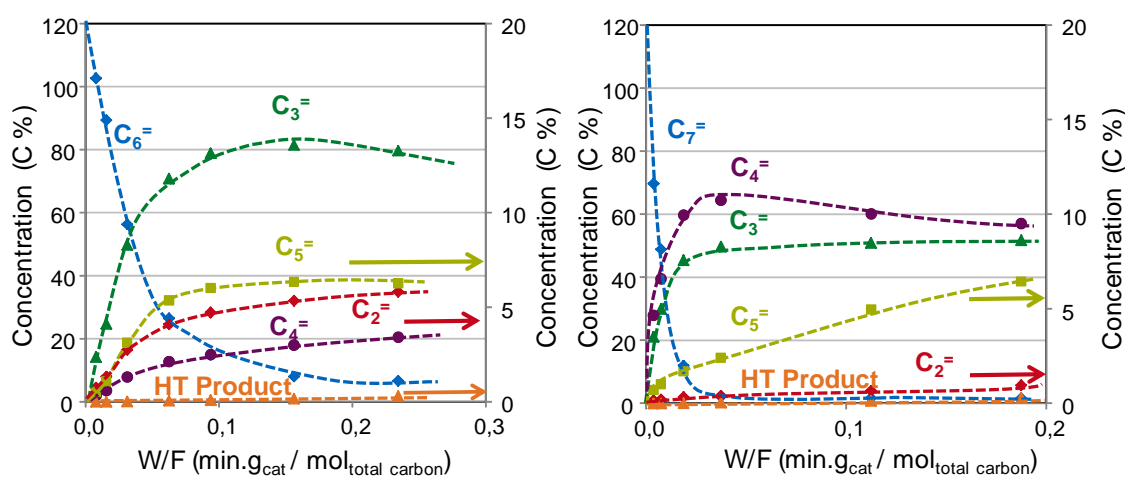
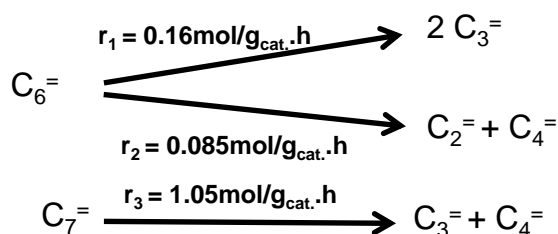


**Figure 6.** Reaction pathway for the 1-hexene (a) and 1-heptene (b) cracking. In both cases, total carbon concentration is 120%. Reaction temperature was 723 K. Water partial pressure was 10 kPa, and partial pressures for 1-hexene and 1-heptene were 2 and 1.7 kPa, respectively, leading to an equivalent 120 C% in each feed mixture (referred to as the 120 C% from a feed containing 100 C% of methanol and 20 C% from the co-fed olefin). Hereby the hydrogen transfer (HT) product includes aromatics and  $C_{2-4}$  paraffins.

We are now in a position to draw the conclusion that two distinct catalytic cycles are operative over HZSM-5 zeolite, with the olefin methylation/cracking route being the dominant reaction pathway in the overall methanol conversion range, and that the final product distribution under typical MTO reaction conditions is dictated to a large extent by  $C_6$ - $C_7$  olefin cracking. Therefore, to gain mechanistic insight into olefin transformations within the complex chemistry involved in and the mechanistic connections among methanol conversion, the conversion of pure olefins, mainly 1-hexene

and 1-heptene, was studied at reaction conditions as close as possible to those industrially practiced in the MTO reaction. As water is formed during the MTO reaction, 10 kPa water vapor (i.e., the outlet partial pressure of water at 100% conversion of 10 kPa methanol) was introduced with the olefin.

Figure 6 illustrates the conversion of 1-hexene and 1-heptene of the same concentration of 120 C% (equivalent to the 120% carbon from a feed containing 100 C% of methanol and 20 C% from olefin co-feed, but no actual methanol in the feed), respectively, as a function of contact time. Different from the previous sections, the contact time in this section is defined as the ratio of carbon molar flow rate to catalyst weight, with a unit of  $\text{min mg}_{\text{cat}} \text{mol}_{\text{total carbon}}^{-1}$ .



**Scheme 3.** Primary reaction routes for 1-hexene and 1-heptene cracking. The reaction rates were evaluated based on the conversions and product distributions at the lowest contact time.

Mechanistically speaking, primary reactions of 1-hexene cracking most likely proceed via two pathways that form ethylene and butene (1:1) or two molecules of propylene, respectively, as shown in Scheme 3. As shown in Figure 6, the former primary reaction is much slower than the latter. The ratio of the reaction rates for these two primary reactions was estimated to be 19, based on the selectivities to propylene and ethylene at the lowest contact time studied (Table 1). Fast secondary reactions of propylene, which was the main product, and 1-hexene, which was abundant at low conversions, led to butenes and pentenes, resulting in the deviation of butenes and ethylene from unity, even at the lowest contact time studied. In the case of 1-heptene, the predominant cracking route forms propylene and butenes, essentially in accord with the stoichiometry (Figure 6 and Table 1). Other products were formed with very low selectivities even at 1-heptene conversion



of 42%. The much faster primary cracking of 1-heptene than that of 1-hexene might be the reason as to why propylene and butenes were observed in parity at 1-heptene conversion of 42%, while the ethylene/butenes ratio deviated from unity when 1-hexene conversion was still 10~20%.

**Table 1.** Conversions and product distributions at low contact times for cracking of 1-pentene or 1-hexene or 1-heptene. Reaction temperature was 723 K. Partial pressure of water vapor was 10 kPa, and partial pressures for 1-pentene, 1-hexene or 1-heptene were 2.4, 2 and 1.7 kPa, respectively, leading to an equivalent 120 C% in each feed mixture (referred to as the 120 C% from a feed containing 100 C% of methanol and 20 C% from the co-fed olefin). The total flow rate was kept identical at 55 ml min<sup>-1</sup>.

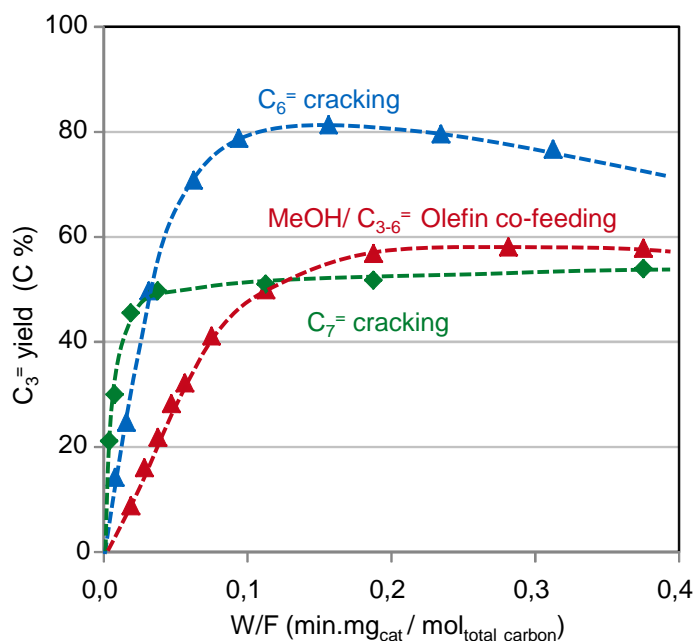
Feed	Catalyst amount (mg)	Conversion ((%)*	Hydrocarbons (C%)					
			C <sub>2</sub>	C <sub>3</sub>	C <sub>4</sub>	C <sub>5</sub>	C <sub>6</sub>	C <sub>7+</sub>
1-C <sub>7</sub>	1	41.9	0.15	21.15	28.0	0.71	0.25	69.74
1-C <sub>6</sub>	2.5	14.5	0.76	14.20	1.93	0.51	102.59	
1-C <sub>5</sub>	2.5	1.55	0.22	0.55	0.43	118.14	0.65	

\* The lowest conversion for each feed.

At longer contact times, the primary olefin products undergo reactions with the reactant and among themselves, resulting in increased formation of olefins which would not be expected from monomolecular pathways mediated by carbenium ions, e.g., pentenes from cracking of 1-hexene. Hydrogen transfer reactions between olefins become detectable with increasing conversion, but remain very low.

Three groups of products, i.e., propylene, ethylene and hydrogen transfer products (C<sub>2-4</sub> light alkanes plus aromatics), deserve special attention in the context of comparing the catalytic performance of HZSM-5 in olefin cracking (pure olefin feeds) and MTO reaction (methanol-olefin mixtures). Analysis of these products can also furnish valuable information about the olefin methylation/cracking route. In terms of the yield of propylene at full reactant conversion, 1-hexene cracking gave rise to a higher value, while 1-heptene cracking produced a lower one, compared to that from the methanol-C<sub>3-6</sub> olefin reaction mixture on the same HZSM-5 catalyst (Figure 7). This is in line with the

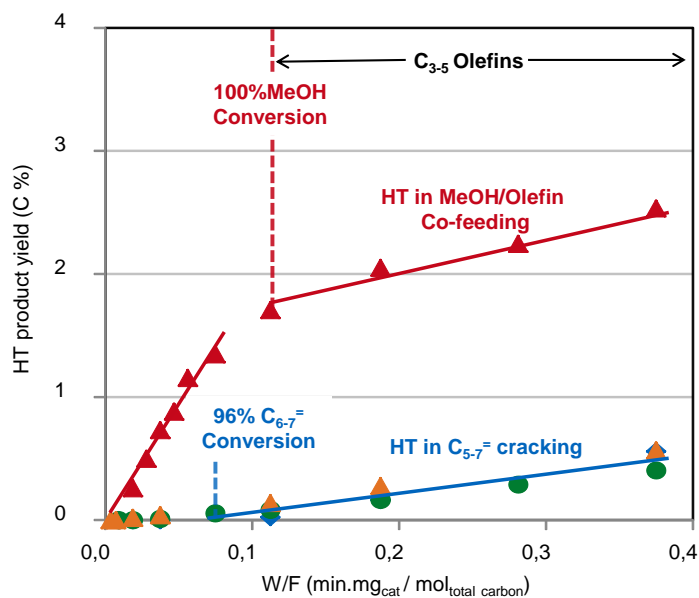
olefin methylation/cracking mechanism for mixed methanol-olefin feeds, in which olefin methylation either terminates at hexenes that are cracked down to propylene (one hexene molecule produces two propylene molecules) or terminates at heptenes that are cracked down to propylene and butenes (one heptene molecule produces one propylene molecule). The fact that propylene yield from mixed methanol-olefin feeds was closer to that from 1-heptene cracking might suggest a higher termination probability at heptenes for conversion of methanol in the presence of co-fed  $C_{3-6}$  1-olefins.



**Figure 7.** Propylene yield as a function of contact time for the feeds of 1-hexene, 1-heptene, and methanol co-fed with 20 C%  $C_{3-6}$  olefins. The total concentration of carbon was 120% and identical for all feeds. Reaction temperature was 723 K in all cases. For cracking of 1-hexene and 1-heptene, water partial pressure was 10 kPa, and partial pressures for 1-hexene, and 1-heptene were 2 and 1.7 kPa, respectively.

$C_{2-4}$  alkanes and aromatics that are referred to as hydrogen transfer (HT) products in this work are undesirable in the MTO reaction. Figure 8 depicts the yield of these HT products, as a function of contact time, for the methanol-olefin feed (molar ratio = 100:20) and various pure  $C_{5-7}$  olefin feeds with the same total carbon concentration. Over the whole range of contact time, hydrogen transfer was significantly higher for the methanol-containing feed compared to pure olefin feeds. Upon reaching full conversion of

methanol, the formation rates of the HT products from the methanol-containing feed and pure olefin feeds became comparable, as indicated by the similar slopes at higher contact times. These HT products were possibly formed via reactions between two olefinic species which should be similar for both cases, as both methanol and higher olefins were converted predominantly to  $C_{3-5}$  olefins at full reactant conversions. Before full conversion of methanol, hydrogen transfer proceeded much faster in the methanol-olefin mixed feed than in pure olefin feeds. Although a molecule-level understanding has not been achieved, it seems that another hydrogen transfer pathway exists that most likely involves methanol or its derived intermediates, proceeding faster than the classical route between two olefinic species.



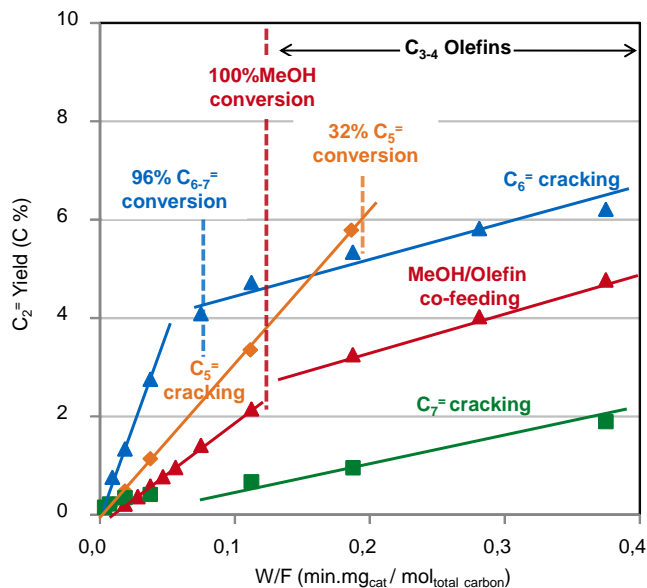
**Figure 8.** Yield of hydrogen transfer products as a function of contact time for the mixed feeds containing methanol (100 C%) and 1-pentene, 1-hexene and 1-heptene. The total carbon concentration was 120% for all feeds. Reaction temperature was 723 K in all cases.

Figure 9 depicts the yield of ethylene as a function of contact time from four different feeds, including a methanol-olefin mixed feed (any  $C_{3-6}$  olefin makes no difference), 1-pentene, 1-hexene and 1-heptene. Before reaching > 90% conversion, 1-hexene cracking gave rise to the highest formation rate of ethylene among all the four feeds, indicating

that the kinetically primary cracking of 1-hexene to ethylene and butenes is very active under realistic MTP reaction conditions. Ethylene formation from 1-pentene cracking was the second highest, while 1-heptene cracking produced ethylene in a much lower rate and yield over the studied range of contact time. From the yield ratio of formed ethylene, propylene and butenes, it is concluded that the bimolecular reaction pathway plays a predominant role in the formation of ethylene, which is essentially formed by cracking of secondary products as hexene cracking (Scheme 4). Compared to that from hexene cracking, the ethylene formation rate from the methanol-olefin feed was lower. This implies that the under realistic reaction conditions, hexene cracking acts as an important route for ethylene formation. Analogous to the situation in the hydrogen transfer rates, with contact times longer than  $0.1 \text{ min mg}_{\text{cat}} \text{ mol}_{\text{MeOH}}^{-1}$ , the ethylene formation showed an identical reaction rate for the feed of methanol,  $\text{C}_6^=$ , and  $\text{C}_7^=$ , respectively. This again was a result of the similar actual feed composition after cracking, predominantly  $\text{C}_{3-4}$  olefins ( $\geq 85 \text{ C}\%$ ). Therefore, the ethylene is formed from the oligomerization of lower olefin and cracking of  $\text{C}_6^=$  intermediates. The only exception is ethylene formation from  $\text{C}_5^=$  conversion. At a contact time of 0.11 min, after which the other feeds have already almost fully converted ( $\geq 96\%$ ), the overall pentene conversion is just 32%. Therefore, the actual feed composition from 1-pentene is highly different from the others and still active in forming ethylene from the bimolecular pathway.

The main conclusion drawn from Figure 9, that hexene cracking is an important route for ethylene, is apparently against the proposal generally accepted in literature that ethylene forms not via the olefin methylation and cracking cycle, but via the aromatics based cycle, as demonstrated by the isotope experiments by Bjørgen et al. [38-39]. However, a detailed comparison of the reaction conditions could identify that for their mechanistic studies, the predominantly adopted reaction temperature was 623 K [38-39], which is much lower than the typical temperature range (723~773 K) for MTO and MTP processes. It is proposed that the reaction temperature is the key factor affecting the dominant formation pathway for ethylene. The olefin based route,  $\text{C}_6^=$  cracking as the key step, has a significantly higher activation energy than the aromatics based cycle. Therefore, although ethylene predominantly forms via the aromatics based cycle at lower

reaction temperatures such as 623 K, the olefin based cycle becomes more significant at 723 K and even higher temperatures.



**Figure 9.** Yield of ethylene as a function of contact time for the feeds containing methanol (100 C%) and 1-pentene, 1-hexene, and 1-heptene. The total carbon concentration was 120% for all feeds. Reaction temperature was 723 K in all cases. For cracking of olefin feeds, water partial pressure was 10 kPa, and partial pressures for 1-pentene 1-hexene and 1-heptene were 2.4, 2.0 and 1.7 kPa, respectively.

This formation route of ethylene via C<sub>6</sub>= olefin cracking is supported from the impact of reaction temperature on the MTO product distributions, as shown on Figure 10. With the increase of reaction temperature, both yields of ethylene and propylene increase. Correspondingly the yield of C<sub>4+</sub> aliphatics decrease with temperature. This indicates the higher olefin cracking capability at higher reaction temperatures that leads to the favored formation of light olefins. Most importantly, the yield of hydrogen transfer products decrease with reaction temperature, most probably due to a lower coverage of olefinic species at higher temperature. The opposite trends of ethylene and aromatics demonstrated that much of ethylene is mechanistically not linked with aromatics, but comes from the other pathways, i.e., C<sub>6</sub>= cracking.

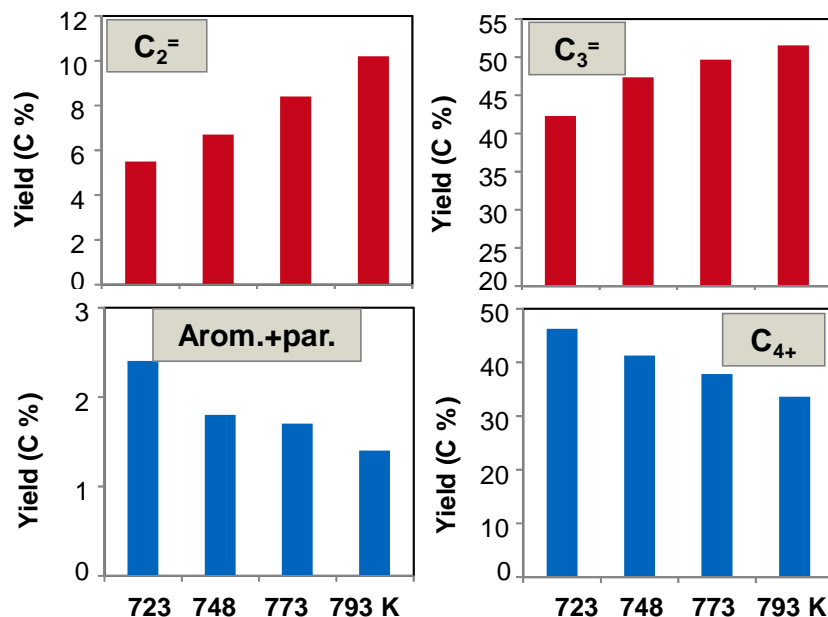


**Figure 10.** Impact of reaction temperature on the MTO product distribution over HZSM-5, in terms of ethylene, propylene, C<sub>4+</sub> aliphatics, and hydrogen transfer products (aromatics plus C<sub>2,4</sub> light olefins). Methanol partial pressure was 22 kPa, diluted by water. The reaction temperature was set as 723, 748, 773 and 793 K, respectively.

### 3.3.4 Impact of methanol to olefin co-feed ratio on product distribution

The finding that product distribution is independent of the nature of the co-fed C<sub>3-6</sub> olefin contradicts with the observation by Wu et al. of a remarkable impact of the identity of co-fed olefins [53]. These authors applied the same partial pressures of methanol and co-fed C<sub>2-6</sub> olefin, corresponding to C-based cofeed-to-methanol ratios of (200-700):100, which is significantly higher than those applied in this work (at most 40:100) [53]. Similarly, it was observed that 1-butene and 1-pentene, when co-fed with methanol in a C-based ratio of 100:100, the product distribution depended on the identity of olefin (Figure 11). A similar or even higher concentration of olefin co-feed relative to methanol would lead to more effective competitive adsorption by olefin-derived species and a greater fraction of methanol being consumed by methylation of such olefin-derived species. In this case, the product distribution at complete methanol conversion is dictated by the subsequent inter-conversion of the formed higher olefins, which reflects the impact of the nature of co-fed

olefin. In contrast, when only a small fraction of olefin is co-fed with methanol, the catalyst surface is dominated by methanol-derived species, and thus the hydrocarbon pool mechanism is responsible for the major part of methanol consumption. Fast olefin methylation/cracking leads to scrambling of co-fed carbon in the products, and thus product distribution becomes independent of the co-feed identity.

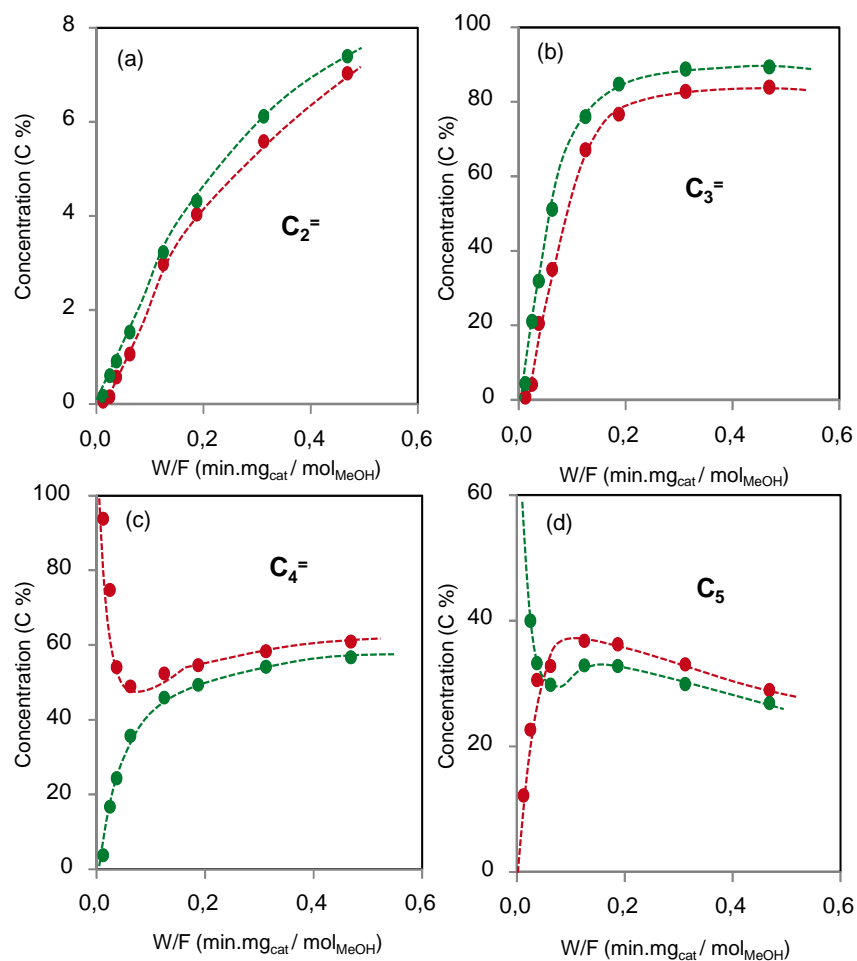


**Figure 11.** Concentrations of different products as a function of contact time for the feed mixture containing 100 C% methanol and 100 C% from 1-butene (in red) or 1-pentene (in green): ethylene (a), propylene (b), butenes (c), C<sub>5</sub> hydrocarbons (d). Reaction temperature was 723 K, methanol partial pressure was 10 kPa, and partial pressures for 1-butene and 1-pentene were 2.5 and 2 kPa, respectively, leading to the equivalent 100 C% in each feed mixture.

To investigate the effect of feed composition on the product distribution, three different feeds of an identical total carbon concentration were studied. Defining the carbon based

concentration as 100% in the mixture of methanol and water with a weight ratio 1 to 2, they were (a) 100 C% methanol, (b) 83C% methanol + 17 C% 2-butanol, (c) 83 C% methanol + 17 C% 2-pentanol, (d) 63 C% methanol + 37 C% 2-butanol, (e) 63 C% methanol + 17 C% 2-butanol 20 C% 2-pentanol, (f) 45 C% methanol + 75 C% 2-butanol, respectively, and the product distributions at 100% methanol conversion were depicted in Table 2. Less methanol in the feed led to less methane while identical yields of ethylene were observed, irrespective of the feed composition. A decrease of the methanol concentration in the feed from 100 C% to 63 C% led to little change in C<sub>3+</sub> product distribution, and at a fixed methanol concentration, the product distribution is independent of the nature of the co-feed. Further decrease in the methanol concentration to 37 % shifted significantly the product spectrum from propylene to butenes and C<sub>5+</sub> aliphatics. The yield of hydrogen transfer product decreased with descending concentration of methanol.

**Table 2.** Detailed product distributions as a function of feed composition. The carbon based concentration was defined as 100% in the mixture of methanol and water with a methanol partial pressure of 22 kPa. The used feed compositions included: (a) 100 C% methanol, (b) 83C% methanol + 17 C% 2-butanol, (c) 83 C% methanol + 17 C% 2-pentanol, (d) 63 C% methanol + 37 C% 2-butanol, (e) 63 C% methanol + 17 C% 2-butanol 20 C% 2-pentanol, (f) 45 C% methanol + 75 C% 2-butanol, respectively. The reaction temperature was 748K. And weight hourly space velocity with respect to carbon was 0.56 g<sub>Carbon</sub> g<sub>cat</sub><sup>-1</sup> min<sup>-1</sup>.

Feed Composition			Product distribution						
Methanol	C <sub>4</sub> <sup>=</sup>	C <sub>5</sub> <sup>=</sup>	C <sub>1</sub>	C <sub>2</sub> <sup>=</sup>	C <sub>3</sub> <sup>=</sup>	C <sub>4</sub> <sup>=</sup>	C <sub>5+</sub>	C <sub>2</sub> -C <sub>4</sub> paraffins	Toluene + xylenes
100	0	0	0.35	6.9	46.9	26.7	14.9	2.8	1.5
83	17	0	0.23	6.9	47.0	27.0	15.0	2.6	1.3
83	0	17	0.23	7.0	47.0	27.0	15.0	2.6	1.3
63	37	0	0.14	7.0	47.1	27.2	15.1	2.5	1.0
63	20	17	0.15	7.1	47.0	27.1	15.3	2.4	1.0
37	63	0	0.08	7.0	44.1	30.2	15.7	2.3	0.6

These results are consistent with the previous findings in this work. With an identical carbon concentration in the feed, the feed containing 100 C% methanol showed the highest yield of hydrogen transfer products, as a methanol-involved hydrogen transfer pathway has a higher rate than the classical route that solely involves olefins (Figure 8).



Although the yield of aromatic products decreased from 1.9% to 1.4% when the concentration of methanol in the feed decreased from 100% to 63%, the yield of ethylene remained very comparable (6.9% compared to 7.0%). Similar to the situation on the impact of the reaction temperature on the ethylene formation as shown in Figure 10, this indicates that at an elevated reaction temperature of 748 K, the ethylene is not much mechanistically linked with aromatics, and the olefin cracking route act as an important pathway for ethylene formation.

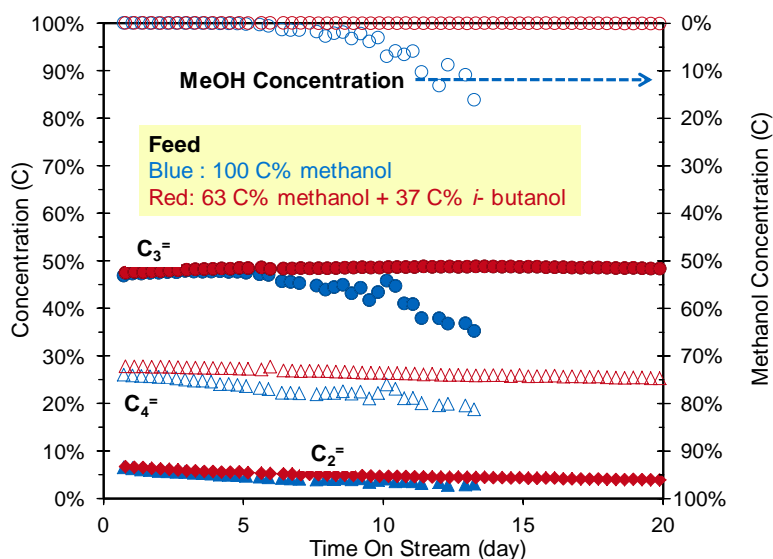


**Figure 12.** Methanol concentration and yields of  $C_2$ - $C_4$  olefin products as a function of time on stream for feeds of (a) 22 kPa Methanol diluted in water (in blue), (b) 13.8 kPa methanol and 2.1 kPa 2-butanol (in red) diluted in water, respectively. Defining the carbon based concentration as 100% in the mixture of methanol and water, they were (a) 100 C% methanol, (b) 62.5 C% methanol + 37.5 C% 2-butanol; i.e., both feeds contained the identical carbon based concentration. Reaction temperature was 748K, and weight hourly space velocity with respect to carbon was  $0.56 \text{ g}_{\text{carbon}} \text{ g}_{\text{cat}}^{-1} \text{ min}^{-1}$ .

A decrease of the methanol concentration from 100% to 63% did not essentially alter the surface chemistry which was still dominated by the presence of methanol/dimethyl ether and its derived  $C_1$  entities, and the olefin methylation/cracking route resulted in a similar product distribution for the three feeds (100 C% methanol, 83 C% methanol + 17 C<sub>4</sub> or C<sub>5</sub>, and 63 C% methanol + 37 C% C<sub>4</sub> or C<sub>5</sub>). However, a further decrease of methanol concentration in the feed to 37 % results in competitive adsorption of the methanol and 1-

butene species. Therefore, analogous to the case shown in this Section, a separate methylation and olefin cracking reaction path will lead to product distribution different from that from a methanol dominant hydrocarbon pool route. It is also demonstrated in Figure 12 that compared to the 100 C% methanol feed the feed with 63% methanol (while with identical carbon concentration in the feed) leads to a longer catalyst lifetime. This is in line with the observations that less methanol in the feed resulted in less hydrogen transfer reactions, which produced the coking precursor deactivating the acid catalyst.

### 3.3.5 Towards elucidating the working mechanism in MTO over HZSM-5

The product selectivity control in MTO reaction calls for in-depth fundamental insights into the reaction mechanism. The dual cycle concept [39] depicts the key reaction steps including olefin methylation and cracking, aromatics methylation and dealkylation, and hydrogen transfer as a bridge step [6]. In the context of elucidating the effect of the zeolite topology, reaction conditions and practical operations on the final product selectivity, more quantitative descriptions of the individual reaction steps of the dual cycle mechanism are, while crucial, yet to be fully developed. Two key persistent questions are:

- 1) for a specific cycle, what influences the intrinsic selectivities to the desired products?
- 2) what accounts for the formation and what is the nature of the prevalent active hydrocarbon species?

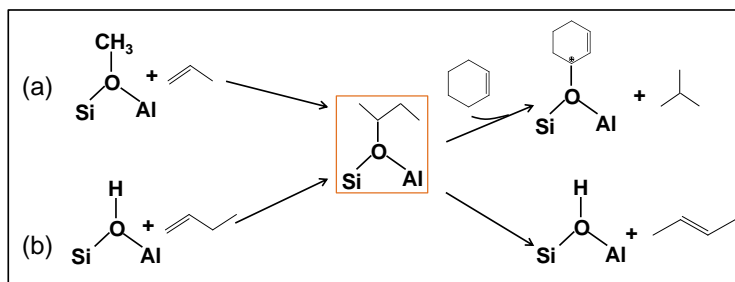
These questions are challenging to answer unequivocally, due to the complex chemistry for the methanol conversion. The key information that we can obtain from the present study over a HZSM-5 catalyst includes:

The aromatics based cycle operates over HZSM-5 zeolite and produce ethylene and propylene with carbon-based intrinsic selectivities 50 to 50 over HZSM-5 under realistic MTO reaction temperatures. The olefin based methylation/cracking route works as well over HZSM-5 zeolite. Growth of the carbon chain terminates predominantly at C<sub>6</sub> or C<sub>7</sub>. The subsequent cracking of these higher olefins mediated by carbenium ion chemistry and β-scission leads to a product spectrum significantly more selective in propylene and

C<sub>4+</sub> than ethylene. An estimate from C<sub>6-7</sub> olefin cracking demonstrated that the relative ratio of carbon based selectivities for ethylene to propylene is 5 to 100.

The final product distribution, however, depends not only on the intrinsic selectivities for a specific cycle, but also relies to a large extent on methanol conversion that each of the catalytic cycles contributes to. The turnover rate for an aromatics or olefin populated site has still not been assessed. It should be noted, however, that the olefin based route is by far the dominant reaction pathway, and its significance increases with methanol conversion to olefins.

A frequently discussed issue is on the dominant source of ethylene and propylene over HZSM-5 zeolite. It has been shown in this work that the olefin based cycle plays the dominant role in methanol conversion over HZSM-5, irrespective of any co-feed, and together with the fact that this cycle is highly selective in favoring the formation of C<sub>3+</sub>, C<sub>3+</sub> olefins are in any case predominantly formed from the olefin based cycle. The formation route of ethylene, on the other hand, is more complex, and depends on multiple parameters. For a feed abundant in aromatics, the aromatics based cycle can be selectively promoted, and correspondingly it acts as the dominant pathway for ethylene formation. However, for the conversion of feeds of methanol with or without olefin co-feeds, ethylene could be formed from both aromatics and olefin based catalytic cycles. In this case, reaction conditions are critical for influencing the relative contributions of the two cycles. The reason is that the aromatics based cycle is comparatively more selective in ethylene formation, but it contributes significantly less to methanol conversion especially at high conversions. On the other hand, the olefin based route is significantly less selective in ethylene formation, while the autocatalytic feature makes it overwhelmingly active in converting methanol, and the selectivity to ethylene increases with increasing reaction temperature. Therefore, the contribution for each cycle depends on the methanol conversion and reaction conditions. At low methanol conversions and relatively low reaction temperatures, a large portion of ethylene is formed via the aromatics based cycle. However, the olefin based cycle contributes more significantly to the ethylene formation with increasing methanol conversion and reaction temperature.



**Scheme 5.** Proposed mechanistic pathway for the methanol enhanced hydrogen transfer via the same intermediate as olefin formation via methylation.

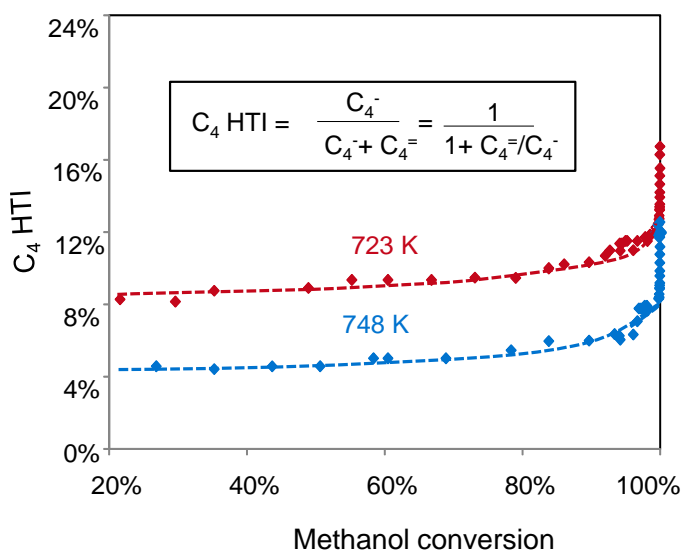


**Figure 13.** C<sub>4</sub> Hydrogen Transfer Index (C<sub>4</sub> HTI) as a function of methanol conversion. Methanol with partial pressure was 22 kPa was diluted in water. Reaction temperature was 723 and 748 K, respectively. Various methanol conversions were measured at different severities of catalyst deactivation.

Hydrogen transfer reaction is undesired in MTO(P) processes. As suggested in Section 3.3.3, a hydrogen transfer pathway involving methanol or its derived intermediates proceeds much faster than the classical route between two olefinic species. Further supports to this proposal were obtained from the experiments performed with varied ratios of methanol to olefin co-feeds (while the total carbon concentration were kept identical), which clearly showed that less methanol in the feed led to less hydrogen transfer products and consequently much alleviated catalyst deactivation rate (Figure 12).

A molecular understanding of it has not been fully achieved. We tentatively proposed that this pathway is linked with intermediates of the olefins methylation, which share a similar chemical nature as the surface species derived directly from an acid site adsorbed olefin, as shown in Scheme 5. Along with this proposal, it is proposed that the olefin based cycle produce light olefins and paraffins in parallel reactions. This proposal gains supports from the plot of C<sub>4</sub> Hydrogen Transfer Index (HTI) as a function of methanol conversion, shown in Figure 13. The C<sub>4</sub> HTI is defined as the ratio of C<sub>4</sub> paraffins (n-butane and iso-butane) concentration to the total C<sub>4</sub> concentration. The C<sub>4</sub> HTI remains almost unchanged over the full range of methanol conversion, indicating a constant ratio of C<sub>4</sub> paraffins to olefins, and that paraffins and olefins are produced in parallel rather than in sequential reactions. This would not have been the case if hydrogen transfers solely occurred between olefins, as the concentration of olefins increases with increasing methanol conversion, and accordingly hydrogen transfer as a secondary reaction would lead to C<sub>4</sub> HTI increase significantly with conversion.

### 3.4 Conclusions

The MTO reaction over HZSM-5 catalysts is better described by an autocatalysis mechanism, with entrained olefins and aromatic products in the zeolite pore as competing co-catalysts. Accordingly, two distinct reaction pathways, aromatics-based and olefin-based catalytic cycles, operate for the production of ethylene and propylene from methanol over HZSM-5 under reaction conditions relevant to practical operations. The aromatics-based cycle starts with toluene as the lowest sufficiently active species, while a complete olefin methylation/cracking cycle begins its turnover with propylene as the lowest sufficiently active species. The aromatics-based cycle produces ethylene and propylene with equal carbon based selectivities, while the olefin-based cycle favors C<sub>3+</sub> olefins over ethylene.

The co-existence of olefins and aromatics species in the zeolite pores leads to a competition between the two cycles for the methanol-activated site. Therefore, their activities depend on the local concentrations of specific hydrocarbon species and methanol conversion. Co-processing of intermediates in each catalytic cycle of the same

concentrations results in identical involvements in the turnover and in turn an identical impact on the product distribution, due to the comparable rate co-efficients in each step of a cycle. While co-feeding lower benzenes propagates the aromatics-based cycle, the olefins produced by the aromatics based cycle will subsequently propagate also the olefin based cycle. In turn, olefin homologation/cracking reactions are more important than the aromatics based cycle at higher methanol conversions, contributing to C<sub>3+</sub> higher olefins formation irrespective of the nature of co-feeds, aromatics or olefins. On the other hand, both the aromatics based route and the olefin based cycle operate for ethylene formation, and the dominant pathway for ethylene formation depends to a large extent on the reaction conditions. With an aromatics-enriched feed and/or at low reaction temperatures, the aromatics based cycle contributed predominantly, while the olefin based cycle contributes significantly as well when a high reaction temperature is adopted (such as in the MT(O)P process). The results shown here also suggest that there is another hydrogen transfer pathway involving methanol-derived intermediates, which proceeds faster than classic hydride transfer between two olefinic species.

### 3.5 Acknowledgements

The authors acknowledge the financial support from Clariant Produkte (Deutschland) GmbH and fruitful discussion within the framework of MuniCat.

### 3.6 References

- [1] C. D. Chang, *Catal. Rev. Sci. Eng.* 25 (1983) 1.
- [2] M. Stöcker, *Micropor. Mesopor. Mater.* 29 (1999) 3.
- [3] T. Mokrani, M. Scurrill, *Catal. Rev. Sci. Eng.* 51 (2009) 1.
- [4] G.A. Olah, *Angew. Chem. Int. Ed.* 44 (2005) 2636.
- [5] U. Olsbye, S. Svelle, M. Bjorgen, P. Beato, T.V.W. Janssens, F. Joensen, S. Bordiga, K.P. Lillerud, *Angew. Chem. Int. Ed.* 51 (2012) 5810.
- [6] S. Ilias, A.Bhan, *ACS Catal.* 3 (2013) 18.
- [7] J. F. Haw, W. Song, D.M. Marcus, J.B. Nicholas, *Acc. Chem. Res.* 36 (2003) 317.
- [8] D. Lesthaeghe, V. Van Speybroeck, G. B. Marin, M.Waroquier, *Angew. Chem.* 118 (2006) 1746
- [9] D. Lesthaeghe, V. Van Speybroeck, G. B. Marin, M.Waroquier, *Ind. Eng. Chem. Res.* 46 (2007) 8832.

- [10] W. Song, D. M. Marcus, H. Fu, J. O. Ehresmann, J. F. Haw, *J. Am. Chem. Soc.* 124 (2002) 3844.
- [11] N.Y. Chen, W.J. Reagan, *J. Catal.* 59 (1979) 123.
- [12] R.M. Dessau, *J. Catal.* 99 (1986) 111.
- [13] R.M. Dessau, R.B. LaPierre, *J. Catal.* 78 (1982) 136.
- [14] B.E. Langner, *Appl. Catal.* 2 (1982) 289.
- [15] T. Mole, J. Whiteside, D. Seddon, *J. Catal.* 82 (1983) 261.
- [16] T. Mole, G. Bett, D. Seddon, *J. Catal.* 84 (1983) 435.
- [17] I.M. Dahl, S. Kolboe, *Catal. Lett.* 20 (1993) 329.
- [18] I.M. Dahl, S. Kolboe, *J. Catal.* 149 (1994) 458.
- [19] I.M. Dahl, S. Kolboe, *J. Catal.* 161 (1996) 304.
- [20] J.F. Haw, J.B. Nicholas, W. Song, F. Deng, Z. Wang, T. Xu, C.S. Heneghan, *J. Am. Chem. Soc.* 122 (2000) 4763.
- [21] J.F. Haw, W. Song, D.M. Marcus, J.B. Nicholas, *Acc. Chem. Res.* 36 (2003) 317.
- [22] Ø. Mikkelsen, P. O. Rønning, S. Kolboe, *Microporous Mesoporous Mater.* 40 (2000) 95.
- [23] B. Arstad, S. Kolboe, *Catal. Lett.* 71 (2001) 209.
- [24] B. Arstad, S. Kolboe, *J. Am. Chem. Soc.* 123 (2001) 8137.
- [25] W. Song, J. F. Haw, J. B. Nicholas, C. S. Henghan, *J. Am. Chem. Soc.* 122 (2000) 10726.
- [26] W. Song, H. Fu, J. F. Haw, *J. Am. Chem. Soc.* 123 (2001) 4749.
- [27] W. Song, H. Fu, J. F. Haw, *J. Phys. Chem. B* 105 (2001) 12839.
- [28] H. Fu, W. Song, J. F. Haw, *Catal. Lett.* 76 (2001) 89.
- [29] J. F. Haw, D. M. Marcus, *Catal. Lett.* 34 (2005) 41.
- [30] M. Bjørgen, U. Olsbye, S. Kolboe, *J. Catal.* 215 (2003) 30.
- [31] M. Bjørgen, U. Olsbye, D. Petersen, S. Kolboe, *J. Catal.* 221 (2004) 1.
- [32] D. Lesthaeghe, J. Van der Mynsbrugge, M. Vandichel, M. Waroquier, V. Van Speybroeck, *ChemCatChem* 3 (2011) 208.
- [33] S. Teketel, S. Svelle, K. P. Lillerud, U. Olsbye, *ChemCatChem* 1 (2009) 78.
- [34] S. Teketel, U. Olsbye, K. P. Lillerud, P. Beato, S. Svelle, *Microporous Mesoporous Mater.* 136 (2010) 33.
- [35] J. Li, Y. Wei, Y. Qi, P. Tian, B. Li, Y. He, F. Chang, X. Sun, Z. Liu, *Catal. Today* 164 (2011) 288.
- [36] J.H. Ahn, B. Temel, E. Iglesia, *Angew. Chem.* 121 (2009) 3872.
- [37] D.A. Simonetti, J.H. Ahn, E. Iglesia, *J. Catal.* 277 (2011) 173.
- [38] S. Svelle, F. Joensen, J. Nerlov, U. Olsbye, K. P. Lillerud, S. Kolboe, M. Bjørgen, *J. Am. Chem. Soc.* 128 (2006) 14770.
- [39] M. Bjørgen, S. Svelle, F. Joensen, J. Nerlov, S. Kolboe, F. Bonino, L. Palumbo, S. Bordiga, U. Olsbye, *J. Catal.* 248 (2007) 195.
- [40] H. Koempel, W. Liebner, *Stud. Surf. Sci. Catal.* 167 (2007) 261.
- [41] H. Bach, L. Brehm, S. Jensen, 2004, EP 2004/018089 A1.

- [42] G. Birke, H. Koempel, W. Liebner, H. Bach, 2006, EP2006048184.
- [43] M. Rothaemel, U. Finck, T. Renner, 2006. EP 2006/136433 A1.
- [44] Chapter 2 within this thesis.
- [45] Svelle, S.; Rønning, P. O.; Olsbye, U.; Kolboe, S. J. *Catal.* 224 (2005), 385.
- [46] Svelle, S.; Rønning, P. O.; Kolboe, S. J. *Catal.* 224 (2004) 115.
- [47] I. M. Hill, Y. S. Ng, A. Bhan, *ACS Catal.* 2 (2012) 1742.
- [48] I. M. Hill, S. A. Hashimi, A. Bhan, *J. Catal.* 291 (2012) 155.
- [49] I. M. Hill, S. A. Hashimi, A. Bhan, *J. Catal.* 285 (2012) 115.
- [50] G. Mirth, J. A. Lercher, *J. Phys. Chem.* 95 (1991) 3736.
- [51] J. Van der Mynsbrugge, M. Visur, U. Olsbye, P. Beato, M. Bjørgen, V. Van Speybroeck, S. Svelle, *J. Catal.* 29 (2012) 201.
- [52] M. Bjørgen, F. Joensen, K. P. Lillerud, U. Olsbye, S. Svelle, *Catal. Today* 142 (2009) 90.
- [53] W. Wu, W. Guo, W. Xiao, M. Luo, *Chem. Eng. Sci.* 66 (2011) 4722.
- [54] X. Sun, S. Mueller, M. Sanchez-Sanchez, A.C. van Veen. J. A. Lercher, unpublished results.



# Chapter 4

## Impact of reaction conditions and catalyst modifications on methanol-to-olefins reaction over HZSM-5 catalysts

*Methanol conversion proceeds generally via two consecutive steps which have highly different dependences on the reaction temperature. An increase of reaction temperature leads to the decoupling of these two steps and shifts the product selectivity to especially propylene, and less undesired hydrogen transfer products, i.e., C<sub>2-4</sub> paraffins and aromatics are formed. A test on the impact of reaction temperature on catalyst lifetime suggests that an optimal operation window of reaction temperature for the MTP reaction exists, which lies between 723 and 753 K. The two consecutive steps have also highly different dependencies on methanol pressure. Analogous to the impact of reaction temperature, a reduced methanol pressure results in the decoupling of these two steps. Phosphorous modification has been applied to zeolites of various Si/Al ratios. It is shown that doping an appropriate concentration of phosphorous to the HZSM-5 zeolites with low Si/Al ratios is able to effectively enhance the propylene selectivity to reach the level on high Si/Al ZSM-5 zeolites, while it has a limited positive impact on the high Si/Al ZSM-5 zeolites with respect to propylene selectivity. A further investigation on the impact of test conditions, i.e., N<sub>2</sub>- or water- diluted feed, leads to the conclusion that the phosphorous doped materials are unstable when interacting with feeds of high water concentrations. While they showed a positive impact on the propylene selectivity when tested under N<sub>2</sub> dilution, decreased propylene selectivity and increased hydrogen transfer ability was observed under water dilution conditions. A 0.1-0.2 wt.% phosphorous loading could prolong the catalyst lifetime.*

## **4.1 Introduction**

Liquid hydrocarbons and light olefins will continue to play an essential role in supplying our planet as energy carriers and platform chemicals, respectively. As a result of the depleting trend of oil reserves, the production of these materials will rely to a large extent on alternative carbon resources in a post-oil society [1-2]. The methanol-to-hydrocarbons (MTH) process acts as a key step in this respect, as methanol can be synthesized from any carbon resources, such as biomass, coal, and natural gas intermediated by synthesis gas [3-4]. The MTH process can be tuned further from producing hydrocarbons in gasoline range (methanol to gasoline; MTG) to light olefins (Methanol-To-Olefins (MTO) with a co-production of ethylene and propylene) or particularly propylene (Methanol-To-Propylene (MTP) with maximized production of propylene, which is very attractive in the current economy due to the increasing market demand) [5]. Compared to the MTO process in which fluidized-bed reactors and the zeotype silicoaluminophosphate SAPO-34 catalyst are employed as the key components, both the ExxonMobil's MTG and Lurgi's MTP processes utilize adiabatic fixed-bed reactors and HZSM-5-based catalysts as the key features [5]. Accordingly, a strong resistance to deactivation for the employed catalyst is demanded in these two ZSM-5 based processes, to reduce the operation cost in intermittent catalyst regenerations via carbon burn-off by diluted air. On the other side, compared to the reported selectivity to light olefins demonstrated in the MTO technologies, the selectivity to the targeted product, i.e., propylene, needs to be further improved in the current MTP technology [6-12]. Optimization of both the catalyst and process operations (including reaction temperature, methanol partial pressure etc.) will contribute remarkably to meeting these specific demands [4-5,13].

ZSM-5 catalyst, of the MFI topology, is a zeolite, which represents a family of microporous, crystalline, acidic aluminosilicates. In addition to methanol conversion, HZSM-5 is extensively applied as catalysts in a wide variety of other industrial processes. Their catalytic performance relies, to a large extent, on their acidity. In addition to various hydrothermal synthesis strategies, several post-synthetic modification approaches have been invented as well, among which steam treatment and phosphorous doping are

two frequently adopted methods to tune the acidity and consequently their catalytic properties in terms of activity, selectivity and stability [4].

Steam treatment of ZSM-5 zeolite at moderate temperatures is able to induce partial dealumination and healing of the defects in zeolite. The effect of mild steaming on the properties of a high Si/Al MFI zeolite was examined in detail by this group recently [14]. On the other hand, zeolite modification by phosphorous anions doping is also a frequently reported approach [15-32]. Various inorganic and organic phosphorous precursors (trimethylphosphite, orthophosphoric acid, trimethylphosphine, and so forth) were reported to have been successfully used [15-32]. After wet impregnation and subsequent calcination in air at elevated temperatures, the modified zeolites usually showed improved catalytic performance for reactions including toluene alkylation, fluid catalytic cracking, and C<sub>4</sub> olefin cracking in addition to the MTO reaction [15-32]. However, its application to the ZSM-5 zeolites of high Si/Al ratios, which are usually regarded as a key requirement for maximizing the selectivities to olefins and especially propylene, has not been fully discussed.

Therefore, in this chapter, efforts were made to investigate and understand the effects of process conditions, especially reaction temperature and methanol partial pressure, on the MTO(P) process over HZSM-5 catalysts. On the other hand, we performed an extensive investigation into the catalytic consequences of the steam treatment and phosphorous modifications in the MTP reaction. Several zeolites with varying Si/Al ratios were employed in the study of phosphorous modification, in which the phosphorous loadings and modification procedures were also varied.

## **4.2 Experimental**

### **4.2.1 Sample preparations**

#### *4.2.1.1 Zeolites*

The Si/Al = 25, 40 zeolite powders were purchased from Zeolyst. The sample MFI-90 (Si/Al = 45) was supplied by Sud-Chemie AG. All samples were calcined in flow air (100 ml/min) for 6 h at 823 K prior to use. A ZSM-5 zeolite powder (Si/Al= 90),

identical to the material used in the previous chapters, was synthesized under hydrothermal conditions using tetrapropylammonium ions ( $\text{TPA}^+$ ) as a template, as reported by Ong et al. [14]. The as-synthesized zeolite was calcined at 823 K in flowing air (100 ml/min) for 6 h to remove the organic template. Subsequently the obtained solid was ion-exchanged at 353 K using a 0.1 M  $\text{NH}_4\text{NO}_3$  solution followed by drying at 393 K overnight and calcination in flowing air (100 ml/min) at 823 K for 6 h. *ortho*-Phosphoric acid (85%) was purchased from Merck. Methanol (99.93%), and trimethylphosphine (97%) were supplied by Sigma-Aldrich.

#### *4.2.1.2 Phosphorous modifications and steaming*

Samples of P modified ZSM-5 zeolite powders ( $\text{Si}/\text{Al}=25, 40, 45$  or 90) with different amounts of phosphorous loading ( $x = 0.1\text{-}2.0$  wt.%) have been obtained by impregnating the powder with an aqueous solution containing the respective amount of orthophosphoric acid ( $\text{H}_3\text{PO}_4$ ). After drying in a rotary v evaporator at 323 K, the sample was dried at 393 K (5 h) and calcined at 823 K (6 h) in flowing air (100 ml/min). The obtained solid was subsequently washed with double distilled water at 353 K (2 h), dried (393 K) and thermally treated (823 K) to study how physicochemical properties can be altered by deposited P containing species and if original properties can be restored.

In addition to the modifications by orthophosphoric acid, another phosphorous source, trimethylphosphine, was also used to “in-situ” modify  $\text{Si}/\text{Al}=25$  zeolite. 200 mg catalyst was charged and placed in a quartz tubing reactor. After the catalyst was activated under helium flow of 50 ml/min for 2 hours at 773K, 0.5 ml of an equi-molar solution of trimethylphosphine and methanol was flowed at a weight-hourly space velocity (WHSV) ( $\text{g}_{\text{feed}}/\text{g}_{\text{cat}}\cdot\text{h}$ ) of  $8\text{ h}^{-1}$  at 773 K and 200 sccm helium. The zeolite was subsequently oxidized at 773 K under 200 sccm air for 10 minutes prior to raising the temperature to 823 K and holding for 1.5 h under the same air flow to form the modified catalyst. After that, reaction temperature was then set to 723 K. Methanol feed was then carried by pass helium with a flow rate of 50 ml/min through a saturator thermostated at 298K. After 5 mins reaction, the catalyst was purged with 50 ml/min helium for 30 mins, and

temperature was raised to 773K for next cycles of trimethylphosphine introduction and oxidation.

Steaming of the zeolite powders was performed in a rotary oven at 753 K for 24 h with water weight hourly space velocity of ( $1 \text{ g}_{\text{H}_2\text{O}}/\text{g}_{\text{cat}}\cdot\text{h}$ ). Water was delivered by a HPLC pump. After steaming, the sample was dried at 393 K for 6 h in flowing air (200 ml/min). to remove the remained water.

## 4.2.2 Catalytic Testing

### 4.2.2.1 Activity and reaction pathway evaluations

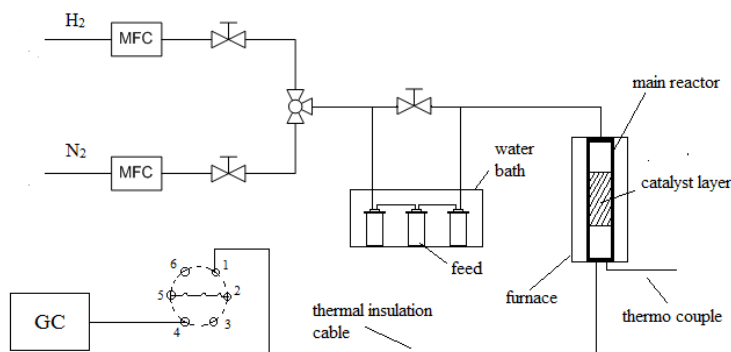


**Figure 1.** Scheme for the single-reactor setup.

Catalytic testing was performed in a fixed bed quartz reactor (with an internal diameter of 6 mm) at 723 K and a constant total pressure of 1.07 bar. The catalysts were press-pelletized, crushed, and used in a sieve fraction ranging from 200-280  $\mu\text{m}$ . The active zeolite was diluted with 300-500  $\mu\text{m}$  silicon carbide beads, in a ratio of 1:20 (wt:wt) to ensure isothermal conditions. Catalyst activation prior to methanol conversion involved heating at 753 K for 1 h under 50 ml/min  $\text{N}_2$  flow. Methanol was fed by passing 50 ml/min  $\text{N}_2$  through a methanol evaporator kept at a fixed temperature. Weight hourly space times of 0.2 to 1.7 ( $\text{h g}_{\text{cat}}/\text{mol}_{\text{MeOH}}$ ) were adjusted by charging varying amounts of catalyst in the reactor. The reactor effluent was on-line analyzed by a gas chromatograph

(HP5890) equipped with a HP-PLOTQ capillary column (30m, 0.32 mm i.d.) and a flame ionization detector.

Due to their rapid inter-conversion, both oxygenates, methanol and dimethyl ether, were counted as reactant. Conversion and yields were calculated on a carbon basis.

#### 4.2.2.2 Catalytic performance testing

A home-made 10-fold parallel plug-flow reaction unit designed from a high throughput concept was employed to evaluate the catalytic performances in terms of catalyst stability, and product distributions under reaction conditions close to industrial operations. The unit consists of 10 parallel sections. For each section, a methanol/water liquid mixture was used as the feed and transferred through a capillary by a HPLC pump (Shimadzu LC-20 AD) to a pre-reactor which was set at 533 K for evaporation. The formed vapor was routed down to the main reactor for catalytic reaction. The partial pressure of methanol was 22 kPa.

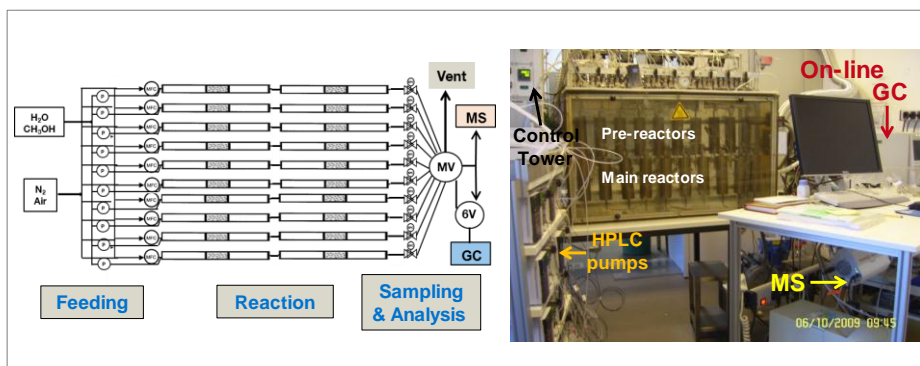


**Figure 2.** The conceptual scheme and image of the home-made 10-fold parallel reaction unit for catalytic testing of MTO conversion over HZSM-5 catalysts.

The catalyst pellets were diluted with silicon carbide (ESK-SIC, 1:12 wt:wt) with a comparable particle size to ensure temperature uniformity, since MTO is a highly exothermic reaction. The catalysts were placed into the pre-determined isothermal zone of a reactor made of 316 stainless steel (316SS) material (22 cm in length, 8.0 mm i.d.)

and supported between two quartz wool plugs. The upper space of the catalyst bed was packed with silicon carbide for preheating the feed. The lower space between the catalyst bed and the metal frit was loaded with silicon carbide in order to regulate the hydrodynamics of the flow. The catalyst samples were activated at 753 K with the temperature control at the external surface of the mantel tube with 30 ml min<sup>-1</sup> nitrogen for 2 h prior to switching to feed. The temperature of the main reactor was set at 723 K, and the total pressure was 104 kPa.

The reactor effluent from each section was routed to the 10-positioned valve, in which 9 out of the 10 ports were routed to vent, and one port was selected and routed to the 6-port sampling valve. The duration of a GC product analysis was 45 minutes, and after that the automated computer-controlled 10-positioned valve was switched to next section and after 10 runs, the valve was rounded back to the original position. During the whole course the reactor effluent was transferred via a heated line kept at 393 K. The reactor effluent was analyzed by a gas chromatograph (Shimadzu GC2010) equipped with a configured multi-column systems connected to two flame ionization detectors for on-line analysis. A mass spectrometer was used to monitor, in a real-time fashion, conversions and flow hydrodynamics/compositions.

The amount of the catalyst loaded is kept at 300 mg, and the flow rate of the liquid feedstock is 0.0246 ml/min, corresponding to a weight hourly space velocity (WHSV) of 1.5 g<sub>MeOH</sub>/(g<sub>cat</sub>·h).

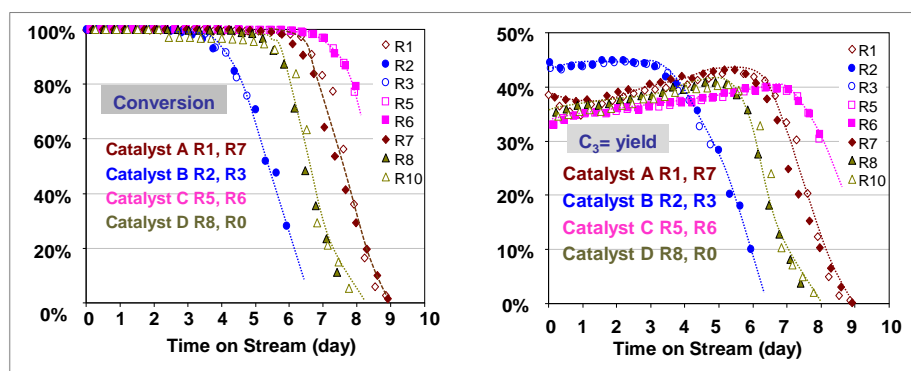


**Figure 3.** Comparison of the performance between different reactors in reproducibility of the 10-fold parallel reaction unit in MTO conversion.

A key concerned issue in the performances of the multi-fold parallel reaction unit is the reproducibility between reactors and runs. As demonstrated in the figure, when the same catalyst was loaded in two reactors, the data obtained from the reactors showed very limited scattering. The performance of different catalysts can be clearly distinguished in terms of catalyst lifetime and propylene yield. Compared to the published data [33], among which the best reported difference between reactors was  $\pm 10\%$  in this reaction, the TUM unit made in-house exhibits significantly better performance in terms of high reproducibility, stability and reliability via rational design and automation. Using test conditions close to realistic industrial conditions, improved performance ( $\pm 3\%$  error) can be achieved.

### **4.3. Results and discussions**

#### **4.3.1 Impact of reaction conditions on MTO reaction**

In this section, we present the results on the effects of reaction temperature and methanol partial pressure on the product distribution of MTO reaction over a HZSM-5 zeolite of a Si/Al ratio of 90.

##### *4.3.1.1 Effect of reaction temperature*

The effect of contact time on the methanol conversion, as depicted in Figure 4-1, clearly showed that a pseudo-first order in methanol proposed in many earlier studies was in fact an invalid assumption for MTO reaction. At low contact times, the main reaction was the transformation of methanol to dimethylether (which was regarded as a reactant rather than product), and the only product detected at the effluent was methane. At low contact times, the formation rate of light olefins was very slow, in accord with the difficulty for the first C-C bond formation from  $C_1$  entities. At longer contact times, the reaction was remarkably sped up by the formation of light olefins, signifying that another methanol conversion route differing from direct mechanisms was opened up. Methanol conversion rose to around 80% in a relatively narrow range of contact times. Such a typical S curve was indicative of an autocatalytic nature of the reaction kinetics, meaning that the formed



products acted as co-catalysts of the reaction [34]. Reaction temperature had a distinct effect on the reaction rate. When the reaction temperature was increased from 623 to 773 K, the induction period was much shortened, while the autocatalytic (-like) S curve still maintained.

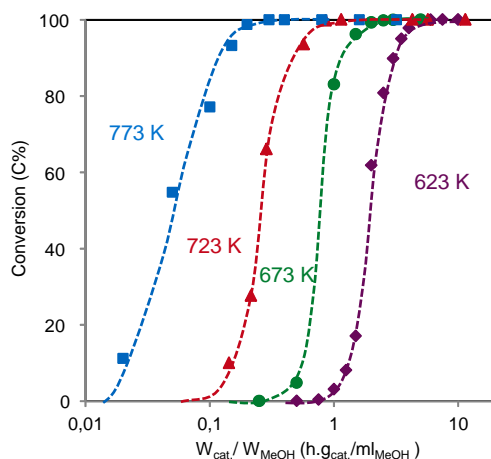


**Figure 4.** Methanol conversion as a function of contact time. Reaction temperatures were 623, 673, 723, and 773 K, respectively. A ZSM-5 catalyst with a Si/Al ratio of 90 was employed. Methanol partial pressure was 17 kPa, diluted in N<sub>2</sub>.

The product distribution on molar C-basis with increasing methanol conversion at 623-773 K was shown in Figure 5. The shape selectivity posed by MFI zeolite 10-ring pore channels led to a narrow range of the product distribution, all the products being in the range of C<sub>1</sub>-C<sub>10</sub>. The effect of contact time on the product distribution clearly showed kinetically sequential steps of the MTO process. At low conversions, the selectivity to light olefins of C<sub>3</sub><sup>=</sup>-C<sub>5</sub><sup>=</sup> range is higher than 80% within which propylene was the dominant product. As the reaction proceeded, olefins underwent homologation and oligomerization and then the selectivity to C<sub>6+</sub> increased, reaching the maximum at 80% conversion. Further reaction led to cracking of the C<sub>6+</sub> to mainly C<sub>3</sub>-C<sub>5</sub> olefins, pinpointing the homologation-cracking route for the C<sub>3</sub>-C<sub>5</sub> olefin formation. The propylene yield as well as the C<sub>5</sub> olefin yield peaked more or less at full conversion and identical contact time. An important note has to be added here that, after full conversion of methanol, prolonged contact times would result in a continuing change of the hydrocarbon distribution because of secondary reactions arising from, at least partly, product diffusion and/or re-adsorption. These secondary reactions mainly refer to

hydrogen transfer which turns the C<sub>3</sub>-C<sub>5</sub> olefins into aromatics and paraffins. Therefore, care must be taken in the interpretation and comparison of product distribution at 100% conversion.

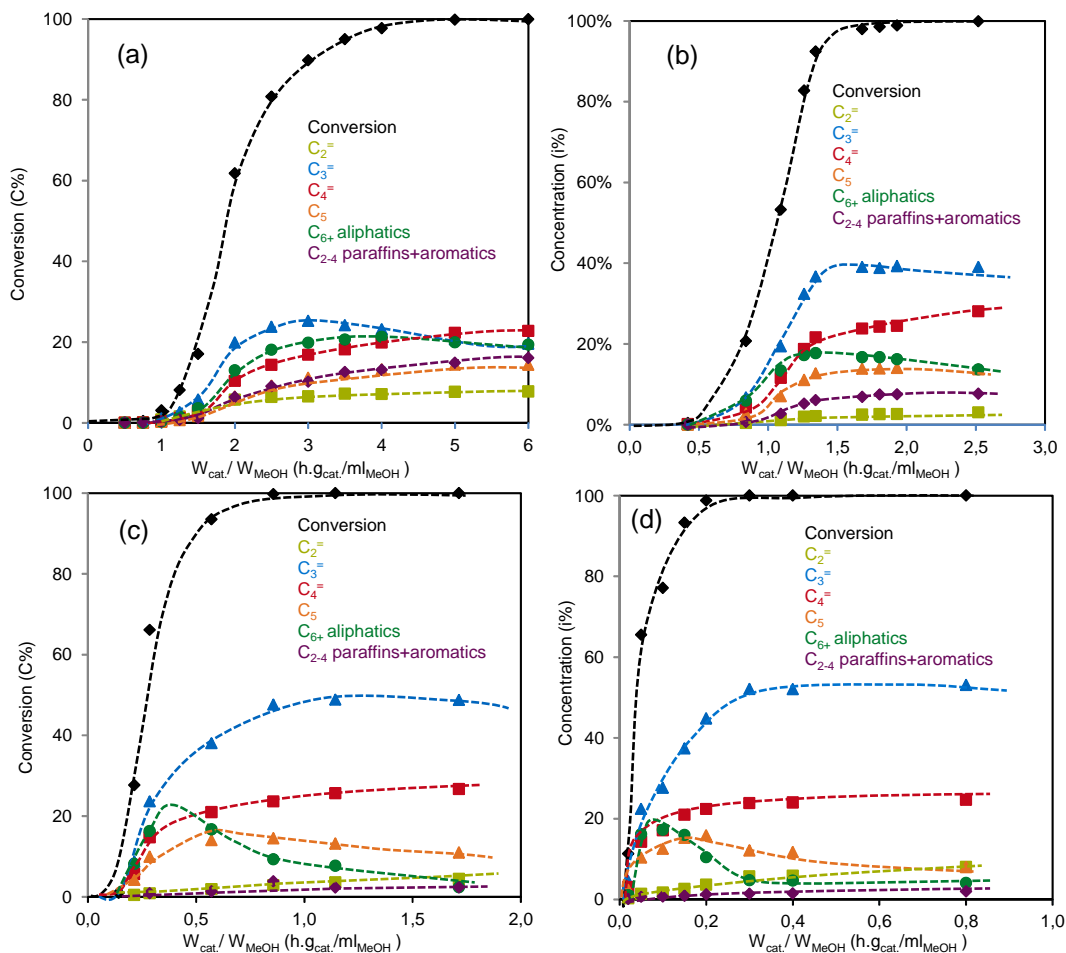
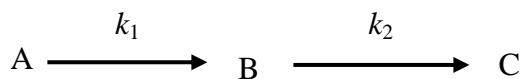


**Figure 5.** MTO Product distribution as a function of contact time. Reaction temperatures were 623 K (a), 673 K (b), 723 K (c), and 773 K (d), respectively. A ZSM-5 catalyst with a Si/Al ratio of 90 was employed. Methanol partial pressure was 17 kPa, diluted in N<sub>2</sub>.

As shown in the reaction pathways, the methanol conversion generally proceeds via kinetically sequential steps of olefin formation and aromatization. This consideration led to a simplified kinetic model [3]. The high temperature conversion of methanol to olefins over ZSM-5 zeolite was based on



where A = Methanol/DME, B = Olefins, C = aromatics + paraffins

The typical experimental data at 673 K were plotted as a function of contact time in Figure 6. Based on the consideration of an autocatalytic nature, the reaction rate for oxygenates conversion can be expressed as:

$$r_A = k_1 * [A] * (1 - [A]),$$

where [A] is the conversion (in C-mole percentage) for methanol/DME.

Given that the hydrogen transfer reaction was generally a bi-molecular reaction between two olefinic species, the aromatization rate was considered as:

$$r_B = k_2 * [B] * [B],$$

where [B] is the yield (in percentage) of olefins.

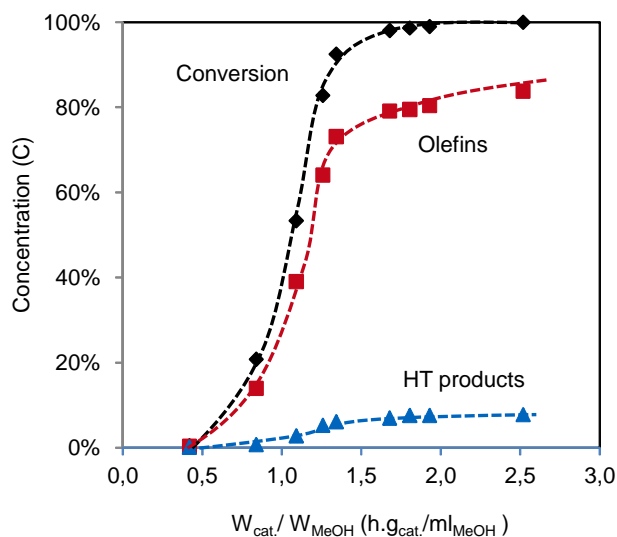


**Figure 6.** Methanol conversion, olefins product and HT products as a function of contact time. Reaction temperatures was 673 K. A ZSM-5 catalyst with a Si/Al ratio of 90 was employed. Methanol partial pressure was 17 kPa, diluted in N<sub>2</sub>.

Arrhenius plots of  $k_1$  and  $k_2$  (olefin formation and aromatics/paraffin formation, respectively) gave an estimation of the apparent activation energies for the two consecutive steps, as indicated in Figures 7. The activation energy for olefin formation was 93 kJ/mol, while the apparent activation energy for hydrogen transfer was only 9 kJ/mol. Due to such a distinct difference in temperature dependence of the reaction rates for the two steps, an increase in reaction temperature would significantly enhance the rate for olefin formation, while the rate for aromatization would only be slightly increased because of the apparently low activation energy. Therefore, higher temperature would help decouple the desired olefin formation and undesired aromatization steps, thereby enhancing selectivity to olefins. The obtained apparent activation energy for hydride transfer was in fair agreement with the reported  $E_{a,app}$  of 18 kJ/mol for hydride transfer reaction in n-hexane cracking over ZSM-5.

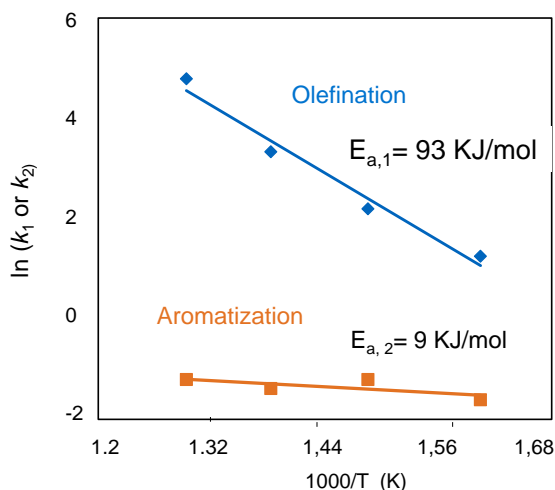


**Figure 7.** Arrhenius plot of rate coefficients of the two consecutive steps, olefination and aromatization, with reaction temperature. A ZSM-5 catalyst with a Si/Al ratio of 90 was employed. Methanol partial pressure was 17kPa, diluted in  $N_2$ .

The concentration profiles for propylene and hydride transfer products over H-ZSM-5 were plotted in Figure 8 as a function of contact time at various temperatures. The effect of a higher temperature on the product distribution in methanol conversion over HZSM-5 catalysts was similar to having a lower partial pressure of methanol at a constant reaction temperature, as will be shown in the next section. At 623 K, the formation of olefins was

highly coupled with the aromatization, and almost equal amount of aromatics and propylene were obtained at full conversion. When the reaction temperature was increased to 723 K, it was clearly shown that the olefin formation was largely decoupled from the aromatization. Increasing the temperature from 623 to 723 K brought the selectivity of propylene up from 25 to 48% at complete conversion, while the aromatics yield remained below 3%. This clearly proved that the increase of the temperature favored the synthesis of propylene.

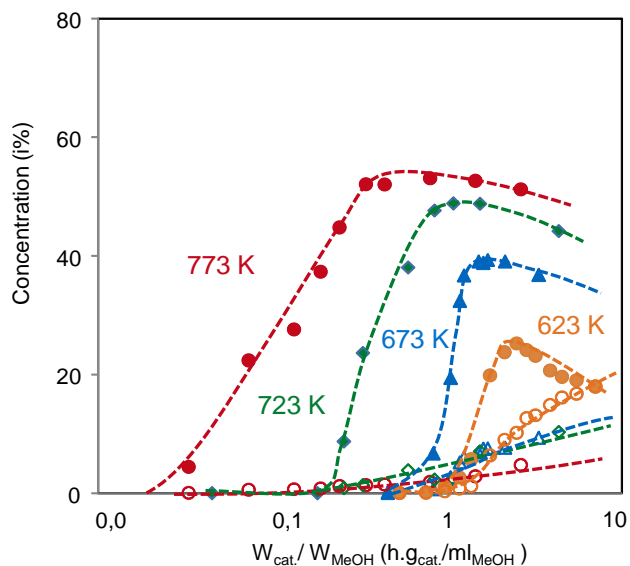


**Figure 8.** Propylene and HT products concentrations as a function of contact time. Reaction temperatures were 623 K (orange), 673 K (blue), 723 K (green), and 773 K (red), respectively. A ZSM-5 catalyst with a Si/Al ratio of 90 was employed. Methanol partial pressure was 17 kPa, diluted in N<sub>2</sub>. Filled symbols represented propylene and empty ones represented HT products.

#### 4.3.1.2 Impact of reaction temperature on MTO long-term performance

We are now in a position to conclude that a higher temperature favors the selectivity to propylene. However, further investigation on the impact of reaction temperature on the catalyst lifetime is needed, which constitutes the main target in this section. The impact of reaction temperature was shown on Figure 9. Higher reaction temperatures led to shortened catalyst lifetime. Even though the impact of reaction temperature on catalyst lifetime between 723 and 748 K was insignificant, a further increase in reaction

temperature significantly shortened the catalyst lifetime, which was defined as the time-on-stream until the conversion dropped to 95%. The lifetime was ca. 280 h at 723 K, while at 748 K this duration decreased to 240 h, and a further increase of reaction temperature to 773 K led to a lifetime of merely 150 h.

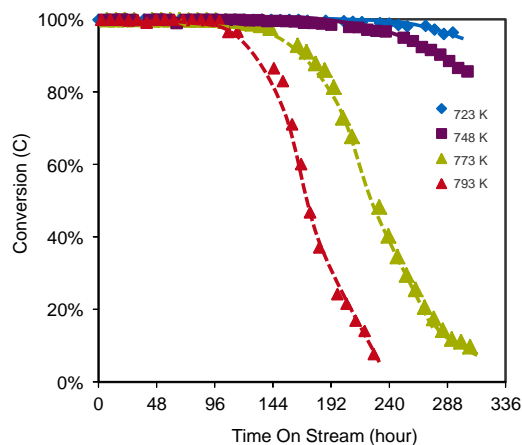


**Figure 9.** Methanol conversion as a function of time on stream. Reaction temperatures were 723 K (blue), 748 K (purple), 773 K (light green), and 793 K (red), respectively. A ZSM-5 catalyst with a Si/Al ratio of 90 was employed. Methanol partial pressure was 17 kPa, diluted in water.

The evolution of each hydrocarbon product was depicted in Figures 10 and 12, and the yield for each product as the initial time on stream was shown in Figure 11. An increase in reaction temperature led to the shift of the product spectrum from  $C_{4+}$  aliphatics to ethylene and propylene, indicating that increased reaction temperature results in higher cracking activity. At higher times on stream, the cracking activity decreased due to catalyst deactivation, and the product selectivity shifted to  $C_{5+}$ , as can be concluded from the peaks in  $C_{5+}$  concentration in Figure 10. Further deactivation led to the step decrease of conversion and the yield of each product.

It is noted that highly different from the observations in the partial pressure and co-feeding test at 723 K, opposite trends were shown for  $C_2^-$  and aromatics, indicative of a  $C_2^-$  formation route other than aromatics based cycle, namely  $C_6$  olefin cracking. This hypothesis obtained additional supports from the previous observation that a rise in reaction temperature leads to higher cracking activities.

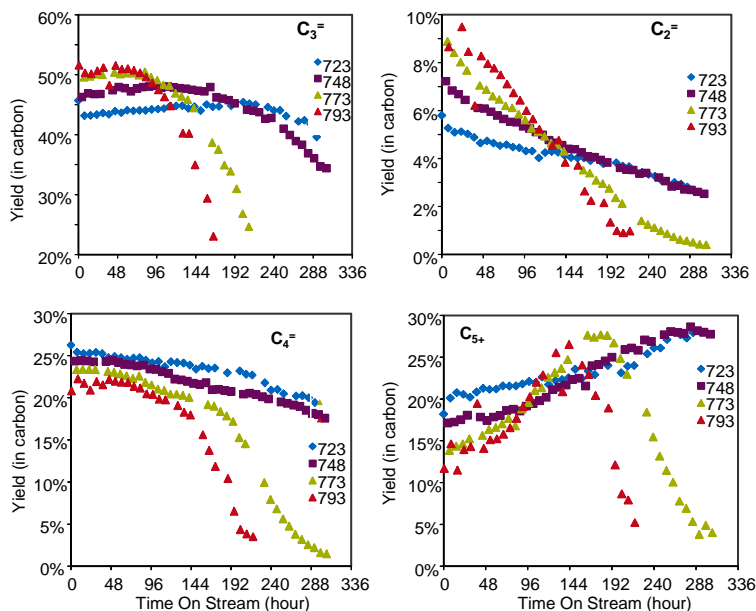


**Figure 10.** Concentration of various products as a function of time on stream, including propylene, ethylene, butenes, and C<sub>5+</sub> aliphatics. Reaction temperatures were 723 K (blue), 748 K (purple), 773 K (light green), and 793 K (red), respectively. A ZSM-5 catalyst with a Si/Al ratio of 90 was employed. Methanol partial pressure was 22 kPa, diluted in water.

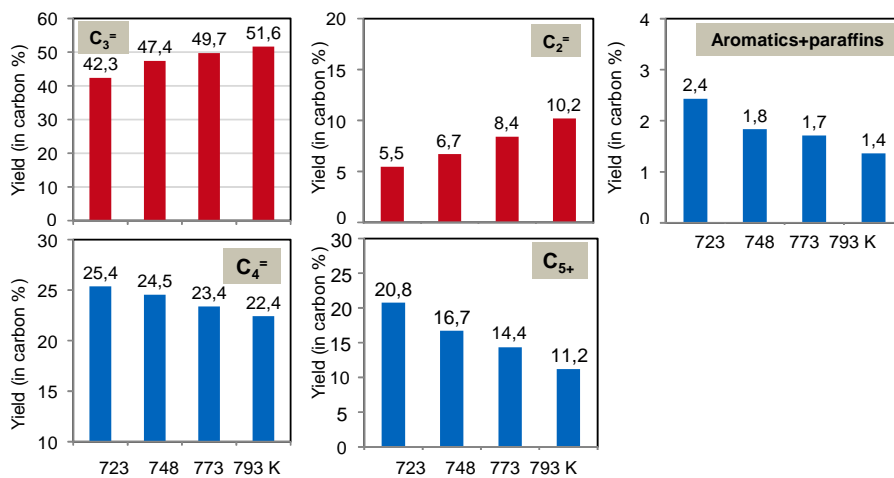


**Figure 11.** Impact of reaction temperature on the product distribution in terms of propylene, ethylene, butenes, and C<sub>5+</sub> aliphatics, and hydrogen transfer products. Reaction temperatures were 723 K, 748 K, 773 K, and 793 K, respectively. A ZSM-5 catalyst with a Si/Al ratio of 90 was employed. Methanol partial pressure was 22 kPa, diluted in water.

The impact of reaction temperature on hydrogen transfer was depicted in Figure 12.  $C_4$  Hydrogen Transfer Index ( $C_4$  HTI) was frequently used in the methanol chemistry to characterize the hydrogen transfer activity, which is defined as the ratio of  $C_4$  paraffins (n-butane and iso-butane) to the total  $C_4$  concentration. The  $C_4$  HTI is highest at 723 K and decreases with increasing reaction temperature. This indicates that the hydrogen transfer activity decreases, in line with the evolution of  $C_{2-4}$  paraffins yield with reaction temperature. The decrease of hydrogen transfer activity with reaction temperature can be ascribed to the decreased coverage of olefinic species with increased temperature because of the exothermic adsorption. However, increased reaction temperature favors the formation of methane from the methylbenzenes de-alkylation, as shown in Figure 12. The methane formation increases with time on stream, indicating that the formation path of methane is linked with the coke formation during catalyst deactivation with time on stream. The faster increase rate for methane formation at elevated reaction temperatures (773 and 793 K) indicates a fast aromatics formation (carbon and hydrogen mass balance).

Given that MTO is a highly exothermic reaction and adiabatic fixed-bed reactors are used in the Lurgi's MTP process, reaction temperature control is a critical issue, and accordingly, multi-staged feeding was employed to regulate the reaction heat [6-9]. The present data indicated that an optimal operation window of reaction temperature for the MTP reaction exists, which lies between 723 and 753 K isothermal reaction conditions under. A rise in reaction temperature within this range leads on the one hand to slightly shortened catalyst lifetime; on the other hand, a more important consequence is that higher temperature results in higher cracking activity which favors the formation of more ethylene and propylene and less hydrogen transfer products. Further increase in the reaction temperature to above 753 K, however, leads to a significant decrease in catalyst lifetime and more formation of unreactive methane simultaneously.



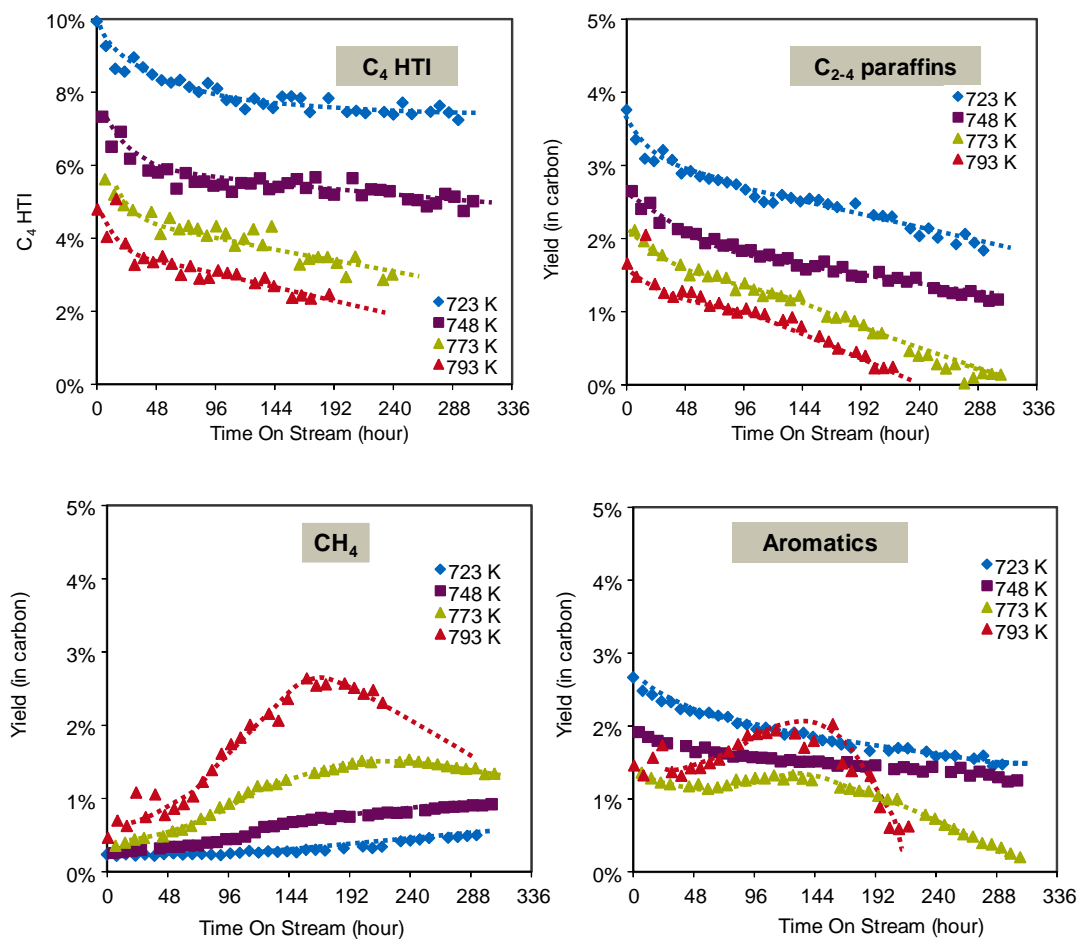


**Figure 12.** Concentration of various products as a function of time on stream, including C<sub>4</sub> HTI, methane, C<sub>2</sub>-C<sub>4</sub> paraffins, aromatics. Reaction temperatures were 723 K (blue), 748 K (purple), 773 K (light green), and 793 K (red), respectively. A ZSM-5 catalyst with a Si/Al ratio of 90 was employed. Methanol partial pressure was 22 kPa, diluted in water.

### 4.3.2 Effect of methanol pressure on product selectivity

Figure 13 showed detailed selectivity patterns for conversion of methanol over H-ZSM-5 at various methanol pressures. Obviously, it was experimentally confirmed that MTO reaction is not zero order in methanol pressure [5,13]. Moreover, at the reaction temperature of 623 K, upon lowering methanol pressure from 13 to 1 kPa, the propylene selectivity increased from 25 to 49% (reported at 100% methanol conversion), while aromatics selectivity decreased sharply from 10 to 1%. A similar impact was also observed at a reaction temperature of 723 K, as shown in Figures 14 and 15. At a fixed

contact time, an increase in methanol partial pressure resulted in increased methanol conversion rate, indicating a positive reaction order with respect to methanol (Figure 14). Furthermore, a decrease in methanol partial pressure increased the selectivity to propylene and decreased the selectivities to ethylene and hydride transfer products, as shown in Figure 15. Therefore, a lower methanol pressure tends to suppress the aromatization reactions and favor the olefin formation reactions, again due to the steeper dependence of hydride transfer rates on gas-phase methanol concentration.

As shown in Figure 15, varying the partial pressure of methanol imposed an evident impact on product selectivities. As previously discussed, the reaction rate constants  $k_1$  and  $k_2$  for olefin formation and aromatization showed different methanol partial pressure dependence, enabling kinetic decoupling of dehydration and hydride transfer steps in a consecutive reaction sequence via methanol pressure modulation. Indeed, a kinetic analysis, as shown in Figure 16, points to the fact that the olefination step has a reaction order of 0.9, while that the aromatization step shows a reaction order of 2.1. This means that the hydrogen transfer reactions have a larger dependence on the pressure than the olefin formation step. Therefore, a decrease in methanol partial pressure leads to the larger decrease of the reaction rate in the second step of hydrogen transfer, shifting the products to more olefins.

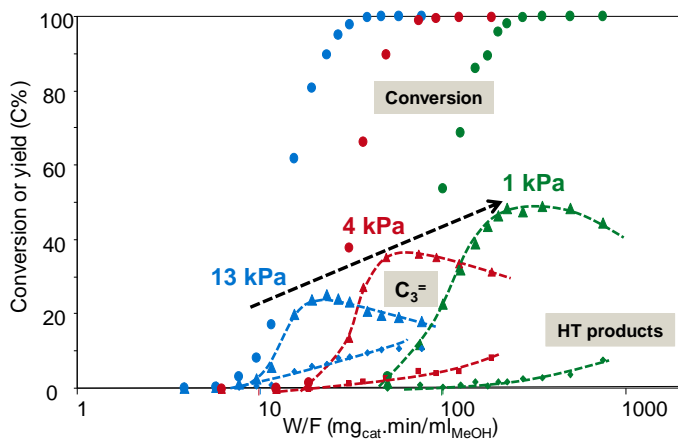


**Figure 13.** Effect of methanol pressure on product selectivities in terms of propylene and hydrogen transfer products. Reaction conditions: reaction temperature was 623 K. A ZSM-5 catalyst with a Si/Al ratio of 90 was employed. Methanol partial pressures were 1, 4 and 13 kPa, respectively.

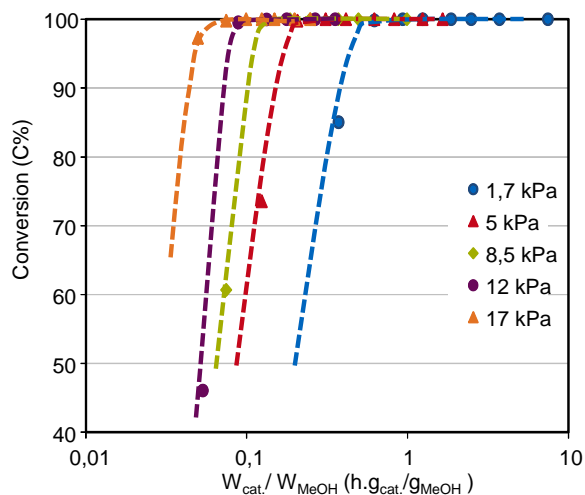


**Figure 14.** Methanol conversion as a function of contact time. Reaction temperature was 723 K. A ZSM-5 catalyst with a Si/Al ratio of 90 was employed. Methanol partial pressures were 1.7, 5, 8.5, 12, 17 kPa, respectively.

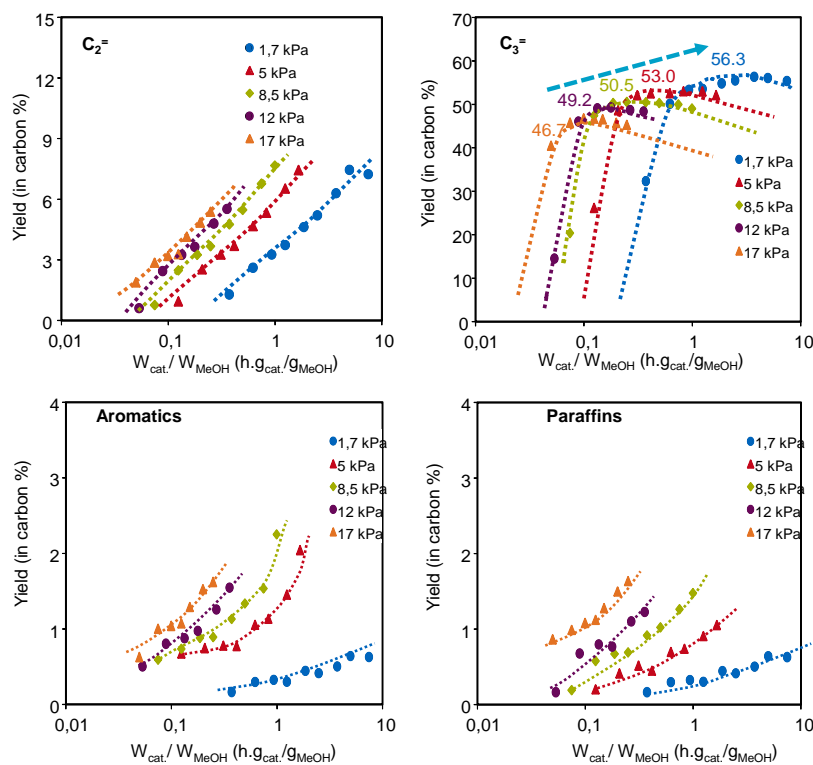


**Figure 15.** Effect of methanol pressure on product distributions in terms of ethylene, propylene, aromatics and paraffins. Reaction temperature was 723 K. A ZSM-5 catalyst with a Si/Al ratio of 90 was employed. Methanol partial pressures were 1.7, 5, 8.5, 12, 17 kPa, respectively.

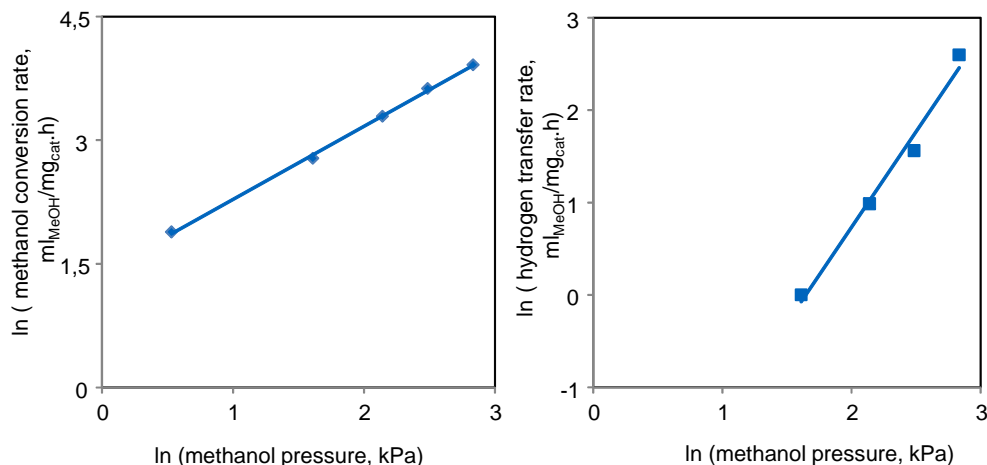


**Figure 16.** Correlations of methanol partial pressure and reaction rates in methanol conversion and hydrogen transfers. Reaction temperature was 723 K. A ZSM-5 catalyst with a Si/Al ratio of 90 was employed. Methanol partial pressures were 1.7, 5, 8, 12, 17 kPa, respectively.

A direct comparison of the product distribution at the identical methanol residence time was depicted in Figure 17. It is shown that lower methanol partial pressure leads to a product spectrum with more  $C_3^=$  and  $C_5$ , less  $C_2^=$ ,  $C_4^=$  and  $C_{6+}$ , and less products of hydride transfer.

A correlation of the maximum propylene yield (obtained from the experiments of changing space velocity) and methanol partial pressure was shown in Figure 18. A lower methanol pressure leads to a higher propylene peak yield. A linear relationship was correlated between the propylene peak yield and methanol partial pressure, suggesting a maximum of 57% at a methanol partial pressure approaching zero. Note that in a very recent literature reportedly at 15 kPa and 723-733 K, the  $C_3^=$  yield reached 55.6% and 57%, respectively (47 % in the reported case), raising concerns about the real carbon/mass balance in the reported literature [31].

From the perspective of industrial operations, especially in the Lurgi's MTP process, methanol was diluted by a large quantity of water which is a co-product of methanol conversion in significant concentrations [6-9]. This approach not only leads a good control of reaction heat, but also lowers the methanol partial pressure, which facilitate the selective production of targeted propylene, and correspondingly the formation of

aromatics that are the precursors leading to the catalyst coking. On the other hand, lowering the partial pressure resulted in a decrease of the methanol conversion rate, simply because the rate of reaction was positively proportional to the partial pressure of methanol. In addition, one apparent drawback of this approach, among others, is the increased difficulty in product separation from more dilute streams.

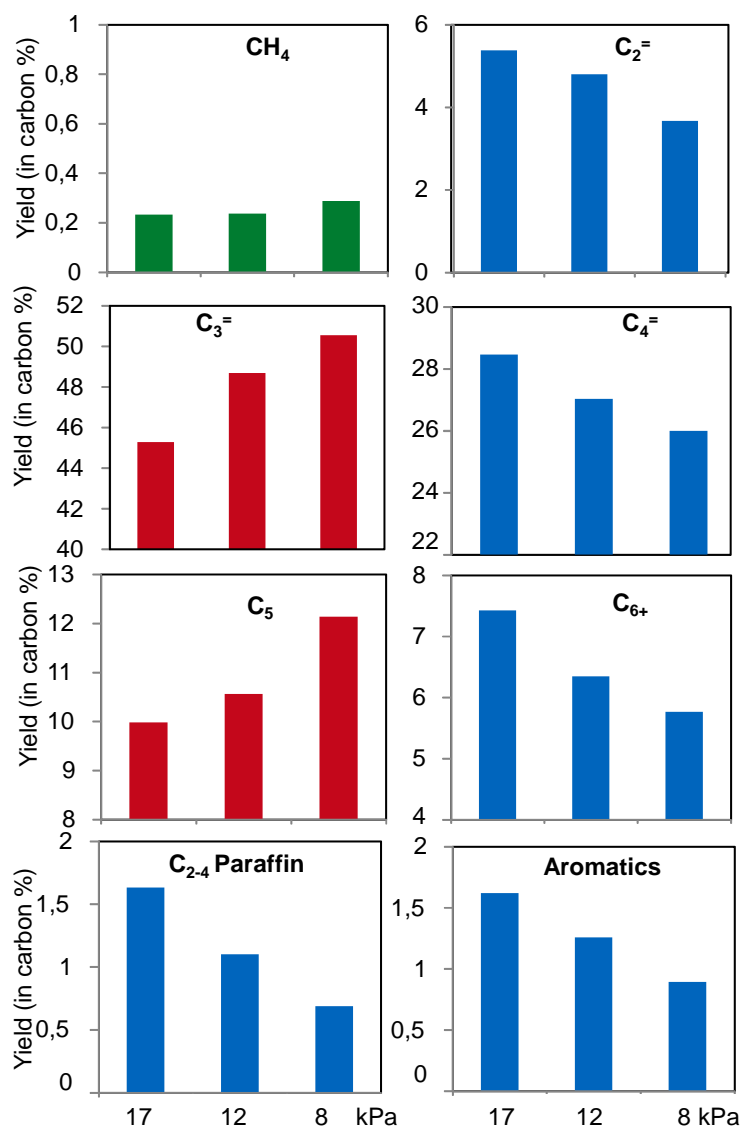


**Figure 17.** Effect of methanol pressure on product distributions in terms of ethylene, propylene, aromatics and paraffins. Reaction temperature was 723 K. A ZSM-5 catalyst with a Si/Al ratio of 90 was employed. Methanol partial pressures were 1.7, 5, 8.5, 12, 17 kPa, respectively.

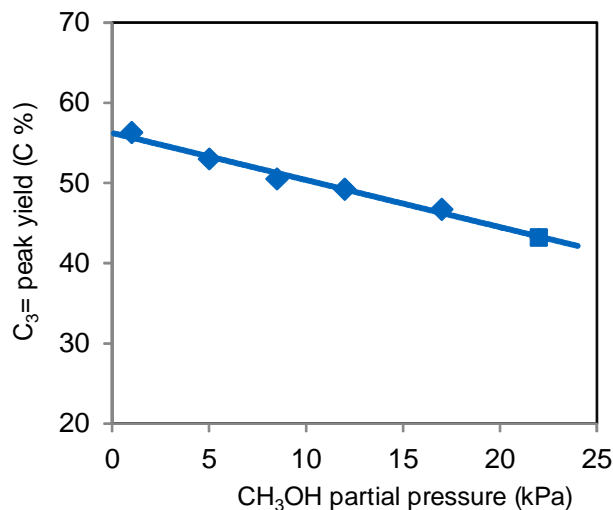


**Figure 18** Correlation of the peak propylene yield and methanol partial pressure. Reaction temperature was 723 K. A ZSM-5 catalyst with a Si/Al ratio of 90 was employed.

### 4.3.3 Impact of P doping

#### 4.3.3.1 Impact of phosphorous doping of ZSM-5 with various Si/Al ratios

Figure 19 depicts the impact of phosphorus loading on the product distribution. The parent material of Si/Al = 45 showed a high activity in methanol conversion. The peak propylene yield of 43.8% was achieved at a contact time when 100% methanol conversion was just reached. A further increase of contact time led to a decreased propylene yield, due to secondary reactions which produced ethylene, aromatics and paraffins (Figure 19 c and d). A phosphorous loading of 1.6 wt.% on the zeolite resulted in decreased activities in methanol conversion and secondary reactions as well (Figure 19). In addition to the decreased activity, the phosphorus doping also induced a significant change in the selectivity to propylene. Compared to a peak propylene yield of 43.8% over the unmodified parent material, the modified zeolite with phosphorus doping of 1.6 wt.% showed a remarkably higher peak propylene yield of 47.4%. A further increase in the phosphorus doping had a limited impact on the peak propylene yield. The P doped material showed a relatively more stable product distribution than the parent material after 100% methanol conversion was reached, due to the lower acidities which

led to slower secondary reactions producing ethylene and hydrogen transfer products, as indicated in Figure 19 c and d.

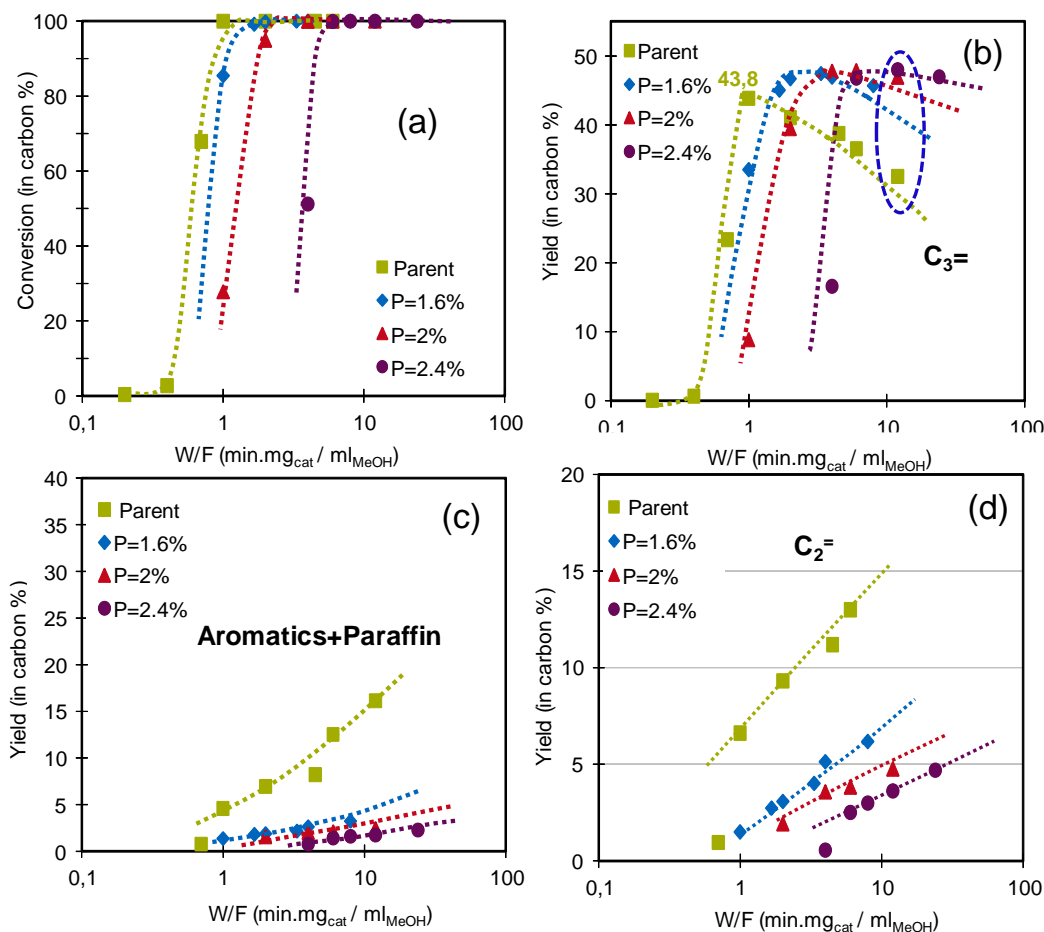


**Figure 19.** Impact of phosphorous loading on the MTO product distributions in terms of conversion (a), propylene (b), ethylene (c), aromatics and paraffins (d). Reaction temperature was 723 K. A ZSM-5 catalyst with a Si/Al ratio of 45 was employed as the parent material. Phosphorous loadings were 0, 1.6%, 2%, 2.4%, respectively.

Table 1 shows a comparison of product distributions at the contact times when the peak propylene yields were reached for each of the parent or phosphorous doped materials. It is clearly shown that phosphorous doping resulted in an improved selectivity to propylene, while further increase in P loading caused little change to the product distribution. The catalytic activity decreased consistently with increasing P loading, as can be seen from the increasing contact time required to reach 100% methanol conversion.

**Table 1.** Product distributions at the contact times when the 100% methanol conversions were initially reached for the parent and phosphorous modified Si/Al=45 HZSM-5 zeolite materials.

Catalyst	Si/Al	P =1.6%	P = 2%	P =2.4%
W/F	1	2.0	3	6
C <sub>2</sub>	6.6	3.9	4.0	3.8
C <sub>3</sub>	43.8	47.0	47.4	47.8
C <sub>4</sub>	27.2	26.7	26.8	26.8
C <sub>5</sub>	9.9	12.7	12.4	12.2
C <sub>6+</sub>	7.0	7.6	7.0	6.9
C <sub>2-4</sub> Paraffins	2.4	1.2	1.1	0.9
Aromatics	1.5	1.0	1.0	1.1

It was noted, however, that the extent of increase in propylene yield (from 43.8% to 47.8%) shown in the present work, though it was significant, was much less than that claimed in literature, in which increases by more than 10% were frequently reported [15-32]. The reason lies in the different criteria in comparison. In most of the reported work, the comparisons were made at a fixed contact time. In such cases, as shown in Figure 19 b, an increase in propylene yield of more than 15% (from 30% to 47%) was apparently observed. However, this kind of comparison showed the combined effects of activity of the zeolite and its intrinsic selectivity, both of which contribute to the final product distribution, as shown in Figure 19. A remarkably higher activity of the parent material would afford a low propylene selectivity at a relatively long contact time (i.e., 100% methanol conversion was already reached), which results from the secondary reactions of olefin transformation and hydrogen transfer. Therefore, we propose that a comparison of the product distribution at the contact times when the 100% methanol conversion was initially reached is more rigorous to reflect the difference in intrinsic selectivities.

Phosphorus doping was also applied to a Si/Al = 40 HZSM-5 zeolite and the results were reported in Figure 20. In addition to phosphoric acid as the P source which was used to modify the zeolites with a Si/Al ratio of 40 and 45, another approach was used to introduce phosphate modifications. Analogous to the method invented by Haw et al., trimethylphosphine was in-situ introduced with methanol to a Si/Al = 25 HZSM-5 zeolite, subsequently followed by an oxidation step at 823 K. The catalytic performance of the



modified materials after each cycle of phosphorous doping was tested and compiled in Table 2. The results shown in Figure 20 and Table 2 are in line with the data shown in Figure 19, evidencing that phosphorous modification led to an improved selectivity to propylene. A comparison of the product distribution for the phosphorous doped materials from three HZSM-5 zeolites with different acid densities, i.e., Si/Al = 25, 40, 45, respectively, led us to conclude that the maximum propylene yield does not exceed 48% under the studied reaction conditions, irrespective of the starting material.

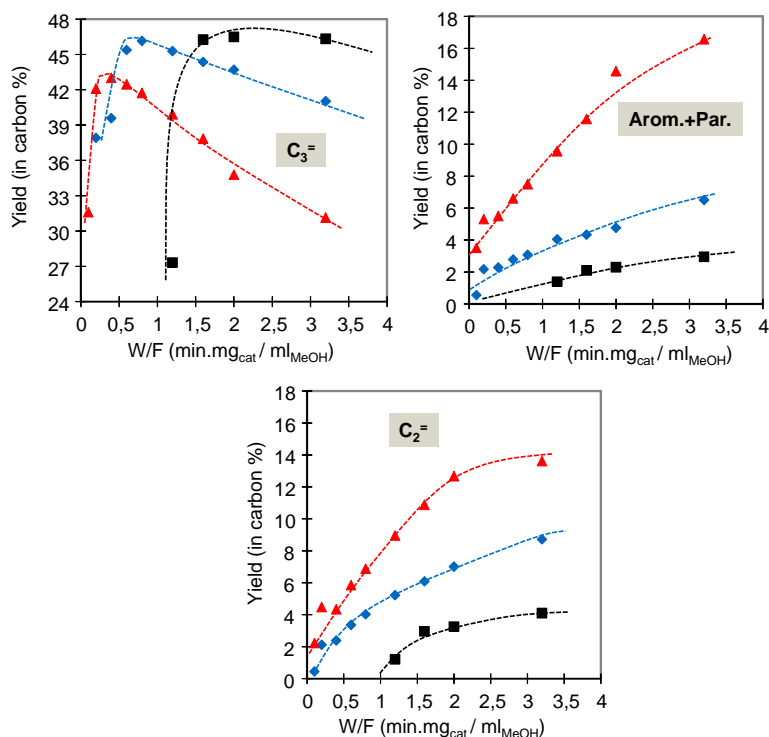


**Figure 20.** Impact of phosphorous loading on the MTO product distributions in terms of propylene (a), aromatics and paraffins (b), ethylene (c), Reaction temperature was 723 K. A commercial ZSM-5 catalyst (Zeolyst) with a Si/Al ratio of 40 was employed as parent material. Phosphorous loadings were 0 (red), 1.2 wt.% (blue), 2 wt.% (black), respectively.

Phosphorous modification was also applied to a zeolite with a high Si/Al ratio of 90, and the results are shown in Figure 21. While phosphorous doping led to a significant enhancement of selectivity to propylene for the zeolites with a low Si/Al ratio, the modified materials from the Si/Al = 90 zeolite showed little improvement on the selectivity to propylene. A loading of 1.2 wt.% resulted in an increase of less than 1% in

peak propylene yield. Consistent with the impact of higher phosphorus loading on the low Si/Al zeolite, the effect of phosphorus doping on the high Si/Al zeolite is mainly to decrease the activity of the materials.

**Table 2.** Product distribution as a function of phosphorous doping cycles for the parent and phosphorous modified Si/Al = 25 HZSM-5 zeolite materials. The procedures of trimethylphosphine introduction and oxidation are analogous to the method reported by Haw et al. [30]. Reaction temperature was 723 K, and catalyst charge is 200 mg. Methanol feed carried by pass N<sub>2</sub> with a flow rate of 50 ml/min through a saturator thermostated at 298K.

Product	Cycle							
	0	1	2	3	4	5	6	
C <sub>2</sub>	16.7	15.8	10.6	11.1	5.7	<b>3.5</b>	2.5	
C <sub>3</sub>	28.5	33.5	37.0	40.5	46.5	<b>47.8</b>	38.7	
C <sub>4</sub>	17.6	21.1	23.7	25.9	28.9	<b>26.9</b>	21.0	
C <sub>5</sub>	8.0	8.5	8.3	8.7	9.7	<b>13.4</b>	15.0	
C <sub>6+</sub> aliphatics	6.0	6.7	6.9	6.9	6.6	<b>6.6</b>	9.0	
Arom. +Par.	23.2	14.4	13.5	6.9	2.7	<b>1.9</b>	0.9	
Conversion	100.0	100.0	100.0	100.0	100.0	<b>100.0</b>	87	

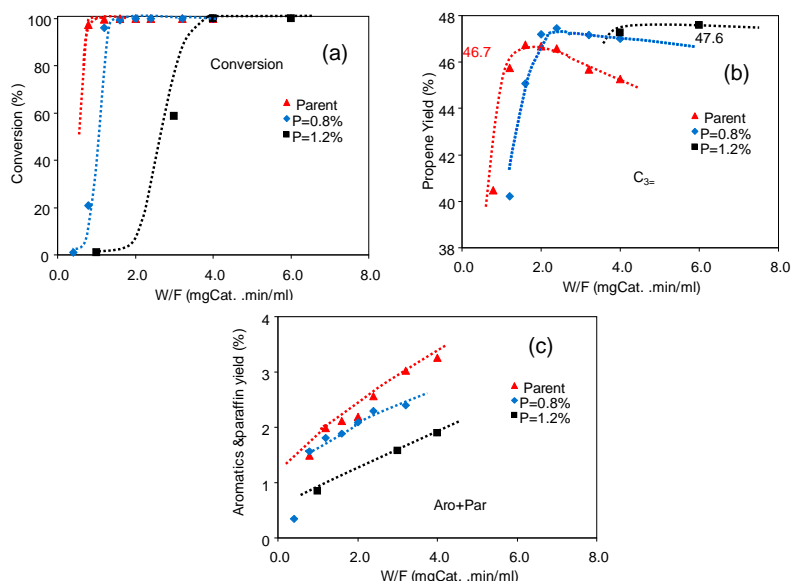


**Figure 21.** Impact of phosphorous loading on the MTO catalytic performance in terms of conversion (a), propylene (b), aromatics and paraffins (c), Reaction temperature was 723 K. A commercial ZSM-5 catalyst

(Zeolyst) with a Si/Al ratio of 90 was employed as parent material. Phosphorous loadings were 0 (red), 0.8% (blue), 1.2% (black), respectively.

The almost identical product distribution at the contact times when the peak propylene yield was reached for the parent and phosphorous modified HZSM-5 zeolite materials with Si/Al = 25, 40, 45, 90, respectively (Table 3), led us to conclude that doping an appropriate concentration of P to the HZSM-5 zeolites with low Si/Al ratios is able to effectively enhance the propylene selectivity to reach the level on high Si/Al ZSM-5 zeolites, while it has a limited ability to further improve the propylene selectivity of high Si/Al ZSM-5 zeolites.

**Table 3.** Product distribution at the contact times when the peak propylene yield were reached for the parent and phosphorous modified Si/Al = 25, 40, 45, 90 HZSM-5 zeolite materials, respectively.

Catalyst	Si/Al=25 P= 2.5%	Si/Al=40 P= 2%	Si/Al=45 P= 2%	Si/Al=90 P= 0%	Si/Al=90 P=0.8%	Si/Al=90 P=1.2%
W/F	6	4.0	6	1.6	2.4	6.0
C <sub>2</sub>	3.5	4.0	3.8	3.2	3.5	2.5
C <sub>3</sub>	47.8	47.4	47.8	46.7	47.5	47.6
C <sub>4</sub>	26.9	26.8	26.9	26.1	26.6	25.6
C <sub>5</sub>	13.4	12.4	12.2	13.4	12.9	14.4
C <sub>6+</sub>	6.9	7.0	6.8	8.2	7.3	8.2
C <sub>2-4</sub> Paraffins	0.9	1.1	0.9	1.3	1.3	1.0
Aromatics	1.0	1.0	1.1	1.0	1.0	0.9

It is well established that the acid density dictates to a large extent the MTO product distribution over HZSM-5 catalysts [3]. A low acid density, associated with a high Si/Al ratio, leads to the decoupling of the two consecutive steps, olefination and aromatization, shifting the product selectivity to C<sub>3+</sub> olefins especially propylene. Through a series of experiments with HZSM-5 zeolites of Si/Al ratios ranging from 20 to 500, Chang et al. reported that the selectivity to propylene increased with increasing Si/Al ratio, and the maximum propylene selectivity was achieved at a Si/Al ratio of ca. 200 [3]. Further increasing the Si/Al decreased the activity further but caused insignificant change on the product selectivity [3]. This is analogous to the effect of phosphorous modification

shown in the present work. It is also well established in literature that phosphorous modification resulted in significantly decreased Brønsted acidity of the zeolite material, though the structures of the directly or indirectly interacting P-species are still controversial [15-32]. Phosphorous doping of the low Si/Al zeolites resulted in a decreased acid density, leading to an improved selectivity to propylene. When the modified material reached an acid density comparable to that of a HZSM-5 zeolite of Si/Al = 100, a further increase in phosphorous loading led to insignificant enhancement on propylene selectivity.

It is noted that Haw et al. [30] reported recently that in addition to the effect of decreased acidity, phosphorous species could interact via hydrogen bonding with adjacent Brønsted acid sites, which resulted in the reduction of the functional channel intersections and thus introduced a transition-state shape selectivity to the space-demanding reactions such as aromatization, which in turn accounted for (in part) the improvement in the selectivity to propylene. Through a repetition of the reported modification method with the same commercial material and the comparison of the MTO product distributions for the various unmodified and modified materials (Table 3), we propose that such an effect is insignificant in comparison with the contribution from the modified acidity.

#### *4.3.3.2 Impact of test conditions and water washing on Phosphorous modified materials*

We are in a position to conclude that phosphorous doping leads to a decreased activity, and enhanced propylene selectivity for the HZSM-5 zeolites with low Si/Al ratios. To evaluate the long-term catalytic performance of these phosphorous modified materials under industrially relevant reaction conditions, two phosphorous doped Si/Al = 45 HZSM-5 zeolites (named as MFI90-1.6%P and MFI90-2.0%P, respectively), were tested in the home-made 10-fold parallel reaction unit. Instead of N<sub>2</sub> dilution used in the previous section, a water diluted methanol feed (methanol pressure 22 kPa) was used in this section to evaluate the catalytic performance of these phosphorous modified materials. Figure 22 shows a comparison of the catalytic performance of two phosphorous doped Si/Al = 45 HZSM-5 zeolites (MFI90-1.6% P and MFI90-2.0% P) and the parent material. These two P-modified zeolites showed in the previous section

comparable activities and selectivity to propylene as the Si/Al = 90 zeolite. Further decreased P loadings (0.2 and 0.4 wt.%) did not improve significantly the catalytic performance in terms of increments in propylene selectivity or decreases in hydrogen transfer activity (results not shown).

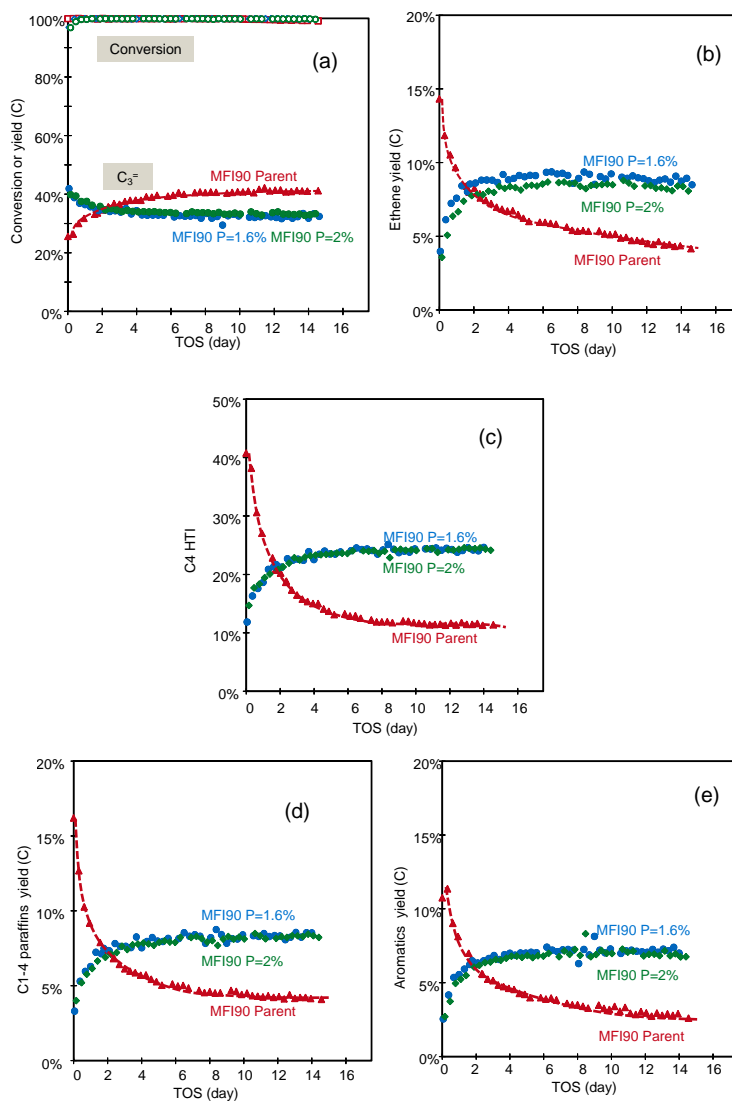


**Figure 22.** Product distributions in terms of conversion and propylene (a), ethylene (b), C<sub>4</sub> HTI (c), paraffins (d) and aromatics (e) as a function of time on stream. Reaction temperature was 723 K. A water diluted methanol feed was used. Methanol pressure was 22 kPa, diluted in water. Weight hourly space velocity (methanol) was 1.5 h<sup>-1</sup>. Three catalysts were evaluated: MFI90 (Si/Al=45) parent material (red), MFI90-1.6% (blue), MFI90-2% (green).

The Si/Al = 45 parent material experienced a large increase of propylene yield from 25 to 40% within the first four days (Figure 22a), along with a decrease in the yield of ethylene (Figure 22b) and hydrogen transfer index (Figure 22c). Specifically, light paraffins (C<sub>1-4</sub>, Figure 22d) and aromatics (Figure 22e) decreased by a factor of 3-4 in the first four days. In contrast, the two phosphorous doped samples showed a higher propylene yield and lower hydrogen transfer ability at the initial time on stream, but their hydrogen transfer activities increased remarkably with time on stream, characterized by the increased C<sub>4</sub> HTI, light paraffins and aromatics and decreased propylene yield, until a steady performance was achieved after 4 days of time on stream. The phosphorous doped samples showed significantly lower propylene yield and higher hydrogen transfer activity compared to parent materials after 2 days time on stream. This is in stark contrast to the results in the previous section, in which the phosphorous doped materials showed increased propylene selectivity and decreased hydrogen transfers when tests were performed under N<sub>2</sub> dilution.

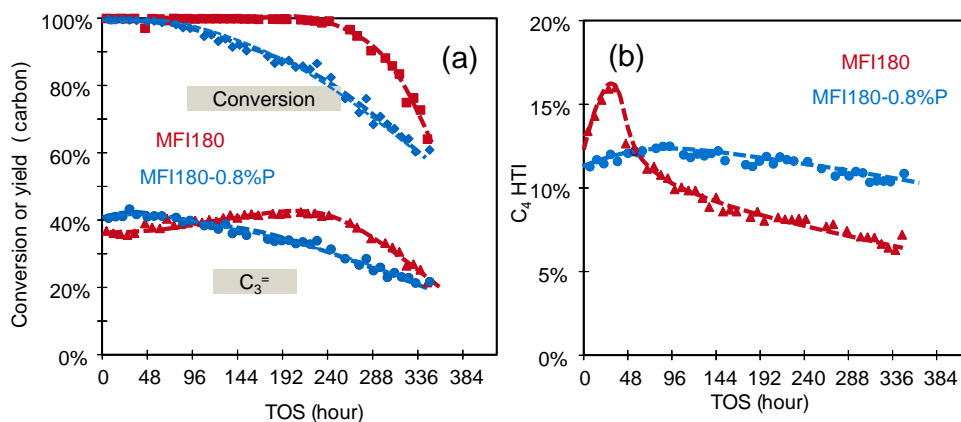


**Figure 23.** Conversion, propylene yield (a) and C<sub>4</sub> HTI (b) as a function of time on stream. Reaction temperature was 723 K. A water diluted methanol feed was used. Methanol pressure was 22 kPa. Weight hourly space velocity (methanol) was 1.5 h<sup>-1</sup>. Two catalysts were evaluated: MFI180 (Si/Al=90) parent material (red), MFI180-0.8% (blue).

Then a HZSM-5 sample with Si/Al = 90 was doped with 0.8 wt.% phosphorous (named as MFI180-0.8%P) and tested also under water dilution. Figure 23 shows a comparison of catalytic performance of the parent Si/Al = 90 HZSM-5 zeolite and the 0.8 wt.%

phosphorous doped material (MFI180-0.8%P). Compared with a lifetime (i.e., the TOS until 95% conversion threshold was reached) of 11 days for the parent material, the 0.8 wt.% phosphorous doped material showed a lifetime of only 4 days (Figure 23a), indicating that doping of 0.8 wt.% phosphorous reduced remarkably the catalyst activity. During the initial time on stream, the parent zeolite showed a decrease in propylene yield and an increase in C<sub>4</sub> HTI (Figure 23 a and b). This can be ascribed to the well-known phenomenon of “in-situ” steaming and generation of some new acid sites which are highly active in hydrogen transfer. The propylene yield started to increase after 2 days of time on stream, due to the decreased in catalyst activity by deactivation. The peak propylene yield for the parent was 1% higher than the doped material. The 0.8 wt.% phosphorous doped material showed a higher C<sub>4</sub> HTI than the parent zeolite, but only after TOS of more than 60 h (Figure 23b).

Figure 24 depicted the C<sub>4</sub> HTI as a function of methanol conversion for the 0.8 wt.% phosphorous doped and parent materials. Compared at the same conversion, The 0.8 wt.% phosphorous doped showed a significantly higher ability in hydrogen transfer than the parent zeolite. Compared to a lifetime of 11 days for the parent material, the 0.8 wt.% phosphorous doped material showed a lifetime of only 4 days, indicating that doping of 0.8 wt.% phosphorous reduced remarkably the catalyst activity.

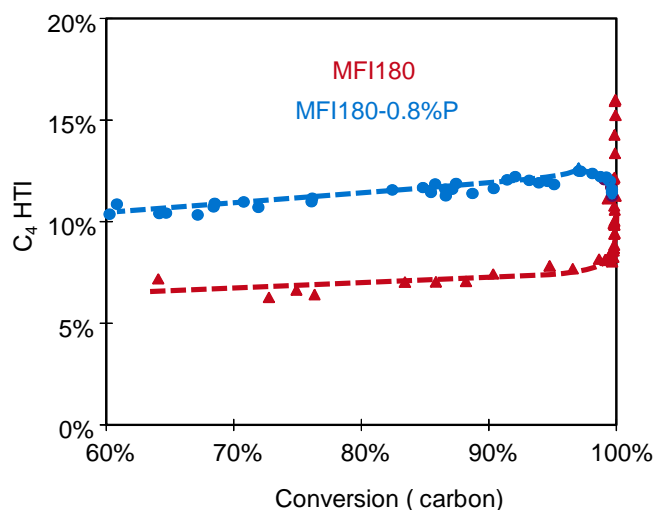


**Figure 24.** C<sub>4</sub> HTI as a function of methanol conversion. Reaction temperature was 723 K. Weight hourly space velocity (methanol) was 1.5 h<sup>-1</sup>. A water diluted methanol feed was used. Methanol pressure was 22 kPa. Two catalysts were evaluated: MFI180 (Si/Al=90) parent material (red), MFI180-0.8% (blue).

Considering that 0.8 wt.% P loading caused a significant decrease in catalyst lifetime due to over-suppressed acid density, the HZSM-5 90 material was modified with a lower P loading, 0.2 wt.%. The sample was evaluated under water dilution and the results were shown in Figure 25. The observations were similar to the case of the Si/Al = 45 HZSM-5, and the 0.2 wt.% phosphorous doping also led to a significantly lower propylene yield and a higher hydrogen transfer activity compared to the parent Si/Al = 90 steamed sample. The positive effect is that, unlike the case of 0.8 wt.% phosphorous modified sample shown in Figure 23, the 0.2 wt.% phosphorous doped material showed significantly prolonged lifetime. As shown in Figure 25, a further steam treatment of the phosphorous doped material before catalytic testing changed little the catalytic performance.

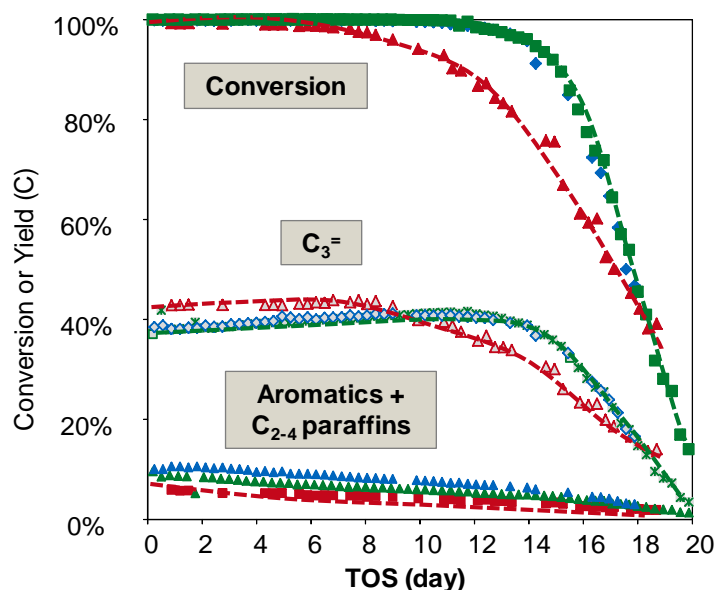


Figure 25. Conversion, propylene, and HT products as a function of time on stream. Reaction temperature was 723 K. A water diluted methanol feed was used. Methanol pressure was 22 kPa. Weight hourly space velocity (methanol) was  $1.5 \text{ h}^{-1}$ . Three catalysts were evaluated: MFI180 (Si/Al=90) parent material (red), MFI180-0.2%P (blue), MFI180-0.2%P-steamed (green).

Therefore, from the above tests of the phosphorous doping effects on both the Si/Al = 45 and 90 zeolites, we can draw the conclusion that under water-dilution conditions, while the catalyst lifetime is prolonged when the P loading is low (0.1-0.2%), a direct



phosphorous doping of the parent material results in a negative effect on the propylene selectivity and enhances the undesired hydrogen transfer ability. The observed negative effect is apparently opposite to the findings in the previous section that a phosphorous doping resulted in enhanced propylene selectivity and suppressed hydrogen transfer activity when tests were performed under N<sub>2</sub> dilution.

To gain insights into the effect of test conditions, i.e., the impact of water on phosphorous doping, the samples with a 1.2-3.4 wt.% phosphorous loading, which showed very low activities in the MTO reaction, was treated with hot water (353 K) to remove most of the phosphorous species. Then, the hot water washed samples were tested under N<sub>2</sub>-dilution conditions. The results were compared with the parent Si/Al = 90 zeolite, and shown in Figure 26 and Table 4. Similar to the performance of a phosphorous modified material directly tested under water-dilution conditions, the phosphorous modified material after hot water washing exhibited lower propylene selectivity and higher hydrogen transfer activity than the parent material (Table 4).

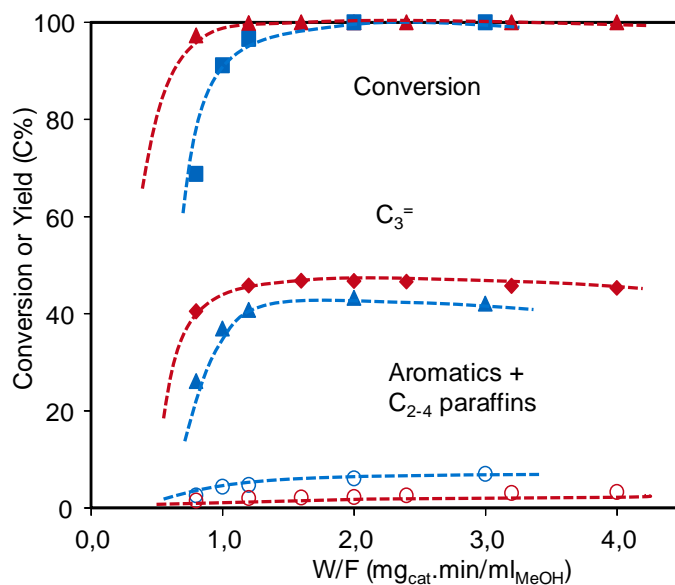


**Figure 26.** Conversion, propylene as a function of time. Reaction temperature was 723 K. Methanol pressure was 17 kPa, diluted in N<sub>2</sub>. Two catalysts were evaluated: MFI180 (Si/Al=90) parent material (red), MFI180-1.2% P-washed (blue).

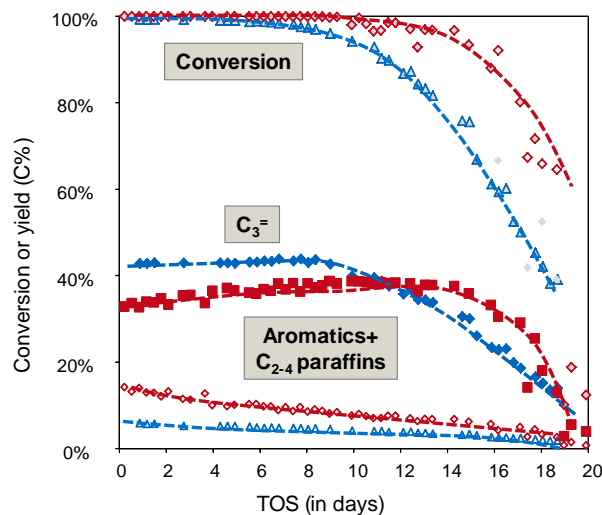


**Figure 27.** Conversion, propylene, and HT products yields as a function of time on stream. Reaction temperature was 723 K. A water diluted methanol feed was used. Methanol pressure was 22 kPa. Weight hourly space velocity (methanol) was  $1.5 \text{ h}^{-1}$ . Two catalysts were evaluated: MFI180 (Si/Al=90) parent steamed material (blue), MFI180-0.2%P-washed (red).

**Table 4.** Effect of the procedure of hot water washing on the catalytic performance of parent HZSM-5 zeolites (Si/Al = 90), and modified materials with various phosphorous loadings. Reaction temperature was 723 K. Methanol partial pressure was 17 kPa, diluted with  $\text{N}_2$ . The flow rate of  $\text{N}_2$  was 50 ml/min. Catalyst charges were shown in the table.

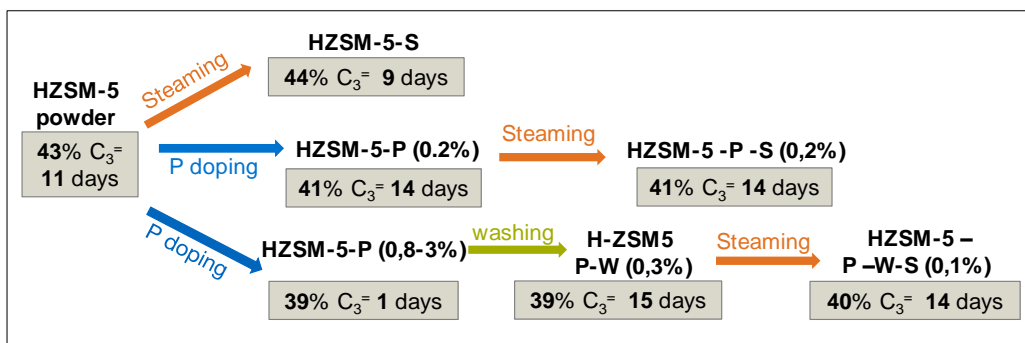
P loading (after washing)	0	1.2 (0.3)	2 (0.5)	3 (0.2)	3.4 (0.4)
Catalyst charge (mg)	100	100	80	60	150
$\text{C}_1$	0.2	0.3	0.3	0.3	0.3
$\text{C}_2$	3.3	5.3	4.4	4.0	7.3
$\text{C}_3$	46.7	44.0	44.4	43.3	42.0
$\text{C}_4$	26.0	25.3	24.4	22.7	26.0
$\text{C}_5$	13.4	11.6	13.1	13.8	9.9
$\text{C}_{6+}$	8.2	8.1	9.2	10.5	7.6
Aromatics	1.1	2.8	2.1	2.2	3.7
$\text{C}_{2-4}$ Paraffins	1.1	2.4	2.2	2.3	3.3
Conversion	100	100	99.7	99.2	100

Figure 27 depicts the catalytic performance tested under water dilution of the parent Si/Al = 90 steamed zeolite and the hot water washed counterpart after phosphorous doping. The

catalytic performance of the hot water washed material is similar to the performance of the directly phosphorous doped zeolite shown in Figure 25.

An overview of the catalytic performance of the phosphorous modified materials tested under water dilution is summarized in Figure 28. It is concluded that a low (0.1-0.2%) phosphorous loading, no matter pre-treated with hot water washing or not, leads to prolonged lifetime but a lower propylene yield.

From the results shown in this section, it can be seen that it is water that changed the catalytic properties of the phosphorous modified samples. Although these phosphorous modified samples are stable when tested with N<sub>2</sub> diluted methanol, their properties, i.e., the interactions between phosphorous species and zeolite, change when the material is subject to water in high concentrations, either if it is pre-treated by hot water washing or directly tested with water-diluted methanol feed. The present work proposes that the structure of the interaction of phosphorous species is dynamic and subject to change when a higher concentration of water exists. More physicochemical analyses are necessary to unravel the intriguing working mechanism.



**Figure 28.** An overview of the catalytic consequences of the phosphorous modified materials tested under water dilution. Reaction temperature was 723 K. Weight hourly space velocity (methanol) was 1.5 h<sup>-1</sup>.

## 4.4 Conclusions

Methanol conversion proceeds generally via two consecutive steps, olefin formation and hydrogen transfer. These two steps have highly different dependences on the reaction temperature, shown by an  $E_{a,app}$  of 93 kJ/mol for the step of olefin formation and 9 kJ/mol

for the second step of hydrogen transfer. Therefore, an increase of reaction temperature leads to the decoupling of these two steps and shifts the product selectivity to C<sub>3+</sub> olefins, especially propylene, and less undesired hydrogen transfer products, i.e., C<sub>2-4</sub> paraffins and aromatics are formed. A test on the impact of reaction temperature on catalyst lifetime suggests that an optimal operation window of reaction temperature for the MTP reaction exists, which lies between 723 and 753 K. A rise in reaction temperature within this range leads on one hand to slightly shortened catalyst lifetime; on the other hand, higher temperature results in higher cracking activity which favors the formation of more ethylene and propylene and less hydrogen transfer products. A further increase in the reaction temperature to above 753 K, however, leads to a significant decrease in catalyst lifetime and simultaneously to an increase in the formation of unreactive methane. The two consecutive steps have highly different dependencies on methanol pressure. The step of methanol conversion to olefins has a positive order between zero and one under reaction temperatures close to the practical MTP operations, while the reaction order with respect to methanol (or olefins) is close to two in the step of hydrogen transfer. Thus, analogous to the impact of reaction temperature, a reduced methanol pressure results in the decoupling of these two steps and shifts the product selectivity to olefins and especially propylene. However, this approach is limited by practical operations. Phosphorous modification has been applied to zeolites of various Si/Al ratios. It is shown that doping an appropriate concentration of P to HZSM-5 zeolites with low Si/Al ratios effectively enhances the propylene selectivity to reach the level on ZSM-5 zeolites with high Si/Al ratios. However, P doping has a limited positive impact on the high Si/Al ZSM-5 zeolites with respect to propylene selectivity. On the other hand, phosphorous doping leads to a reduced activity. A further investigation on the impact of test conditions, i.e., N<sub>2</sub>- or water- diluted feed, leads to the conclusion that the phosphorous doped materials are unstable when interacting with feeds with high water concentrations. While these P doped materials showed a positive impact on the propylene selectivity when tested under N<sub>2</sub> dilution, a decrease in propylene selectivity and an increase in hydrogen transfer ability was observed under water dilution conditions. This conclusion applies to phosphorous doped material either directly tested with water- diluted methanol feed or

after pre-treatment with hot water washing. Only low phosphorous loadings of 0.1-0.2 wt.% were effective in prolonging the catalyst lifetime.

## **4.5 Acknowledgements**

The authors acknowledge the financial support from Clariant Produkte (Deutschland) GmbH and fruitful discussion within the framework of MuniCat.

## **4.6 References**

- [1] T. Mokrani, M. Scurrrell, *Catal. Rev. Sci. Eng.* 51 (2009) 1.
- [2] G.A. Olah, *Angew. Chem. Int. Ed.* 44 (2005) 2636.
- [3] C. D. Chang, *Catal. Rev. Sci. Eng.* 25 (1983) 1.
- [4] M. Stöcker, *Micropor. Mesopor. Mater.* 29 (1999) 3.
- [5] U. Olsbye, S. Svelle, M. Bjorgen, P. Beato, T. V. W. Janssens, F. Joensen, S. Bordiga, K. P. Lillerud, *Angew. Chem. Int. Ed.* 51 (2012) 5810.
- [6] H. Koempel, W. Liebner, *Stud. Surf. Sci. Catal.* 167 (2007) 261.
- [7] H. Bach, L. Brehm, S. Jensen, 2004, EP 2004/018089 A1.
- [8] G. Birke, H. Koempel, W. Liebner, H. Bach, 2006, EP2006048184.
- [9] M. Rothaemel, U. Finck, T. Renner, 2006. EP 2006/136433 A1.
- [10] B. V. Vora, T. L. Marker, P. T. Barger, H. R. Nielsen, S. Kvisle, T. Fuglerud, *Stud. Surf. Sci. Catal.* 107 (1997) 87.
- [11] *Chem. Eng. News* 2005, 83 (50) 18.
- [12] J. Liang, H. Li, S. Zhao, W. Guo, R. Wang, M. Ying, *Appl. Catal.* 64 (1990) 31.
- [13] S. Ilias, A. Bhan, *ACS Catal.* 3 (2013) 18.
- [14] L. H. Ong, M. Domok, R. Olindo, A. C. van Veen, J. A. Lercher, *Micropor. Mesopor. Mater.* 164 (2012) 9.
- [15] W. W. Kaeding, C. Chu, L. B. Young, B. Weinstein, S. A. Butter, *J. Catal.* 67 (1981) 159.
- [16] W. W. Kaeding, C. Chu, L. B. Young, S. A. Butter, *J. Catal.* 69 (1981) 392.
- [17] J. A. Lercher, G. Rimplmayr, *Appl. Catal.* 25 (1986) 215.
- [18] J. A. Lercher, G. Rimplmayr, H. Noller, *Acta Phys. Chem.* 31 (1985) 71.
- [19] J. C. Vedrine, A. Auroux, P. Dejaifve, V. Ducarme, H. Hoser, S. Zhou, *J. Catal.* 73 (1982) 147.
- [20] H. Vinek, G. Rimplmayr, J. A. Lercher, *J. Catal.* 115 (1989) 291.
- [21] J. Caro, M. Bülöw, M. Derewinski, J. Haber, M. Hunger, J. Kärger, H. Pfeifer, W. Storek, B. Zibrowius, *J. Catal.* 124 (1990) 367.
- [22] G. Seo, R. Ryoo, *J. Catal.* 124 (1990) 224.

- [23] G. Oehlmann, H.G. Jerschke, G. Lischke, R. Eckelt, B. Parlitz, E. Schreier, B. Zibrowius, E. Loeffler, *Stud. Surf. Sci. Catal.* 65 (1991) 1.
- [24] G. Lischke, R. Eckelt, H.G. Jerschke, B. Parlitz, E. Schreier, W. Storek, B. Zibrowius, G. Oehlmann, *J. Catal.* 132 (1991) 229.
- [25] D. Liu et al. *Catalysis Today* 164 (2011) 154.
- [26] N. Xue, X. Chen, L. Nie, X. Guo, W. Ding, Y. Chen, M. Gu, Z. Xie, *J. Catal.* 248 (2007) 20.
- [27] T. Blasco, A. Corma, J. Martinez-Triguero, *J. Catal.* 237 (2006) 267.
- [28] D. Van VU, Y. Hirota, N. Nishiyama, Y. Egashira, K. Ueyama, *J. Japan Petroleum Inst.* 53 (2010) 232.
- [29] W. Dehertog, G. Froment, *Appl. Catal.*, 71 (1991) 153.
- [30] S. Abubakar, D. Marcus; J. Lee; et al. *Langmuir* 22 (2006) 4846.
- [31] J. Liu, C. Zhang, Z. Shen, M. Hua, Y. Tang, W. Shen, Y. Yue, H. Xu, *Catal. Comm.* 10 (2009) 1506.
- [32] J. Nunan, H. Cronin, J. Cunningham, *J. Catal.* 87 (1984) 77.
- [33] T. V. W. Janssens, *J. Catal.* 264(2009) 130.
- [34] N. Y. Chen, W.J. Reagan, *J. Catal.* 59 (1979) 123.

# *Chapter 5*

## **Summary and conclusions**

The catalytic conversion of methanol to olefins (MTO) is regarded as an alternative to alleviate the dependence on crude oil for the production of platform petrochemicals, i.e., ethylene and propylene. The control of product selectivity, as one of the key issues in MTO, necessitates an in-depth fundamental understanding on the extremely complex reaction network.

Methanol conversion proceeds generally via two consecutive steps, olefin formation and hydrogen transfer. These two steps have highly different dependences on the reaction temperature and pressure, shown by apparent activation energies and reaction orders. Therefore, an increase of reaction temperature or a decrease of methanol pressure decouples these two steps and shifts the product selectivity to propylene, and less undesired hydrogen transfer products, i.e., C<sub>2-4</sub> paraffins and aromatics are formed. A test on the impact of reaction temperature on catalyst lifetime suggests an optimal operation window of reaction temperature (723-753 K) for the MTO reaction.

The reaction patterns of the MTO conversion over HZSM-5 catalysts have been systematically investigated under industrially relevant conditions. The MTO reaction is an autocatalysis, and olefins and aromatic products act as entrained catalysts. Co-feeding a low concentration of aromatic molecules, which are free of diffusion constraints, significantly propagates the aromatics based catalytic cycle and greatly suppresses the olefin based route, leading to enhanced methane, ethylene formation and aromatics methylation at the expense of propylene and C<sub>4+</sub> higher olefins. In stark contrast, co-feeding small amount (10~40 C%) of C<sub>3-6</sub> olefins with 100 C% methanol does NOT selectively suppress the aromatics based cycle, resulting in unchanged selectivities to ethylene and higher olefins (C<sub>3+</sub><sup>+</sup>). Within the C<sub>3+</sub> fraction, propylene selectivity decreases and the selectivity to butenes is enhanced with increasing concentration of the co-fed olefin. Due to the relatively fast rates in methylation and cracking of C<sub>3-6</sub> olefins in the olefin-based cycle, the same product distributions at high methanol conversion were observed when co-feeding C<sub>3-6</sub> olefins with the same carbon concentrations.

This work provides further insights into the two distinct catalytic cycles operating for the methanol conversion HZSM-5 catalysts. It was concluded that two distinct catalytic cycles operate over HZSM-5 catalysts for methanol conversion to produce ethylene and propylene. However, their essential contributions to the final product distribution depend



on both their activities and intrinsic selectivity. The aromatics based cycle produces ethylene and propylene with an almost equal carbon based selectivity, while the olefin based methylation/cracking cycle favor  $C_{3+}$  olefins over ethylene. The co-existence of olefins and aromatics species in the zeolite channels leads to the competition between the two cycles. Therefore, their activities depend on the local concentrations of specific carbon species and methanol conversion. Olefin homologation/cracking are more active than the aromatics based route and responsible for most of methanol conversion, contributing to  $C_{3+}$  higher olefins formation irrespective of the nature of co-feeds, aromatics or olefins. On the other hand, ethylene comes from both the aromatics based route (intrinsic selectivity contributes) and the olefin based cycle (overall activities contribute). Their contribution, therefore, depends to a large extent on the reaction conditions. With an aromatics-enriched feed or at a low reaction temperature, the aromatics based cycle contributes more than the olefin based cycle, while the olefin based cycle contributes significantly at high reaction temperatures (such as in the MTO process). In addition to the classical hydride transfer between light olefins, It was proposed that a distinct and kinetically faster hydrogen transfer pathway involving methanol-derived intermediates exists and proceeds faster than the classic hydride transfer route.

Phosphorous modification has been applied to zeolites of various Si/Al ratios. It is shown that doping an appropriate concentration of P to the HZSM-5 zeolites with low Si/Al ratios is able to effectively enhance the propylene selectivity to reach the level on high Si/Al ZSM-5 zeolites, while it has a limited positive impact on the high Si/Al ZSM-5 zeolites with respect to propylene selectivity. In the meantime, phosphorous doping leads to a reduced activity. A further investigation on the impact of test conditions, i.e.,  $N_2$ - or water- diluted feed, leads to the conclusion that the phosphorous doped materials are unstable when interacting with feeds of high water concentrations. While these phosphorous doped materials showed a positive impact on the propylene selectivity when tested under  $N_2$  dilution, decreased propylene selectivity and increased hydrogen transfer ability was observed under water dilution conditions. Only low phosphorous loadings of 0.1-0.2 wt.% phosphorous loading were effective in prolonging the catalyst lifetime.

## **Curriculum vitae**

Xianyong Sun was born on August 2nd, 1981 in Hubei, China. After completing his high-school education in 1999, he was matriculated into the Department of Petroleum Refining at China University of Petroleum (East China), where he studied applied chemistry and received his bachelor's degree in Science in July 2003. His education as a master student continued in Taiyuan at Institute of Coal Chemistry, Chinese Academy of Sciences, under the supervision of Prof. Dong WU. In July 2006, he earned his master's degree in Engineering with distinctions from the Graduate University of the Chinese Academy of Sciences. In September of the same year, he was admitted to SINOPEC Research Institute of Petroleum Processing, Beijing, where he got research training in hydrotreating catalysis under the supervision of Prof. Da-Dong Li, a member of the Chinese Academy of Engineering. In February 2009, he joined the research group of Prof. Johannes A. Lercher and pursued his Ph.D. study at Catalysis Research Center and Institute of Technical Chemistry II of Technische Universität München, Germany. He was employed and working on an applied research project "Methanol to Propylene" in a close collaboration with partners from Clariant Produkte (Deutschland) GmbH (previous Süd-Chemie AG), sponsored by the BMBF (2008-2011) and MuniCat – an alliance of TUM and Clariant (2011-present). His research focuses on the fundamental understanding of catalytic conversion of methanol to olefins over HZSM-5 catalysts, the results of which constitute the current dissertation.

## **List of publications (to be submitted)**

**1. Catalytic conversion of methanol to olefins over HZSM-5 catalysts - Part 1: Impact of co-feeding aromatics and olefins.** Xianyong Sun, Sebastian Mueller, Hui Shi, Gary L. Haller, Maricruz Sanchez-Sanchez, Andre C. van Veen , Johannes A. Lercher, Journal of Catalysis, *to be submitted*.

**2. Catalytic conversion of methanol to olefins over HZSM-5 catalysts - Part 2: Insight into reaction pathways.** Xianyong Sun, Sebastian Mueller, Hui Shi, Gary L. Haller, Maricruz Sanchez-Sanchez, Andre C. van Veen , Johannes A. Lercher, Journal of Catalysis, *to be submitted*.

**3. Catalytic consequences of phosphorous modification of HZSM-5 zeolites in the methanol-to-olefins reaction.** Xianyong Sun, Muthusamy Vishnuvarthan, Sebastian Mueller, Roberta Olindo, Andre C. van Veen, Maricruz Sanchez-Sanchez, Johannes A. Lercher, *in preparation*.

**4. On the Reversibility of the Modification of HZSM-5 with Phosphate Anions.** Miroslaw Derewenski, Priit Sarv, Xianyong Sun, Sebastian Mueller, Andre C. van Veen, Johannes A. Lercher, The Journal of Physical Chemistry C, *submitted*.

## **List of presentations**

**On the impact of co-feeding aromatics and olefins in the methanol-to-olefins conversion over HZSM-5 catalysts.** Xianyong Sun, Sebastian Mueller, Andre C. van Veen, Johannes A. Lercher, Deutsche Wissenschaftliche Gesellschaft (DGfMK) Annual Conference, 2012, Berlin, Germany.(Oral)

**Towards engineering the active sites in the methanol-to-olefins reaction over HZSM-5 catalysts.** Xianyong Sun, Sebastian Mueller, Maricruz Sanchez-Sanchez, Andre C. van Veen, Johannes A. Lercher, IDECAT Conference, 2013, Brixen, Italy.(Oral)

**Impact of co-feeding olefins or aromatics in the methanol-to-hydrocarbons conversion over H-ZSM-5 catalysts.** Xianyong Sun, Sebastian Mueller, Andre C. van Veen, Johannes A. Lercher, Jahrestreffen Deutscher Katalytiker, 2013, Weimar, Germany. (Poster)